University of Alberta

Energy and Carbon Dioxide Transfers in a Barley-Fallow System in Southern Alberta

By

Zhaozhan Zhong ©

A thesis submitted to the Faculty of Graduate Studies and Research in partial fulfillment of the requirements for the degree of Master of Science

in

Water and Land Resources

Department of Renewable Resources

Edmonton, Alberta

Fall, 2002

University of Alberta

Library Release Form

Name of Author: Zhaozhan Zhong
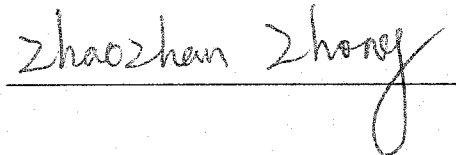
Title of Thesis: Energy and Carbon Dioxide Transfers in a Barley-Fallow System in Southern Alberta

Degree: Master of Science

Year this Degree Granted: 2002

Permission is hereby granted to the University of Alberta Library to reproduce single copies of this thesis and to lend or sell such copies for private, scholarly or scientific research purposes only.

The author reserves all other publication and other rights in association with the copyright in the thesis, and except as herein before provided, neither the thesis nor any substantial portion thereof may be printed or otherwise reproduced in any material form whatever without the author's prior written permission.

Zhaozhan Zhong
_____

204 Vanier House, Michener Park

T6H 4N1, Edmonton, Alberta

Date: Aug. 7, 2002

University of Alberta

Faculty of Graduate Studies and Research

The undersigned certify that they have read, and recommended to the Faculty of Graduate Studies and Research for acceptance, a thesis entitled Energy and Carbon Dioxide Transfers in a Barley-Fallow System in Southern Alberta submitted by Zhaozhan Zhong in partial fulfillment of the requirements for the degree of Master of Science in Water and Land Resources.
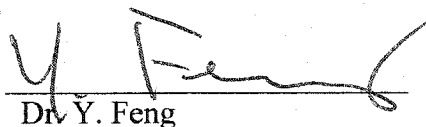
Dr. R. F. Grant
(Supervisor)

Dr. N. G. Juma

Dr. J. King

Dr. Y. Feng

Date: 7 Aug. '02

Abstract

Crop-fallow is a major cropping system used to conserve soil moisture and maintain stable yield in semi-arid regions, but there is still uncertainty about net CO_2 exchange by this ecosystem. Examining the energy and CO_2 transfers within this cropping system is therefore important for calculating agricultural sources and sinks of carbon. The objective of this paper is to study the energy and CO_2 transfers, carbon balance, soil carbon dynamics over a barley-fallow rotation in Lethbridge. Simultaneous measurements of net radiation, sensible heat, latent heat and CO_2 fluxes were made by two Bowen Ratio systems, which were used to test modeled results from the ecosystem model *ecosys*. Long-term soil carbon dynamics was predicted using *ecosys*, through which the effects of land use change and climate change on soil carbon were examined. Results indicates that crop-fallow is a net C source in drier years while a small sink in wetter years before harvest, but soil loses C in both cases after harvest, causing a negative NBP.

Acknowledgement

I am very grateful to my supervisor, Dr. Robert F. Grant (Department of Renewable Resources, University of Alberta), for his insight in ecosystem modeling, and for his encouragement, supervision throughout my studies at University of Alberta. His master-touch on every draft of the manuscript has contributed immensely to this thesis.

I am also very grateful to Dr. Sean McGinn, Mr. Hugh McLean and Mr. Trevor Coates (Lethbridge Research Center, Agriculture and Agri-Food Canada) for not only providing the experimental data, the great help during the field experiments in Lethbridge, but also the thoughtfulness and friendships. In particular, Dr. Sean McGinn gave me lots of supports, guidance and instructions in the experimental work on the Bowen Ratio measurements, all of which are sincerely appreciated.

Thanks are given to Dr. Noorallah G. Juma, Dr. Yongsheng Feng (Department of Renewable Resources, University of Alberta) and Dr. Jane R. King (Department of Agricultural, Food and Nutritional Science, University of Alberta) for serving on my supervisory committee, for their valuable suggestions, and for their time and efforts spent in reviewing my thesis.

Special thanks are extended to Dr. Peter H. Crown, for his advice, assistance and encouragement. I enjoy the friendship and discussion with my graduate fellows, especially Dr. Shusen Wang (Canada Centre for Remote Sensing, Ottawa), Isaac Amponsah, Dr. Yinsuo Zhang (Post Doc.), and Tao Li. Also, I want to take this opportunity to thank all other faculty and staff members in Department of Renewable Resources, University of Alberta.

I express my great gratitude to my family, especially my wife, Huayong Wei, for the love, support and encouragement at all times.

Table of Contents

List of Tables

List of Figures

Chapter 1   Introduction

1.1 The importance of studying energy and CO_2 exchange

With global change, the human population explosion and the increasing need for food and fiber around the world, research in natural resources management, greenhouse gas (GHG) emission, and agro-ecosystem sustainability, has attracted more and more attention. Energy and CO_2 transfers in agricultural ecosystem are important issues, in that they are not only the key to understanding greenhouse gas emissions from agricultural ecosystems, but they also provide the theory and mechanism for crop photosynthesis, water use efficiency, and crop yield formation. These transfers determine whether an ecosystem is a source or sink of carbon and therefore it contributes to or reduces the rates of atmospheric CO_2 accumulation.

CO_2 is a major atmospheric trace gas with a concentration that currently is 25% higher than in pre-industrial times (Watson et al., 1990). The atmospheric concentration of CO_2 has increased by 31% since 1750 (IPCC, 2001). The rate of increase of atmospheric CO_2 concentration has been about 1.5 ppm (0.4%) per year over the past two decades (IPCC, 2001). During the 1990s the year to year increase varied from 0.9 ppm (0.2%) to 2.8 ppm (0.8%) (IPCC, 2001). Moreover, CO_2 is the most abundant trace gas and is radioactively active in the atmosphere that is responsible for 50% of the greenhouse warming effect (Bouwman, 1990). Therefore, quantifying by direct measurement or ecosystem modeling the CO_2 exchange, NPP (net primary productivity), NEP (net ecosystem productivity), and NBP (net biome productivity) allows valuable insights into the dynamics of the long-term carbon of ecosystem. This work provides useful information in evaluating CO_2 emissions from terrestrial ecosystems and building carbon inventories for the purpose of greenhouse gas mitigation in response to the Kyoto Protocol.

CO_2 emission from land-use change is a major source that causes the increase in atmospheric CO_2 concentration. About 10 to 30% of the current total anthropogenic emissions of CO_2 are estimated to be caused by land-use conversion (IPCC, 2001). The

annual flux of carbon from land-use change for the period from 1990 to 1995 has been estimated to be 1.6 Pg C yr^{-1} (Houghton, 2000). During the period 1850–1998, net cumulative global CO_2 emissions from land-use change are estimated to have been 136 ± 55 Gt C (IPCC, 2001). Of these emissions, about 87 percent were from forest areas and about 13 percent from cultivation of mid-latitude grasslands (Houghton, 1999; Houghton et al., 1999, 2000). Houghton (1991) assessed seven types of land-use change for carbon stock changes: (1) conversion of natural ecosystems to permanent croplands, (2) conversion of natural ecosystems to shifting cultivation, (3) conversion of natural ecosystems to pasture, (4) abandonment of croplands, (5) abandonment of pastures, (6) harvest of timber, and (7) establishment of tree plantations. Change in land use contributes C to the atmosphere in two principal ways: 1) release of C in the biomass which is either burnt or decomposed, and 2) release of soil organic carbon (SOC) following cultivation due to enhanced mineralization brought about by change in soil moisture and temperature regimes and low rate of return of biomass to the soil (Lal et al., 1998).

On the west Canadian prairies, land use change from continuous cropping to crop-fallow rotation is a widely-used approach for conserving soil moisture while ensuring stable crop yields. The area of crop-fallow in western Canada was estimated to be 8.1 Mha in 1989 and 6.0 Mha in 1999, accounting for 29.6% and 21.7% of the cropland, respectively (Statistical Handbook, 1999). But how this land use change affects CO_2 exchange, and soil carbon storage is still uncertain. Therefore, examining the CO_2 exchange from the crop-fallow system is very important in determining the agriculture's contribution to GHG emission and global change.

The following is a summary review of major factors influencing the CO_2 flux in agricultural ecosystems related to this study (although some other factors such as nutrient, soil pH etc. are also important, they are not included), followed by a discussion of the main methods used in energy and CO_2 exchange studies. The main study contents and objectives of this study are given at end of this chapter.

1.2 Factors affecting the ecosystem CO_2 exchange

The terrestrial carbon cycle involves a series of processes. Higher plants acquire CO_2 by diffusion through tiny pores (stomata) into leaves and thus to the sites of photosynthesis. Most of this CO_2 diffuses out again without participating in photosynthesis. The amount that is "fixed" from the atmosphere, i.e., converted from CO_2 to carbohydrate during photosynthesis, is known as gross primary production (GPP) or CO_2 fixation. Part of GPP is used for plant growth, i.e. incorporated into new plant tissues such as leaves, roots and wood, and the rest is converted back to atmospheric CO_2 by autotrophic respiration (respiration by plant tissues) (Lloyd and Farquhar, 1996; Waring et al., 1998). Net primary production (NPP) is the difference between GPP (photosynthesis) and autotrophic respiration (R_a), which is the annual plant growth.

Eventually, virtually all of the carbon fixed in NPP is returned to the atmospheric CO_2 pool through two processes: heterotrophic respiration (R_h) by decomposers (bacteria and fungi feeding on dead plant tissue and exudates) and herbivores; and combustion in natural or human-set fires. Net ecosystem production (NEP) is the difference between NPP and R_h, which determines how much carbon is lost or gained by the ecosystem in the absence of disturbances that remove carbon from the ecosystem (such as harvest or fire). When other losses of carbon are accounted for, including fires, harvesting/removals (eventually combusted or decomposed), erosion and export of dissolved or suspended organic carbon (DOC) by rivers to the oceans (Schlesinger and Melack, 1981; Sarmiento and Sundquist; 1992), what remains is the net biome production (NBP), i.e., the carbon accumulated by the terrestrial biosphere (Schulze and Heimann, 1998).

The energy and CO_2 exchange in agricultural ecosystem are controlled by many factors. Being the interface between atmosphere, biosphere and pedosphere, the agricultural field is the place where energy and CO_2 transfers occur in agricultural ecosystems. Therefore, energy and CO_2 transfers in agricultural ecosystems are simultaneously controlled by atmospheric, biospheric, and pedospheric factors, and by their dynamic interactions. In addition, agricultural practices such as crop rotation, land use change, irrigation, field mulch, fertilizer application, and tillage, also greatly influence the heat and CO_2 transfers in agricultural ecosystems (Fig. 1.1).

3

Atmospheric Factors
Radiation
Temperature
Precipitation
Wind speed
Air pressure
Humidity

Biospheric factors
Crop varieties
Stomatal function
Respiration
Water use efficiency
Evapotranspiration
Photosynthesis
Crop species

Pedospheric Factors
Soil texture
Soil water content
Soil organic matter
Soil biota
Soil pH
Soil salinity
Nutrient
Structure

Agricultural practices
Crop rotation
Land use
Irrigation
Field mulch
Fertilization
Tillage

Fig. 1.1   Schematic representation of factors in agricultural ecosystems
that control energy and carbon dioxide exchange.

1.2.1 Environmental factor affecting CO_2 exchange

1.2.1.1 Photosynthesis (GPP)

Photosynthesis is the primary process in plant growth and production, providing both energy and carbon for plant processes. Photosynthesis can be conveniently treated as three components: (1) light reaction, in which radiant energy is absorbed and used to generate the high energy compounds; (2) dark reaction, i.e. enzymatic processes

including the biochemical reduction of CO_2 to sugars using the high energy compounds generated in the light reaction; and (3) diffusion process which bring about exchange of CO_2 and O_2 between the chloroplasts and the external air (Jones, 1983; Larcher, 1995).

Atmospheric factors

Radiation

Radiation is the driving variable for photosynthesis in three ways: the photosynthesis light response curve of leaves, the radiation intercepted by leaf canopies and the distribution of light within canopies (Penning de Vries et al., 1989). At light intensities below the light compensation point, photosynthesis fixes less CO_2 than is set free by respiration. Once the compensation point has been passed, CO_2 uptake increases rapidly. If crop leaves are exposed to increasing intensities of illumination, the CO_2 uptake increases at first in proportion to light intensity and then more slowly to a maximum value. The relationship between net photosynthesis and radiation is represented by a rectangular hyperbolic response curve, which can be expressed by Equation 1.1.

$$P = \frac{\alpha I P_{max}}{\alpha I + P_{max}} \tag{1.1}$$

where P is photosynthetic rate; α is a constant; I is the light flux density incident on the leaf; P_{max} is the value of P at saturating light level.

Various species of plants differ greatly with respect to the light dependency of their carbon dioxide fixation rates (Rosenberg et al., 1983). Leaves of C_4 species (e.g. corn, sorghum, sugar cane) show a continual increase in carbon dioxide uptake rate with increasing level of irradiance. Leaves of C_3 species (e.g. soybeans, sugar beets, many range and forage species) are less productive and may become light saturated at levels of irradiance as low as one-fourth the full sunlight of the mid-latitudes (Rosenberg et al., 1983). Therefore, C_4 plants are not light-saturated even at the highest intensities, and

even at intermediate irradiance they operate more efficiently than C_3 plants (Larcher, 1995). Some woody species and shade plants are light saturated at very low irradiance. Leaves of shade and woody species are light saturated at about 350 W m^{-2} of incandescent light. The orchard grass group appears light saturated at about 700 W m^{-2}, whereas the corn leaves are still unsaturated at 1400 W m^{-2} (Moss, 1965).

Temperature

Most metabolic reactions are strongly influenced by temperature. An equation attributed to Arrhenius is often used to describe the temperature dependence of the rate constant k of a biochemical reaction. Both the temperature sensitivities of photosynthesis and growth respiration (see **autotrophic respiration** below) can be expressed by the Arrhenius equation (Equation 1.2).

$$K = A\exp[-E_a /(RT)] \tag{1.2}$$

where A is a constant; E_a is activation energy of the reaction; R is the gas constant; T is the absolute temperature.

The effects of temperature on photosynthesis are defined by three regions: the cold limit or the temperature minimum, the temperature optimum, and the heat limit or the temperature maximum (Larcher, 1995). At cool, suboptimal temperatures the rate at which carbon is fixed increase as the temperature rises, until an optimal value is reached. At temperatures above the optimal range the ratio of soluble CO_2/O_2 decreases due to reductions in the comparative solubilities of CO_2 versus O_2; this results in a decrease in carboxylation efficiency of the enzyme RuBP (ribulose bis-phosphate) carboxlase/oxygenase. Very high temperatures impair the interplay between the various reactions involved in carbon metabolism and transport of material. This, together with the inhibition of the membrane-bound photochemical processes, results in a rapid breakdown of photosynthesis.

The effect of temperature minimum on photosynthesis has been of special interest recently (Oquist, 1983). Air temperatures between 0 and 15°C are defined by Raison

and Lyons (1986) as chilling temperatures which reduce photosynthetic activity in chill-sensitive plants (Lee and Estes, 1982; Larcher, 1983; Long, 1983; Potvin, 1985, 1988; Potvin et al., 1985). Reduced photosynthesis occurs following chilling in darkness and chilling in light, the latter case being more severe (Oquist, 1983). Long et al. (1983) reported a 93% reduction in CO_2 exchange in maize plants exposed to a decrease in air temperature from 20 to 5°C, accompanied by a reduction in stomatal conductance. One effect of low temperature is an increase in CO_2 inside the leaf (Hallgren et al., 1982), which also occurs with decreased stomatal conductance and reduced photosynthesis. Larcher (1983) reported that chilling temperatures inhibit enzymatic activity, in particular that of pyruvate photodikinase, thus decreasing photosynthesis. Potvin (1988) reported that chilling temperatures reduced photosynthesis assimilate transport to the phloem. Detailed information on the effects of chilling temperatures on photosynthesis can be found in Basra (2001).

The C_4 plants have a generally greater photosynthetic potential under higher temperature because soluble CO_2 concentrations are maintained by phosphoenolpyruvate (PEP) carboxylase. Under controlled environment conditions, maize assimilates carbon dioxide more efficiently as temperatures increase from 10 to 30°C, however, an optimum temperature exists between 30 and 40°C (Moss, 1965). Sugar production in sugar beets, on the other hand, is benefited by a decreased temperature in the range of 15-29°C (Thomas and Hill, 1949). In a field study with alfalfa, Baldocchi et al. (1981a) found the flux of CO_2 from air to crop decreased with temperature in the range 23-32°C. This effect may be due not only to the direct influence of temperature on photosynthesis, but also to an increase in soil and root respiration that would cause a greater release of carbon dioxide from below. Such an increased release might diminish the need for CO_2 from the air above.

Atmospheric CO_2 concentration

The sensitivity of photosynthesis to CO_2 concentration can be expressed by Michealis-Menten equation (Farquhar et al., 1980). The rate, V_c, of the carboxylation of RuBP in the presence of competitive inhibition by O_2 with saturating RuBP is:

$$V_c = \frac{V_{cmax} \times C}{C + K_C(1 + O/K_O)} \qquad (1.3)$$

where V_c is CO_2 limited leaf carboxylation rate; V_{cmax} is the maximum leaf carboxylation rate at saturating CO_2 and in the absence of O_2; C and O are the partial pressures of CO_2 and O_2 in equilibrium with dissolved gases in chloroplast stroma, respectively; and Kc, Ko are Michaelis-Menten constants for CO_2 and O_2, respectively.

The fixation of CO_2 can generally be increased by increasing the ambient CO_2 concentration level (Lemon, 1983). The ability of leaf photosynthesis to respond to increased CO_2 concentration depends on various external and internal limits to CO_2 uptake, their dependence on CO_2 concentration, and their interactions with other environmental factors. The strength of the response of photosynthesis to an increase in CO_2 concentration depends on the photosynthetic pathway used by the plants. C_4 plants differ from C_3 plants in response to increased CO_2, since the C_4 pathway serves, in effect, as an internal CO_2 concentrating mechanism. In C_4 plants, photosynthesis is not inhibited by O_2, and it is only slightly limited by the present atmospheric CO_2 concentration. C_3 plants generally show an increased rate of photosynthesis in response to increases in CO_2 concentration above the present level (Koch and Mooney, 1996; Curtis, 1996). C_4 plants already have a mechanism to concentrate CO_2 and therefore show either no direct photosynthetic response, or less response than C_3 plants (Wand et al., 1999).

Wind and turbulence

Wind and turbulence are among the environmental factors that influence photosynthesis. The re-supply of carbon dioxide to levels at which it has been depleted by the actively photosynthesizing plant should generally be adequate whenever there is effective turbulent mixing. Baldocchi et al. (1981a) studied the interacting effects of windiness and irradiance on the flux of CO_2 to an alfalfa crop. CO_2 flux is seen to response to an increase in the flux density of net radiation. However, the rates at any irradiance level increase with increasing windiness (described in terms of friction

velocity). This effect may be due to distortion of canopy shape by the wind, thus facilitating the penetration of radiation to the lower, light-unsaturated leaves (Rosenberg et al., 1983).

Pedospheric factors

Water

Water is an essential component in the photosynthesis reaction. Shortages of soil moisture or extreme dryness of the atmosphere create a water stress that affects the efficiency of the photosynthetic reaction in the plant. The moisture affects photosynthesis through a number of mechanisms: by affecting the levels of metabolic intermediates; by inhibiting the photosynthetic electron transport system; by causing stomatal closure; by altering rates of respiration; and by lowering CO_2 diffusion into plants (Boyer, 1970; Lemon, 1983). One very direct influence of water availability on photosynthesis is through the impact on stomatal aperture. As stomata close in response to stress, resistance to the diffusion of carbon dioxide into the leaves increases. Moss (1965) speculated on the influence of soil moisture stress and atmospheric evaporative demand on photosynthesis at varying levels of irradiance. With increasing in soil moisture stress (increasing dryness), the optimum photosynthetic rate is reached at a lower irradiance. When soil moisture stress is low and with little atmospheric evaporative demand, photosynthesis continues to rise even at high irradiance. High atmospheric stress and, particularly, extreme atmospheric stress reduce photosynthesis, probably because rapid evaporation reduces turgor in the guard cells causing stomata to close (Rosenberg et al., 1983).

Biospheric factors

Stomatal conductance

Stomata are pores formed by a pair of specialized cells, the guard cells, which are found in the surface of aerial parts of most higher plants and which can open and close

to control gas exchange between a plant and its environment. Stomata act as portals for entry of CO_2 into the leaves and exit of water vapor from the leaves, which control two of the most important plant process, namely photosynthesis and transpiration (Willmer, 1983). Stomata control 95% or more of the CO_2 exchange between the leaf and the atmosphere. They therefore control rates of crop photosynthesis.

Stomata influence crop photosynthesis through stomatal resistance r_s. Stomata of most plants, with an exception in CAM (crassulacean acid metabolism) plants, open in response to light and close in response to darkness (Heath and Russell, 1954; Neales, 1975), and their responses to light vary according to species, the age of the leaf or plant, the pretreatment of leaf or plant and other environmental factors. Relatively low levels of light (about 1 and 10 percent of full sunlight) stimulate stomatal opening in leaves and the level needed to saturate the opening response is usually well below full sunlight (Willmer, 1983). Stomata may also close during part of daylight and open during part of the night because of an endogenous effect (Circadian rhythms) (Pittendrigh, 1954; Martin and Meidner, 1971; Martin and Stevens, 1979; Mansfield and Heath, 1963, 1964), and certain species exhibit midday stomatal closure (Tenhunen et al., 1980).

In general, as ambient CO_2 concentrations increase stomata close, while as CO_2 concentrations decrease stomata open (Heath and Russell, 1954). Stomata of C_4 species appear more sensitive to CO_2 than those of C_3 species and closure in C_4 species occurs at much lower CO_2 levels than in C_3 species (Willmer, 1983). CO_2 levels below about 100 μl l^{-1} may not cause further stomatal opening, at least in C_3 species, while in C_4 species stomata are apparently sensitive down to zero levels of CO_2. Raschke (1979) studied the mechanism by which CO_2 regulates stomata movements.

Temperature increase will affect internal CO_2 concentrations which, in turn, will affect stomatal aperture. If respiration outpaces photosynthesis as temperatures increase, CO_2 levels will increase within the leaf which will tend to bring about closure. Also, an increase in leaf temperature will result in an increase of vapor pressure (humidity) gradient between the leaf and the surrounding air which may cause stomatal closure either through a direct atmospheric humidity response or by increasing transpirational water loss, resulting in plant water stress. Therefore, there is considerable variation in temperatures for optimal stomatal opening (Stalfelt, 1962; Schulze et al., 1973; Losch,

1977; Willmer, 1980). In addition, increased temperature can counteract the effects of increased CO_2 levels and darkness on stomatal closure (Mansfield, 1965).

Stomata of some species such as coffee and onion show a distinct "mid-day" closure, particularly when growing under hot, sunny conditions (Tenhunen et al., 1980). Initially the closure was attributed to water stress brought about by the high temperature which occurred during the middle of the day (Loftfield, 1921). Later, it was considered to be a CO_2 effect (Meidner and Heath, 1959). As temperatures increase, respiration outpaces photosynthesis and high CO_2 levels accumulate in the leaves which close their stomata.

Stomata respond to bulk leaf water potential by closing if the leaf water content becomes too low and opening as the leaf water content increases. In some species stomata remain open until a threshold level of leaf water deficit is reached and then close rapidly. Under field conditions leaf water potentials may drop to very low values before the stomata close (Willmer, 1983). Stomata of some species also respond to changes in atmospheric humidity (atmospheric water vapour pressure deficit) by opening as humidity increases and closing as the atmosphere becomes drier (Watts and Neilson, 1978). There is some evidence that leaf water stress increases stomatal sensitivity to humidity while high light intensity reduces stomatal sensitivity to humidity (Willmer, 1983).

1.2.1.2 Autotrophic respiration

The oxidation of carbohydrate to CO_2 and H_2O in living cells is generally termed as autotrophic respiration (R_a). In photosynthetic organisms there are two main types of respiration. The first is called dark respiration (R_d) and includes various pathways of substrate oxidation such as glycolysis, the oxidative pentose phosphate pathway and the tricarboxylic acid cycle that conserve some of the free energy in carbohydrate in the high energy bonds of ATP (adenosine triphosphate) and reduced pyridine nucleotide (NADH). This also includes the further oxidation of NADH by transfer of electrons along the oxidative phosphorylation pathway in the mitochondrial membranes to O_2 as the final electron acceptor, with the formation of 3 ATP per NADH oxidized. The second type of respiration in plants is called photorespiration or light respiration (R_l).

11

This is the pathway of CO_2 production via the photorespiratory carbon oxidation (PCO) cycle (Jones, 1983). R_l only occurs in photosynthetic cells in the light, while R_d can occur in all cells in the dark or light. The autotrophic respiration discussed here refers to R_d only.

Autotrophic respiration significantly influences the carbon balance of a crop since often about half the carbon assimilated during photosynthesis is eventually lost by respiration (Amthor, 1989). The energetics of crop growth and yield are closely bound up with respiratory activity and the production of CO_2. It is generally considered that autotrophic respiration in plants is concerned with two metabolic functions: growth (R_g) and maintenance (R_m) respiration. Growth respiration includes processes such as the synthesis of plant material from the sugars produced by photosynthesis, the conversion of stored carbohydrates from the stems of crop plants into grain material, and the conversion of sugars and nitrogen into plant proteins. Respiration accompanying growth is sometimes referred to as "conversion", or "constructive" respiration (France and Thornley, 1984). The maintenance function is concerned with maintaining the existing plant material. Factors influencing autotrophic respiration include temperature, soil water, and crop species (Rosenberg et al., 1983; Larcher, 1995).

Atmospheric factors

Temperature

Maintenance respiration (R_m) is proportional to dry weight and strongly temperature sensitive, while R_g is directly dependent on photosynthesis and therefore follow the same response to temperature as photosynthesis (Equation 1.1). The rates of R_m increase exponentially with temperature, other factors being equal (Larcher, 1995; Rosenberg et al., 1983; Amthor, 1989). The increase in reaction rate of R_m from a temperature increase of 10°C is expressed by the temperature coefficient Q_{10}, given approximately by:

$$Q_{10} = \exp[\frac{10E_a}{RT(T+10)}] \qquad (1.4)$$

In practice, the Q_{10} may be obtained from the reaction rates k_1 and k_2 at any two temperatures T_1 and T_2 by:

$$\ln Q_{10} = \frac{10}{T_2 - T_1} \ln \frac{k_2}{k_1} \qquad (1.5)$$

where T_1 and T_2 are two absolute temperatures, and k_1 and k_2 are the associated reaction rates.

Temperature has a direct effect on the rate of maintenance respiration (Penning de Vires et al., 1989). It corresponds to a doubling of the rate for each 10°C rise in temperature up to temperatures that will kill a plant (45-60°C) (McCree, 1974). This dependence between temperature and the rate of maintenance respiration generally corresponds with a Q_{10} of 2.0 (McCree, 1974; Kase and Catsky, 1984).

As the temperature rises R_m increases exponentially. Below 5 °C the energy of activation (E_a) for various processes involved in R_m is large, and the Q_{10} is high. In tropical plants the Q_{10} is around 3, or even more, at temperatures below 10 °C. Above 25-30 °C the temperature coefficient for R_m in most plants falls to 1.5 or less. At still higher temperatures biochemical processes occur so rapidly that the supply of substrate and metabolites cannot keep pace with the turnover of matter and energy. The rate of R_m thus declines in a short time. At temperatures between 50° and 60 °C enzymes and functionally important membrane structures are damaged by heat, and R_m ceases (Larcher, 1995). Hofstra and Hesketh (1969) observed an increase in leaf R_m rate to 45°C in maize, which remained constant between 45 and 50°C; an increase in R_m rate to 50°C in soybean leaves, although the rate of increase declined above 40°C; and a decrease in sugar beet leaf R_m rate above 45°C. Nevins and Loomis (1970) observed increases in R_m to at least 35°C in sugar beet leaves. The rate of R_m of leaves of bean, cotton, and sorghum all increased exponentially with an increase in temperature to at least 40°C (Brown and Thomas, 1980). Kase and Catsky (1984) observed that the R_m rate of maize leaves increased exponentially with temperature increase to at least 60°C.

13

R_m rate of cotton leaves increased exponentially with temperature to 30-35°C, but then increased only slightly to 40°C (Ludwig et al., 1965). Rice and Eastin (1986) found that root specific R_m rate of grain sorghum increased significantly from 25 to 30°C, but with further temperature increases (up to 40°C) only slight increases in R_m rate occurred. However, R_m is not often dramatically influenced by lower temperatures experienced by major crops (Amthor, 1989). Crawford and Huxter (1977) examined R_g and R_m in pea and maize seeding roots at low temperatures as low as 2°C. They concluded that although respiration rate was reduced by a low temperature, a reduced supply of substrate to the root is the factor likely to be limiting growth at low temperature, not slow respiration per se. Some other effects of low temperature on R_m have been reviewed by Raison (1980).

Pedospheric factors

Soil moisture

Although the availability of soil moisture affects autotrophic respiration in plants, the response of autotrophic respiration to changes in soil moisture is less marked than those for temperature. However, since water stress (water deficit) usually limits both plant photosynthesis and growth, it reduces the rate of plant autotrophic respiration. This can be assumed to be due simply to (1) decreases in growth rate and hence decreases in growth respiration, and (2) decreases in total metabolic activity and in the amount of living phytomss (compared to a non-stressed crop) and hence decreases in maintenance respiration (Amthor, 1989). In their studies of *Populus deltoides*, Regehr et al. (1975) stressed the plant by withholding water until an internal leaf water potential of about -1.8 MPa was reached. Autotrophic respiration decreased significantly in the range -0.4 to -0.8 MPa. This decreasing respiration rate was linked to the decrease in photosynthesis that occurred in the leaf as a result of water stress. Respiration recovered rapidly after watering.

Biospheric factors

Crop species

Autotrophic respiration differs between plant species, changing with the availability of respirable substrate, with the state of development and activity, and with temperature. Larcher (1995) summarized the specific respiratory activities for different plant species. To facilitate comparison, the specific respiratory activity is expressed as the rate of respiration measured in the dark at a standard temperature (usually at 20 or 25 °C). Herbaceous species, especially those with a rapid growth rate, respire twice as rapidly as deciduous trees under the same conditions, and the latter in turn respire on the average at five times the rate of evergreens. Within a given group, heliophytes respire more rapidly than sciophytes at 20 °C, and plants of the artic and high mountains respire more strongly than those of warmer regions and valleys.

1.2.1.3 Heterotrophic respiration

Heterotrophic respiration (R_h) is the process by which carbon dioxide produced by soil microorganisms is released to the atmosphere. Therefore, heterotrophic respiration here refers to soil respiration, excluding root respiration. Major environmental variables that control soil respiration are temperature, soil property, soil moisture and carbon input (Singh and Gupta, 1977; Lloyd and Taylor, 1994; Davidson et al., 1998; Akinremi et al., 1999).

Atmospheric factors

Temperature

All respiratory processes are sensitive to temperature, as is the rate of population growth of respiring organs—particularly the fine roots and heterotrophic organisms in the soil. Thus, heterotrophic respiration is a function of soil temperature (Boone et al., 1998). The response of heterotrophic respiration to increasing temperatures also follows the exponential equation (Equation 1.4-1.5) (Lloyd and Taylor, 1994). The Q_{10} values reported for soil respiration generally fall between 2 and 4. However, Q_{10} values vary

with temperature, and are sensitive to the depth of the active soil layer and the depth at which temperature is measured (Kirschbaum, 1995). Akinremi et al. (1999) found that the integrated daily CO_2 flux under fallow fields was strongly related to daily soil moisture and mean soil temperature.

Pedospheric factors

Soil properties

The rate of R_h varies with the soil properties. Clay in soils reacts with residues from litterfall and microorganisms to form humus which is less vulnerable to loss by disturbance than plant and litterfall carbon. Therefore, R_h decreases as clay content increases in soils. For a given rate of litterfall, soils with higher clay content accumulate more humus than sandier soils, and are therefore better for increasing carbon storage from changes in land use practices since humus undergoes R_h much slowly than litterfall (Anderson et al., 2001).

Soil moisture

Availability of soil moisture affects respiration in the plant as well as in the soil. Generally, too low or too high soil moisture contents restrict R_h. When soil is too dry, soil microbes lack habitat and therefore access to litterfall and humus, R_h is slower. Lack of soil water also inhibits the metabolic activity of microbes, causing reduction in R_h. At a high moisture content, the reduction in R_h is caused by lack of oxygen and the accumulation of CO_2 as a result of the soil pore spaces becoming filled with water (Glinski and Stepniewski, 1985). Between the low and high moisture limits, the change in soil moisture content has little or no obvious effect on R_h (Tesarova and Gloser, 1976). Soil respiration has been found to decrease at very high and very low water content at boreal sites (Schlentner and Van Cleve, 1985; Savage et al., 1997), in temperate deciduous forest (Davidson et al., 1998), and in arctic tundra (Luken and Billings, 1985; Oberbauer et al., 1991). Lower (more negative) soil water potential, which is a function of diminished soil water content, has been shown to decrease rates of R_h. The influence of soil water availability on respiratory processes has also been

demonstrated in the field studies on nocturnal CO_2 release in soybeans (Da Costa et al., 1986). In the early part of the growing season, soil moisture content was low. The respiratory rate appeared to be related to air temperature. In early August extensive rains increased the soil profile moisture content and the increase in respiration was more closely related to soil moisture availability through its general influence on photosynthesis. Temperature in the upper 30-100 mm of the soil was fairly uniform throughout the growing season. Respiration rose rapidly after the rainfall but diminished as the season progressed. Part of the increased production of CO_2 in the soil can be related to the greater photosynthetic activity after rain; a part is also attributable to increased activity of microorganisms for which soil organic materials provide the substrate. Both soil moisture and temperature are known to influence microbial activities (Monteith et al., 1964; Norman et al., 1992; Grant and Rochette, 1994) and therefore soil respiration. Norman et al. (1992) obtained an empirical relationship between CO_2 flux from grasslands, soil temperature at 10 cm, volumetric moisture in the top 10 cm, and leaf area index. Rochette et al. (1995) obtained a linear relationship between the hourly flux of CO_2 and soil temperature at 7 cm depth.

Biospheric factors

Carbon input

Heterotrophic respiration depends on carbon input to the soil. Most dead biomass enters the detritus and soil organic matter pools as litterfall where it is respired at a rate that depends on the chemical composition of the dead tissues and on environmental conditions (for example, low temperatures, dry conditions and flooding slow down decomposition). The composition of litterfall affects both its rate of decomposition and the fate of its decomposition residues (Anderson et al., 2001). Woody litterfall decomposes much more slowly than foliar or root litterfall because of its high cellulose content, and so tends to reside longer in the soil. Litterfall from coniferous forests decomposes more slowly than that from deciduous forest because of the higher lignin content and the low pH (high acidity) of its residues. Higher lignin contents in litterfall

17

also yield more residues that react to form humus in the soil, so less CO_2 is lost through R_h. Undisturbed coniferous forests therefore tend to accumulate large amounts of soil carbon over time, unless other environmental conditions favor litterfall decomposition.

Agricultural practices also affect the rate of R_h through influencing carbon input into the ecosystem. Because the soil microbial community is generally limited by the availability of organic substrates, enhanced addition of labile carbon to the soil tends to increase heterotrophic respiration unless inhibited by other factors such as low temperature (Hungate et al., 1997; Schlesinger and Andrews, 2000). Field studies have indicated that increases in soil organic matter could increase soil respiration at about 30%, under elevated CO_2 (Schlesinger and Andrews, 2000). In general, daily soil respiration from crop fields is higher than from fallow (Biscoe et al., 1975; McGinn and Akinremi, 2000). Under cropped fields, CO_2 fixation by crop photosynthesis serves as a carbon input into the ecosystem, which causes a higher growth respiration. Moreover, higher microbial activity for soil under cropped field also results in a higher rate of heterotrophic respiration.

1.2.2 Agricultural practices affecting CO_2 exchange

Agricultural practices affect CO_2 exchange mainly through their influences on soil carbon and therefore R_h. R_h is strongly affected by agricultural practices such as summer fallow, crop rotation, tillage, fertilizer that determines inputs of carbon to the soil, as well as soil temperatures and water contents. Strategies for increasing carbon in cultivated soil can be broadly classified into four main approaches: 1) reduction in tillage intensity; 2) intensification of cropping systems; 3) adoption of yield-promoting practices, including improved nutrient amendments; and 4) reestablishment of permanent perennial vegetation (Janzen et al., 1998; Bruce et al., 1999).

1.2.2.1 Summer fallow

Gains in carbon storage by agricultural soils require continuous inputs of plant litterfall. These inputs are interrupted by several land use practices that cause soil carbon to be lost. One of such practices is summer fallow, which has caused

considerable loss of organic carbon from Canada's soils, especially in the Prairies (Anderson et al., 2001). Summer fallow is used as a means of conserving moisture and ensuring an economic yield in the semi-arid regions of the world (Akinremi et al., 1999). However, frequent summer fallow causes soil erosion (Monreal et al., 1995), soil organic matter loss (Havlin et al., 1990), nitrate and nutrient leaching (Campbell et al., 1984). Discrepancies exist in studies comparing soil respiration from fallow to cropped soil. Rochette et al. (1992) measured equal fluxes of CO_2 in fallow and barley plots during the early part of the growing season, but a difference in CO_2 fluxes from fallow and barley plots was observed in July, which grew large as the soil became drier under barley. Their results showed that soil respiration under barley was 25% lower than in fallow soil. Their observation suggests that soil respiration from fallow may contribute more CO_2 to the atmosphere compared to continuous cropping. Monteith et al. (1964) reported that the flux of CO_2 from cropped soil (beans, kale, grass) was 2-3 g C m^{-2} d^{-1} more than from fallow early in the growing season. The difference was attributed to root respiration. Between July and harvest the CO_2 produced under barley decreased and was smaller for several weeks than the corresponding flux from fallow. The lower flux of CO_2 from barley was attributed to soil moisture deficit under barley during this latter period. Biscoe et al. (1975) reported that approximately one-half of the CO_2 produced could be ascribed to root respiration. Summer fallow causes loss of soil carbon (Campbell et al., 1991; Janzen 1987; Bremer et al., 1994). This is because more crop residues are added to the soil, and soil disturbance is less under continuous cropping compared with fallow systems (Doran and Smith, 1987; Blevins and Frye, 1993).

1.2.2.2 Tillage

Cropland soils can lose carbon as a consequence of soil disturbance (e.g., tillage). The influence of tillage management and crop rotation on soil organic matter C has been investigated extensively throughout the world (Blevins and Frye, 1993). Tillage increases aeration and soil temperatures (Tisdall and Oades, 1982; Elliott, 1986), making soil aggregates more susceptible to breakdown and physically protected organic material more available for decomposition (Elliott, 1986; Beare et al., 1994). Tillage

removes the crop cover, resulting in warmer and moister conditions that accelerate microbial decomposition processes. Tillage also increases the supply of oxygen to soil microorganisms by increasing aeration. In addition, erosion can significantly affect soil carbon stocks through the removal or deposition of soil particles and associated organic matter. As a result, adoption of practices with reduced tillage can result in significant accumulation of soil carbon (Lal et al., 1998; Paustian et al., 1997). Generally, organic carbon in the surface 15 cm of non-tilled soils is greater than for tilled soil (Lal, 1976; Blevins et al., 1977; Doran, 1980).

1.2.2.3 Cropping systems

Many cropping systems can be intensified by increasing the duration of photosynthetic activity, thus increasing soil carbon. Use of perennial forages often enhances soil carbon, because these crops have extended periods of active growth and allocate greater proportions of carbon below ground (Paustian et al., 1997). Other opportunities for intensification of cropping systems include the use of winter cover crops (Kuo et al., 1997) and the elimination of summer fallow. Intensification of cropping systems not only increases the amount of carbon entering the soil, it may suppress decomposition rates by drying the soil. Soil carbon content can be protected and even increased through alteration of tillage practices, crop rotations, residue management, reduction of soil erosion, improvement of irrigation and nutrient management, and other changes in forestland and cropland management (Kern and Johnson, 1993; Lee et al., 1993).

1.2.2.4 Fertilization

Application of nutritive amendments, including commercial fertilizers and organic amendments, favors soil carbon by increasing yield and, consequently, the amount of residues returned to the soil (Paustian et al., 1997). Addition of organic amendments like livestock manure also promotes soil carbon by adding carbon directly, although this carbon is merely a recycling of crop carbon and does not necessarily represent a new input. Other agronomic options that may furnish higher yields include improved crop varieties, better pest control, more efficient fertilizer practices, and improved water

management (including irrigation). These higher yields will translate into higher soil carbon contents, provided the higher residue amounts are returned to the soil (Bruce et al., 1999). However, it was concluded that fertilization would result in only small increase in soil carbon where summer fallow is part of the crop rotation, especially in semi-arid climates (Campbell et al., 1996).

1.3 Methods for studying energy and CO_2 exchange

There are commonly two ways for studying the energy and CO_2 exchange in any ecosystem: direct measurement and modeling. Measuring and modeling energy and CO_2 exchanges between ecosystem and the atmosphere are essential to achieve a better understanding of the role of terrestrial ecosystems in determining atmospheric CO_2 concentrations, the ecosystem's contribution to GHG emissions, and global change.

1.3.1 Direct measurements

Ecosystem-atmosphere energy and CO_2 exchange on short time-scales can be measured using micrometeorological techniques, of which Bowen ratio/energy balance (BREB) and eddy-covariance (EC) are the most widely used (Jones, 1983; Rosenberg et al., 1983; Dabberdt et al., 1993; Baldocchi et al., 1988; IPCC, 2001). BREB is an indirect approach wherein sensible heat H, latent heat (LE) and CO_2 fluxes are calculated from measurements of temperature, and vapor and CO_2 concentration gradients, assuming the equality of turbulent diffusivity for water vapor (K_v), heat (K_h) and CO_2 (K_c) (Rosenberg et al., 1983). The most direct method available for estimating energy and CO_2 fluxes above a canopy is the eddy covariance method proposed by Swinbank (1951), which measures H, LE and CO_2 fluxes by correlating fluctuations of vertical wind speed with fluctuation of temperature and vapor density, respectively.

Through BREB and EC methods, many successful measurements of H, LE and CO_2 fluxes have been achieved over different ecosystems, such as soybean (Baldocchi et al., 1981b), forest (Denmead et al., 1993; Janssens et al., 2001); bare soil (Dugas, 1993), wheat (Dugas et al., 1991; Pruger et al., 1997; Tanner, 1960; Verma and Rosenberg, 1975); maize (McGinn and King, 1990; Steduto and Hsiao, 1998), Alfalfa

(McGinn and King, 1990; Todd et al., 2000), barley (McGinn and Akinremi, 2000); grassland (Blad and Rosenberg, 1974; Dugas et al., 1999; Angell et al., 2001), and sorghum (Dugas et al., 1999).

The carbon density of vegetation and soils has been measured in numerous ecological field studies that have been aggregated to a global scale to assess carbon stocks and NPP (Atjay et al., 1979; Olson et al., 1983; IPCC, 2001). The annual integral of the measured CO_2 exchange is approximately equivalent to NEP (Wofsy et al., 1993; Goulden et. al, 1996; Aubinet et al., 2000). This innovation has led to the establishment of a rapidly expanding network of long-term monitoring sites (FLUXNET) with many sites now operating for several years, improving the understanding of the physiological and ecological processes that control NEP (Valentini et al., 2000). Current flux measurement techniques typically integrate processes at a scale less than 1 km^2. Detailed discussion on measurement methods can be found in the **introduction** of Chapter 2.

1.3.2 Modeling methods

Modeling provides alternative effective ways to study energy and carbon exchange in any ecosystem when the direct measurements are not available. Modelling is considered important because it provides the opportunities to test future scenarios, to separate various component processes and to study their interactions, and its results can be used as a reference for measurements in the field (Ehleringer and Field, 1993; Van Gardingen et al., 1997; Cernusca et al., 1998). Moreover, a simulation model may provide a further framework for analysis of the effect of climate change on energy balance, crop growth, carbon dioxide exchange, annual carbon balance, and soil carbon dynamics.

Models can be generally classified into two types: statistical or empirical models and process-based models. Statistical or empirical models usually employ statistical regression with specific climatic parameters such as temperature, soil moisture, radiation, precipitation, etc. (Rajvanshi and Gupta, 1986; Grahammer et al., 1991; Bridgham and Richardson, 1992; Peterjohn et al., 1994; Thierron and Laudelout, 1996). However, the lack of physiological and biological bases in statistical and empirical

models, makes it difficult to explain processes that take place in the ecosystem. Therefore, their applications are greatly restricted to the conditions under which they are parameterized.

Another type of model, which is more useful and powerful than the statistical and empirical model, is the process-based model. Since this type of models is built based on the physiological and biological theories that control the component processes in the ecosystem, such as energy exchange, carbon fixation, carbon respiration, evapotranspiration, nutrient uptake, crop growth, etc., it is extensively used in ecosystem studies, such as plant growth (Goudriaan, 1977; Penning de Vries and Laar, 1982; Penning de Vries et al., 1989); photosynthesis (de Wit et al., 1978; Farquhar et al., 1980); stomatal behavior (Ball et al., 1987); energy exchange (Grant et al., 1999); water balance and transpiration (Stroosnijder, 1982; Stewart and Gay, 1989); microbial decomposition and soil respiration (Juma and Paul, 1981; Grant, 1994; Grant and Rochette, 1994); nutrient uptake (Barber and Cushman, 1981; Keulen and Seligman, 1987); carbon sequestration and soil carbon dynamics (Grant et al., 2001); climate change (Grant et al., 1999). A detailed discussion on modeling methods can be found in the **introduction** of **Chapter 3.**

1.4 Main study contents and objectives

1.4.1 Main study contents

The main objectives of this study are to study the energy and CO_2 exchange, and to predict long-term soil carbon dynamics over a barley-fallow rotation in Lethbridge, southern Alberta. To achieve this objective, both direct field measurements and ecosystem modeling, two commonly used methods in the energy and CO_2 exchange studies in any ecosystem, were used. Modeled results were test against field measurements to examine the energy and CO_2 exchange variation in the growing seasons of 1996 and 1998.

A general introduction, with an emphasis on discussion of possible factors influencing the energy and CO_2 transfers in agricultural ecosystems, followed by a brief

introduction to the commonly-used methods in energy and CO_2 flux studies, was given in this chapter. The methods, Bowen ratio and ecosystem modeling, adopted in this study were introduced in Chapter 2 and Chapter 3, respectively. Results were given in Chapter 4 and Chapter 5. In Chapter 4, the accuracy of modeled energy fluxes was first tested with the Bowen Ratio measurements. The variation of energy exchange was then discusses followed by a discussion. Chapter 5, following the same format as Chapter 4, dealt with the carbon dioxide exchange, annual carbon balance, and long-term soil carbon dynamics. General conclusions from this study and some future considerations were given in Chapter 6.

1.4.2 Main study objectives

1. Measure energy and CO_2 exchange over a barley-fallow rotation;

2. Simulate energy and CO_2 exchange over a barley-fallow rotation through *ecosys*, and test the modelled results using the field measurements;

3. Examine the energy and CO_2 exchange variations and the corresponding environmental factors that control these variations;

4. Predict long-term soil carbon dynamics under current climate and climate change conditions using the model *ecosys*, and improve the understanding of factors controlling the long-term soil carbon of this semiarid ecosystem.

References

Akinremi, O.O., McGinn, S.M., McLean H.D.J., 1999. Effects of soil temperature and moisture on soil respiration in barley and fallow plots. Can. J. Soil Sci. 79, 5-13.

Amthor, J.S., 1989. Respiration and crop productivity. Springer-Verlag, New York.

Anderson, D., Grant, R.F., Rolfe, C., 2001. Climate of change: taking credit, Canada and the role of sinks in international climate negotiations. David Suzuki Foundation.

Angell, R.F., Svejcar, T., Bates, J., Saliendra, N.Z., Johnson, D.A., 2001. Bowen ratio and closed chamber carbon dioxide flux measurements over sagebrush steppe vegetation. Agric. For. Meteorol. 108, 153-161.

Atjay, G.L., Ketner, P., and Duvigneaud, P., 1979. Terrestrial primary productivity and phytomass. In: Bolin, B., Degens, E.T., Kempe, S., and Ketner, P. (eds.), The Global Carbon Cycle. John Wiley & Sons, Chichester, 129-181.

Aubinet, M., Grelle, A., Ibrom, A., Rannik, U., Moncrieff, J., Foken, T., Kowalski, A.S., Martin, P.H., Berbigier, P., Bernhofer, C., Clement, R., Elbers, J., Granier, A., Grunwald, T., Morgenstern, K., Pilegaard, K., Rebmann, C., Snijders, W., Valentini, R., and Vesala, T., 2000. Estimates of the annual net carbon and water exchange of forests: The EUROFLUX methodology. Advances in Ecological Research 30, 113-175.

Baldocchi, D.D., Hicks, B.B., Meyers, T.P., 1988. Measuring biosphere-atmosphere exchanges of biologically related gases with micrometeorological methods. Ecology 69, 1331-1340.

Baldocchi, D.D., Verma, S.B., and Rosenberg, N.J., 1981a. Mass and energy exchange of a soybean canopy under various environmental regimes. Agron. J. 73, 706-710.

Baldocchi, D.D., Verma, S.B., and Rosenberg, N.J., 1981b. Environmental effects on the CO_2 flux and CO_2-water flux ratio of Alfalfa. Agric. Meteorol. 24, 175-184.

Ball, J.T., Woodrow, I.E., Berry, J.A., 1987. A model predicting stomatal conductance and its contributions to the control of photosynthesis under different environmental conditions. In: Biggens, J. (Ed.), Progress in Photosynthesis Research, Vol. IV, Martinus Nijhoff, Dordrecht, The Netherlands, 221-225.

Barber, S.A., Cushman, J.H., 1981. Nitrogen uptake model for agronomic crops. In: Iskandar, I.K. (ed.), Modeling waste water renovation-land treatment. Wiley-Interscience, New York.

Basra, A.S. (Ed.), 2001. Crop responses and adaptation to temperature stress. The Haworth Press, Inc., New York.

Beare, M.H., P.F. Hendrix, and D.C. Coleman, 1994. Water-stable aggregates and organic matter fractions in conventional- and no-tillage soils. Soil Sci. Soc. Am. J. 58, 777-786.

Biscoe, P.V., Scott, R.K., and Monteith, J.L., 1975. Barley and its environment III. Carbon budget of the stand. J. Appl. Ecol. 12, 269-291.

Blad, B.L., Rosenberg, N.J., 1974. Lysimetric calibration of the Bowen ratio/energy balance method for evapotranspiration estimation in the central Great Plains. J. Appl. Meteorol. 13, 227-236.

Blevins, R.L., Frye, W.W., 1993. Conservation tillage: An ecological approach to soil management. Adv. Agron. 51, 33-78.

Blevins, R.L., Thomas, G.W., Cornelius, P.L., 1977. Influence of no-tillage and nitrogen fertilization on certain soil properties after five years of continuous corn. Agron. J. 69, 383-386.

Boone, R.D., K.J. Nadelhoffer, J.D. Canary, and J.P. Kaye, 1998: Roots exert a strong influence on the temperature sensitivity of soil respiration. Nature 396, 570–572.

Bouwman, A.F., 1990. Soils and the greenhouse effect. John Wiley and Sons, Chichester.

Boyer, J.S., 1970. Differing sensitivity of photosynthesis to low leaf water potentials in corn and soybean. Plant Physiol. 46, 236-239.

Bremer, E., Janzen, H.H., Johnson, A.M., 1994. Sensitivity of total, light fraction and mineralizable matter to management practices in a Lethbridge soil. Can. J. Soil Sci. 74, 131-138.

Bridgham, S.D., Richardson, C.J., 1992. Mechanisms controlling soil respiration (CO_2 and NH_4) in southern peatlands. Soil Biol. Biochem. 27, 279-286.

Brown, K.W., Thomas, J.C., 1980. The influence of water stress preconditioning on dark respiration. Physiologia Plantarum 49, 205-209.

Bruce, J.P., Frome, M., Haites, E., Janzen, H., Lal, R., Paustian, K., 1999. Carbon sequestration in soils. J. Soil and Water Conserv., 382-389.

Campbell, C.A. McConkey, B.G., Zentner, R.P., Sellers, F., Curtin, D., 1996. Long-term effects of tillage and crop rotations on soil organic C and total N in a clay soil in southwest Saskatchewan. Can. J. Soil Sci. 76, 395-401.

Campbell, C.A., Biederbeck, V.O., Zentner, R.P., Lafond, G.P., 1991. Effects of crop rotations and cultural practices on soil organic matter, microbial biomass and respiration on a thin Black Chernozem. Can. J. Soil Sci. 71, 363-376.

Campbell, C.A., De Jong, R., and Zentner, P., 1984. Effect of cropping, summer fallow and fertilizer nitrogen on nitrate-nitrogen lost by leaching on a brown chernozemic loam. Can. J. Soil Sci. 64, 61-74.

Cernusca, A., Bahn, M., Chemini, C., Graber, W., Siegwolf, R., Tappeiner, U., Tenhunen, J., 1998. ECOMONT: a combined approach of field measurements and process-based modelling for assessing effects of land-use changes in mountain landscape. Ecol. Model. 113, 167-178.

Crawford, R.M.M., Huxter, T.J., 1977. Root growth and carbohydrate metabolism at low temperature. J. Exp. Bot. 28, 917-925.

Curtis, P.S., 1996. A meta-analysis of leaf gas exchange and nitrogen in trees grown under elevated carbon dioxide. Plant Cell and Environment 19, 127-137.

Da Costa, J.M.N., Rosenberg, N.J., Verma, S.B., 1986. Joint influence of air temperature and soil moisture on CO_2 release by a soybean crop. Agric. For. Meteorol. 37, 219-227.

Dabberdt, W.F., Lenschow, D.H., Horst, T.W., Zimmerman, P.R., Oncley, S.P., Delany, A.C., 1993. Atmosphere-surface exchange measurements. Science 260, 1472-1481.

Davidson, E.A., Belk, E., Boone, R.D., 1998. Soil water content and temperature as independent to confounded factors controlling soil respiration in a temperate mixed hardwood forest. Global Change Biol. 4, 217-227.

de Wit, C.T., 1978. Simulation of assimilation, respiration and transpiration of crops. John Wiley & Sons, New York.

Denmead, O.T., Dunin, F.X., Wong, S.C., Greenwood, E.A.N., 1993. Measuring water use efficiency of eucalypt trees with chambers and micrometeorological techniques. J. Hydrol. 150, 649-664.

Doran, J.W. 1980. Soil microbial and biochemical changes associated with reduced tillage. Soil. Sci. Soc. Am. J. 44, 765-771.

Doran, J.W., Smith, M.S., 1987. Organic matter management and utilization of soil and fertilizer nutrients. In: Mortvedt, J.J., Buxton, D.R., Mickelson, S.H., (eds.), Soil fertility and organic matter as critical components of production systems. SSSA Special Publication No. 19, 53-72.

Dugas, W.A., 1993. Micrometeorological and chamber measurements of CO_2 flux from bare soil. Agric. For. Meteorol. 67, 115-128.

Dugas, W.A., Fritschen, L.J., Gay, L.W., Held, A.A., Matthias, A.D., Reicosky, D.C., Steduto, P., Steiner, J.L., 1991. Bowen ratio, eddy correlation, and portable chamber measurements of sensible and latent heat flux over irrigated spring wheat. Agric. For. Meteorol. 56, 1-20.

Dugas, W.A., Heuer, M.L., Mayeux, H.S., 1999. Carbon dioxide fluxes over bermudagrass, native prairie and sorghum. Agric. For. Meteorol. 93, 121-139.

Ehleringer, J.R., Field, C.B., (Eds.), 1993. Scaling photosynthesis processes, leaf to global. Academic Press. San Diego, USA.

Elliott, E.T., 1986. Aggregate structure and carbon, nitrogen, and phosphorus in native and cultivated soils. Soil Sci. Soc. Am. J. 50, 627–633.

Farquhar, G.D., von Caemmerer, S., and Berry, J.A., 1980. A biological model of photosynthetic CO_2 assimilation in leaves of C_3 species. Planta 149, 78-90.

France, J., Thornley, J.H.M., 1984. Mathematical models in agriculture. Butterworths, London.

Glinski, J., Stepniewski, W., 1985. Soil aeration and its role for plant. CRC Press, pp. 176-178.

Goudriaan, J., 1977. Crop micrometeorology: a simulation study. Centre for Agriculture Publishing and Documentation, Wageningen, the Netherlands.

Goulden, M.L., Munger, J.W., Fan, S.M., Daube, B.C., and Wofsy, S.C., 1996. Exchange of carbon dioxide by a deciduous forest: Response to interannual climate variability. Science 271, 1576-1578.

Grahammer, K., Jawson, M.D., Skopp, J., 1991. Day and night soil respiration from a grassland. Soil Biol. Biochem. 23, 77-81.

Grant, R.F., 1994. Simulation of ecological controls on nitrification. Soil Biol. Biochem. 26, 305-315.

Grant, R.F., Black, T.A., den Hartog, G., Berry, J.A., Neumann, H.H., Blanken, P.D., Yang P.C., Russell, C., Nalder, I.A., 1999. Diurnal and annual exchanges of mass and energy between an aspen-hazelnut forest and the atmosphere: Testing the

mathematical model *Ecosys* with data from the BOREAS experiment. J. Geophys. Res. 104, 27699-27717.

Grant, R.F., Juma, N.G., Robertson, J.A., Izaurralde, R.C., McGill, W.B., 2001. Long-term changes in soil carbon under different fertilizer, manure, and rotation: testing the mathematical model *ecosys* with data from the Breton plots. Soil Sci. Soc. Am. J. 65, 205-214.

Grant, R.F., Rochette, P., 1994. Soil microbial respiration at different water potentials and temperatures: theory and mathematical modeling. Soil Sci. Soc. Am. J. 58, 1681-1690.

Hallgren, J.E., Sundbom, E., and Strand, M., 1982. Photosynthetic responses to low temperature in *Betula pubescens* and *Betula totuosa*. *Physiol*. Plant. 54, 275-282.

Havlin, J.L., Kissel, D.E., Maddux, L.D., Claasen, M.M. and Long, J.H., 1990. Crop rotation and tillage effects on soil organic carbon and nitrogen. Soil Sci. Soc. Am. J. 54, 448-452.

Heath, O.V.S., Russell, J., 1954. Studies in stomatal behavior. VI. An investigation of the light responses of wheat stomata with the attempted elimination of control by the mesophyll. J. Exp. Bot. 5, 1-15.

Hofstra, G., Hesketh, J.D., 1969. Effects of temperature on gas exchange of leaves in the light and dark. Planta 85, 228-237.

Houghton, R.A. J.L. Hackler, and K.T. Lawrence, 1999. The U.S. carbon budget: contributions from land-use change. Science 285, 574–578.

Houghton, R.A., 1991. Tropical deforestation and atmospheric carbon dioxide. Climate Change 19, 99–118.

Houghton, R.A., 1999. The annual net flux of carbon to the atmosphere from changes in land use 1850-1990. Tellus 52B, 298-313.

Houghton, R.A., 2000. A new estimate of global sources and sinks of carbon from land-use change. EOS 81, supplements 281.

Houghton, R.A., D.L. Skole, C.A. Nobre, J.L. Hackler, K.T. Lawrence, and W.H. Chomentowski, 2000. Annual fluxes of carbon from deforestation and regrowth in the Brazilian Amazon. Nature 403, 301–304.

Hungate, B.A., Holland, E.A., Jackson, R.B., Chapin, F.S., Mooney, H.A., Field, C.B., 1997. The fate of carbon in grasslands under carbon dioxide enrichment. Nature 388, 576-579.

IPCC, 2001. IPCC Third Assessment Report - Climate Change 2001: The Scientific Basis. http://www.ipcc.ch.

Janssens, I.A., Kowalski, A.S., Ceulemans, R., 2001. Forest floor CO_2 fluxes estimated by eddy covariance and chamber-based model. Agric. For. Meteorol. 106, 61-69.

Janzen, H.H., 1987. Soil organic matter characteristics after long-term cropping to various spring wheat rotation. Can. J. Soil. Sci. 67, 845-856.

Janzen, H.H., Campbell, C.A., Gregorich, E.G., Ellert, B.H., 1998. Soil carbon dynamics in Canadian agroecosystems. In: Lal, R., Kimble, J.M., Follett, R.F., and Stewart, B.A.(eds.), Soil processes and the carbon cycle. CRC Press, New York.

Jones, H.G., 1983. Plant and microclimate: A quantitative approach to environmental plant physiology. Cambridge University Press. Cambridge.

Juma, N.G., Paul, E.A., 1981. Use of tracers and computer simulation techniques to assess mineralization and immobilization of soil nitrogen. In: Simulation of nitrogen behavior of soil-plant system- papers of a workshop models for the behavior of nitrogen in soil and uptake by plant. Wageningen, the Netherlands.

Kase, M., Catsky, J., 1984. Maintenance and growth components of dark respiration rate in leaves of C_3 and C_4 plants as affected by leaf temperature. Biologia Plantarum 26, 461-470.

Kern, J., Johnson, M., 1993. Conservation tillage impacts on national soil and atmospheric carbon levels. Soil Sci. Soc. Am. J. 57, 200–210.

Keulen, H. van, Seligman, N.G., 1987. Simulation of water use, nitrogen nutrition and growth of a spring wheat crop. Simulation Monographs. Pudoc, Wageningen.

Kirschbaum M.U.F., 1995. The temperature dependence of soil organic matter decomposition, and the effect of global warming on soil organic C storage. Soil Biol. Biochem. 27, 753-760.

Koch, G.W., Mooney, H.A., 1996. Response of terrestrial ecosystems to elevated CO_2: a synthesis and summary. In: Kock, G.W., Mooney, H.A. (eds.), Carbon Dioxide and Terrestrial Ecosystems. Academic Press, San Diego, 415-429.

Kuo, S., Sainju, U.M., Jellum, E.J., 1997. Winter cover crop effects on soil organic carbon and carbohydrate in soil. Soil Sci. Soc. Am. J. 61, 145-152.

Lal, R., 1976. No-tillage effects on soil properties under different crops in western Nigeria. Soil Sci. Soc. Am. Proc. 40, 762-768.

Lal, R., Kimble, J.M., Follett, R.F., and Stewart, B.A.(eds.), 1998. Management of carbon sequestration in soil. CRC Press, New York. 1-10.

Larcher, W., 1983. Effects of low temperature stress and frost injury on plant productivity. In: C.B. Johnson (Editor), Physiological Processes Limiting Plant Productivity. Butterworths, London, 253-269.

Larcher, W., 1995. Physiological Plant Ecology. Springer, Austria.

Lee, J., Phillips, D., Liu, R., 1993. The effect of trends in tillage practices on erosion and carbon content of soils in the US corn belt. Water, Air, and Soil Pollution, 70, 389–401.

Lee, S.S., Estes, G.O., 1982. Corn physiology in short season and low temperature environments. Agron. J. 74, 325-331.

Lemon, E.R., 1983. CO_2 and plants. The response of plants to rising levels of atmospheric carbon dioxide. AAAS Selected Symposium Series 84, Westview Press, Washington.

Lloyd, J., Farquhar, G.D., 1996. The CO_2 dependence of photosynthesis, plant growth responses to elevated atmospheric CO_2 concentrations, and their interaction with soil nutrient status. I. General principles and forest ecosystems. Functional Ecology 10, 4-32.

Lloyd, J., Taylor, J.A., 1994. On the temperature dependence of soil respiration. Funct. Ecol. 8, 315-323.

Loftfield, J.V.G., 1921. The behaviour of stomata. Publ. Carnegie Inst., Wash. Publ. No. 314, 1-104.

Long, S.P., 1983. C_4 photosynthesis at low temperature. Plant Cell Environ. 6, 345-363.

Long, S.P., East, T.M., and Baker, N.R., 1983. Chilling damage to photosynthesis in young *Zea mays*. I. Effects of light and temperature variation on photosynthetic CO_2 assimilation. J. Exp. Bot. 34, 177-188.

Losch, R., 1977. Responses of stomata to environmental factors-experiments with isolated epidermal strips of Polypodium vulgare. 1. Temperature and humidity. Oecologia 29, 85-97

Ludwig, L.J., Saeki, T., Evans, L.T., 1965. Photosynthesis in artificial communities of cotton plants in relation to leaf area. I. Experiments with progressive defoliation of mature plants. Australian Journal of Biological Sciences 18, 1103-1118.

Luken, J.O., Billings, W.D., 1985. The influence of microtopographic heterogeneity on carbon dioxide efflux from a subartic bog. Holarct. Ecol. 8, 306-312.

Mansfield, T.A., 1965. Stomatal opening in high temperature in darkness. J. Exp. Bot. 16, 721-731.

Mansfield, T.A., and Heath, O.V.S., 1963. Studies in stomatal behaviour. IX. Photoperiodic effects on rhythmic phenomena in Xanthium pennsylvanicum. J. Exp. Bot. 15, 334-352.

Mansfield, T.A., Heath, O.V.S., 1964. Studies in stomatal behaviour. X. An investigation of responses to low intensity illumination and temperature in Xanthium pennsylvanicum. J. Exp. Bot. 15, 114-124.

Martin, E.S., and Meidner, H., 1971. Endogenous stomatal movements in Tradescantia virginiana. New Phytol. 70, 923-928.

Martin, E.S., and Stevens, R.A., 1979. Circadian rhythms in stomatal movements. In: Sen, D.N. (ed.), Structure, Function and Ecology of Stomata. Bishen Singh and Mahendra Pal Singh, Dehra Dun, India.

McCree, K.J., 1974. Equations for the rate of dark respiration of white clover and grain sorghum, as functions of dry weight, photosynthetic rate, and temperature. Crop Sci. 14, 509-514.

McGinn, S.M. and Akinremi, O.O., 2000. Carbon dioxide balance of a crop-fallow rotation in western Canada. Can. J. Soil Sci. 81, 121-127.

McGinn, S.M., and King, K.M., 1990. Simultaneous measurements of heat, water vapor and CO_2 fluxes above alfalfa and maize. Agric. For. Meteorol. 49, 331-349.

Meidner, H., Heath, O.V.S., 1959. Stomatal responses to temperature and carbon dioxide concentration in *Allium cepa* L. and their relevance to midday closure. J. Exp. Bot. 10, 206-219.

Monreal, C.M., Zentner, R.P., and Robertson, J.A., 1995. The influence of management on soil loss and yield of wheat in Chernozemic and Luvisolic soils. Can. J. Soil Sci. 75, 567-574.

Monteith, J.L., Szeicz, G. and Yabuki, K., 1964. Crop photosynthesis and the flux of carbon dioxide below the canopy. J. Appl. Ecol. 1, 321-337.

Moss, D.N., 1965. Capture of radiant energy in plants. Agricultural Meteorology (P.E. Waggoner, ed.), Chapter 5, Meteorol. Monogr. 6(28): 90-108. Am. Meteorol. Soc., Boston.

Neales, T.F., 1975. The gas exchange patterns of CAM plants in The environmental and Biological Control of Photosynthesis (Ed. R. Marcelle). Junk, The Hague.

Nevins D.J., Loomis, R.S., 1970. A method for determining net photosynthesis and transpiration of plant leaves. Crop Sci. 10, 3-6.

Norman, J.M., Garcia, R., and Verma, S.B., 1992. Soil surface CO_2 flux and the carbon budget of a grassland. J. Geophys. Res. 97, 18845-18853.

Oberbauer, S.F., Tenhunen, J.D., Reynolds, J.F., 1991. Environmental effects on CO_2 efflux from water track and tussock tundra in artic Alaska. U.S.A. Artc. Alp. Res. 23, 162-169.

Olson, J.S., Watts, J.A., and Allison, L.J., 1983. Carbon in live vegetation of major world ecosystems. Oak Ridge, Tennessee: Oak Ridge National Laboratory. ORNL-5862.

Oquist, G., 1983. Effects of low temperature on photosynthesis. Plant Cell Environ. 6, 281-300

Paustian, K., Andren, O., Janzen, H., Lal, R., Smith, P., Tian, G., Tiessen, H., van Noordwijk, M., Woomer, P., 1997. Agricultural soil as a C sink to offset CO_2 emission. Soil Use and Management 13, 230-224.

Penning de Vries, F.W.T., Laar, H.H. van (eds.), 1982. Simulation of plant growth and crop production. Simulation Monographs. Pudoc Wageningen.

Penning de Vries, F.W.T., Jansen, D.M., ten Berge, H.F.M., Bakema, A., 1989. Simulation of ecophysiological processes of growth in several annual crops. Pudoc Wageningen.

Peterjohn, W.T., Melillo, J.M., Steudler, P.A., Newkirk, K.M., Bowles, F.P., Aber, J.D., 1994. Response of trace gas fluxes and N availability to experimentally elevated soil temperature. Ecol. Appl. 4, 617-625.

Pittendrigh, L.S., 1954. On the temperature independence in the clock system controlling emergence time in Drosophila. Proc. Natl. Acad. Sci., USA, 40, 1018.

Potvin, C., 1985. Amelioration of chilling effects by CO_2 enrichment. Physiol. Veg. 23, 345-353.

Potvin, C., 1988. Differences between the effects of partial and whole plant chilling on carbon translocation of a C_4 grass. Plant Cell Environ. 11, 51-54.

Potvin, C., Strain, B.R., and Goeschl, J.D., 1985. Low light temperature effect on photosynthate translocation of two C_4 grasses. Oecologia (Berlin) 67, 305-309.

Pruger, J.H., Hatfield, J.L., Ase, J.K., Pikul, J.L., 1997. Bowen ratio comparisons with lysimeter evapotranspiration. Agron. J. 89, 730-736.

Raison, J. K., and Lyons, J. M., 1986. Chilling injury: a plea for uniform terminology. Plant Cell Environ. 9, 685-686.

Raison, J.K., 1980. Effect of low temperature on respiration. In: The Biochemistry of Plants. Vol. 2, Metabolism and Respiration (ed. D.D. Davies). Academic Press, New York.

Rajvanshi, R., Gupta, S.R., 1986. Soil respiration and carbon balance in a tropical Dalbergia sissoo forest ecosystem. Flora 178, 251-260.

Raschke, K., 1979. Movements of stomata. In: Haupt, W. and Feinlieb, M.E. (eds.), Encyclopedia of plant physiology. Vol. 7, Physiology of movements. Springer-Verlag, Berlin.

Regehr, D.L., F.A. Bazzaz, and W.R. Boggess, 1975. Photosynthesis, transpiration and leaf conductance of *Populus deltoides* in relation to flooding and drought. Photosynthetica 9, 52-61.

Rice, J.R., Eastin, J.D., 1986. Grain sorghum root response to water and temperature during reproductive development. Crop Sci. 26, 547-551.

Rochette, P., Desjardins, R.L., Gregorich, E.C, Pattey, E., and Lessard, R., 1992. Soil respiration in barley (*Hodeum vulgare* L.) and fallow fields. Can. J. Soil Sci. 72, 591-603.

Rochette, P., Desjardins, R.L., Pattey, E., and Lessard, R., 1995. Crop net carbon dioxide exchange rate and radiation use efficiency in soybean. Agron. J. 87, 22-28.

Rosenberg, N.J., Blad, B.L., and Verma, S.B., 1983. Microclimate, the biological environment. John Wiley & Sons, Inc. New York.

Sarmiento, J.L., and E.T. Sundquist, 1992. Revised budget for the oceanic uptake of anthropogenic carbon- dioxide. Nature 356, 589-593.

Savage, K., Moore, T.R., Grill, P.M., 1997. Methane and carbon dioxide exchanges between the atmosphere and northern boreal forest soils. J. Geophys. 102, 279-288.

Schlentner, R.E., Van Cleve, K., 1985. Relationship between CO_2 evolution from soil, substrate temperature, and substrate moisture in four mature forest types in interior Alske. Can. J. For. Res. 15, 97-106.

Schlesinger, W.H., Andrews, J.A., 2000. Soil respiration and the global carbon cycle. Biogeochemistry 48, 7-20.

Schlesinger, W.H., J.M. Melack, 1981. Transport of organic-carbon in the worlds rivers. Tellus 33, 172-187.

Schulze, E.D., and M. Heimann, 1998. Carbon and water exchange of terrestrial ecosystems. In: Galloway, J.N. and J. Melillo (eds.), Asian change in the context of global change. Cambridge University Press, Cambridge.

Schulze, E.D., Lange, O.L., Kappen, L., Buschbom, U., Evanari, M., 1973. Stomatal responses to changes in temperature at increasing water-stress. Planta 110, 29-42.

Singh, J.S., Gupta, S.R., 1977. Plant decomposition and soil respiration in terrestrial ecosystem. Bot. Rev. 43, 449-528.

Stalfelt, M.G., 1962. The effect of temperature on opening of stomatal cells. Physiol. Plant. 10, 752-792.

Statistical Handbook, 1999. Canadian Grains Industry, Winnipeg, MB.

Steduto, P., Hsiao, T.C., 1998. Maize canopies under two soil water regions - IV. Validity of Bowen ratio - energy balance technique for measuring water vapor and carbon dioxide fluxes at 5-min intervals. Agric. For. Meteorol. 89, 215-228.

Stewart, J.B., Gay, L.W., 1989. Preliminary modeling of transpiration from the FIFE site in Kansas. Agric. Forest Meteorol. 48, 305-315

Stroosnijder, L., 1982. Simulation of the soil water balance. In: Penning de Vries F.W.T., van Laar, H.H. (Eds.). Simulation of plant growth and crop production. Centre for Agriculture Publishing and Documentation, Wageningen, 175-193.

Swinbank, W.C., 1951. The measurement of the vertical transfer of heat and water vapor by eddies in the lower atmosphere. J. Meteorol. 8, 135-145.

Tanner, C.B., 1960. Energy balance approach to evapotranspiration from crops. Soil Sci. Soc. Am. Proc. 24, 1-9.

Tenhunen, J.D., Lange, O.L., Braun, M., Meyer, A., Losch, R., and Pereira, J.S., 1980. Midday stomatal closure in Arbunus unedo leaves in a natural macchia and under simulated habitat conditions in an environmental chamber. Oecologia 47, 365-367.

Tesarova, M., Gloser, J., 1976. Total CO_2 output from alluvial soils with two types of grassland communities. Pedobiologia 16, 364-372.

Thierron, V., Laudelout, H., 1996. Contribution of root respiration to total CO_2 efflux from the soil of a deciduous forest. Can. J. For. Res. 26, 1142-1148.

Thomas, M.D., and Hill, G.R., 1949. Photosynthesis under field conditions. Photosynthesis in plants. In: J. Frank and W.E. Loomis (eds.), Plant Physiol. Monogr. Iowa State University Press, Ames, 19-52.

Tisdall, J.M. and J.M. Oades, 1982. Organic matter and water-stable aggregates in soils. J. Soil Sci. 33, 141.

Todd, R.W., Evett, S.R., Howell, T.A., 2000. The Bowen ratio-energy method for estimating latent heat flux of irrigated alfalfa evaluated in a semi-arid, advective environment. Agric. For. Meteorol. 103, 335-348.

Valentini, R., Matteucci, G., Dolman, A.J., Schulze, E.D., Rebmann, C., Moors, E.J., Granier, A., Gross, P., Jensen, N.O., Pilegaard, K., Lindroth, A., Grelle, A., Bernhofer, C., Grunwald, T., Aubinet, M., Ceulemans, R., Kowalski, A.S., Vesala, T., Rannik, U., Berbigier, P., Loustau, D., Guomundsson, J., Thorgeirsson, H., Ibrom, A., Morgenstern, K., Clement, R., Moncrieff, J., Montagnani, L., Minerbi, S., and Jarvis, P.G., 2000. Respiration as the main determinant of carbon balance in European forests. Nature 404, 861-865.

Van Gardingen, P.R., Foody, G.M., Curran, P.J., (Eds.), 1997. Scaling-up: From Cell to Landscape. Society of Experimental Biology Seminar Series 63. Cambridge University Press, Cambridge.

Verma, S.B., Rosenberg, N.J., 1975. Accuracy of lysimetric, energy balance, and stability corrected aerodynamic methods of estimating above-canopy flux of CO_2. Agron. J. 67, 699-704.

Wand, S.J.E., Midgley, G.F., Jones, M.H., Curtis, P.S., 1999. Response of wild C_4 and C_3 grass (Poaceae) species to elevated atmospheric CO_2 concentration: a meta-analytic test of current theories and perceptions. Global Change Biology 5, 723-741.

Waring, R.H., J.J. Landsberg, and M. Williams, 1998. Net primary production of forests: a constant fraction of gross primary production? Tree Physiology 18, 129-134.

Watson, R.T., Rhode, H., Oeschger, H., Siegenthaler, U., 1990. Greenhouse gases and aerosols. In: Houghton et al., (ed.), Climate change: The IPCC scientific assessment. Cambridge Univ. Press, Cambridge, UK.

Watts, W.R., and Neilson, R.E., 1978. Photosynthesis in Sitka spruce (Picea sitchensis [Bong.] Carr.) VIII. Measurements of stomatal conductance and $^{14}CO_2$ uptake in controlled environments. J. Appl. Ecol. 15, 245-255.

Willmer, C.M., 1980. Some characteristics of phosphoenolpyruvate carboxylase activity from leaf epidermal tissue in relation to stomatal functioning. New Phytol. 84, 593-602.

Willmer, C.M., 1983. Stomata. Longman, New York.

Wofsy, S.C., Goulden, M.L., Munger, J.W., Fan, S.M., Bakwin, P.S., Daube, B.C., Bassow, S.L., Bazzaz, F.A., 1993. Net exchange of CO_2 in a mid-latitude forest. Science 260, 1314-1317.

Chapter 2 Field experiment

2.1 Introduction

Measurements of latent heat (LE), sensible heat (H) and CO_2 flux (Fc) density in agricultural fields are useful for understanding physical and biological processes in agro-ecosystems, and for field water management, crop planting management, carbon sequestration strategies, and for global change monitoring. These measurements are also important in calibrating and validating various soil-plant-atmosphere models of crop growth, water balance, energy balance and carbon balance etc..

Two widely-used micrometeorological techniques to measure energy fluxes are Bowen ratio/energy balance (BREB) and eddy-covariance (EC) (Dabberdt et al., 1993). EC provides a direct measurement of sensible and latent heat fluxes by correlating fluctuations of vertical wind speed with fluctuation of temperature and vapor density, respectively (Swinbank, 1951), whereas BREB is an indirect approach wherein H and LE are calculated from measurements of temperature and vapor density gradients, assuming the equality of turbulent diffusivity for water vapor (K_v) and heat (K_h). The BREB method is not well suited to very rough surfaces (e.g. forest), because vertical velocity fluctuations are large and the vertical gradients of scalars are correspondingly small (Verma, 1990). In such cases, EC is preferred over BREB (Angell et al., 2001).

There are two commonly used approaches for measuring CO_2 fluxes: micrometeorological techniques (both BREB and EC) and chamber methods. The gradient-based BREB method to measure CO_2 flux is again based on the assumption that the turbulent diffusivities of water vapor (K_v), heat (K_h) and CO_2 (K_c) are equal. Many researchers have used the BREB method to measure both energy and CO_2 fluxes (e.g. Baldocchi et al., 1981; Denmead et al., 1993; Dugas, 1993; Dugas et al., 1999; Prueger et al., 1997; Tanner, 1960; Todd et al., 2000; Verma and Rosenberg, 1975). BREB relies on several other assumptions (Fritschen and Simpson, 1989). Transport of heat, water vapor and CO_2 are assumed to be one-dimensional, with no horizontal gradients, and further, the sensors which measure the vertical gradients are assumed to

38

be located within the equilibrium sublayer, i.e. the "fully adjusted" layer to the new boundary conditions (Rosenberg et al., 1983). Fluxes within this layer are also assumed to be constant with height. These assumptions are not usually violated if measurements are made at appropriate height and adequate upwind fetch is present (Angell et al., 2001). Rosenberg et al. (1983) established a requirement for a 100:1 fetch/height-above surface ratio as a rule of thumb. Steduto and Hsiao (1998) concluded that the assumption of one-dimensional transport, which underlies the technique, is justified. However, advection, the transport of energy or mass in the horizontal plane in the downwind direction (Rosenberg et al., 1983) can be present under certain conditions. Sensible heat advection could result in underestimation of latent heat flux, and it was suggested that the underestimation is due to an inequality of K_v and K_h (Blad and Rosenberg, 1974). Further studies by Verma et al. (1978) showed that $K_h > K_v$ when conditions of regional sensible heat advection prevail. There is also possibility of discontinuous data when the Bowen ratio (β) approaches -1, causing the calculation of LE and H to become impossible because they lose their physical meaning. The values $\beta \approx -1$ appear at sunrise and sunset and during precipitation when the direction of temperature gradient changes to be opposite to that of the vapor pressure gradient (Perez et al., 1999). Thus the measurement precision of BREB is of great concern, since errors in estimating LE are propagated in the calculation of CO_2 flux (Sinclair et al., 1975) and can lead to bias. However, Dugas et al. (1999) successfully employed the BREB method to measure CO_2 fluxes over plant canopies, and the validity of the method has been demonstrated in several earlier studies (Dugas et al., 1991; Held et al., 1990; Malek and Bingham, 1993). Its advantages include straight-forward, simple measurements; it requires no information about the aerodynamic characteristics of the surface of interest; it can integrate latent heat flux over large areas (hundreds to thousands of square meters); it can estimate fluxes on fine time scales (less than an hour) (Todd et al., 2000); and it does not disturb the soil environment (Janssens et al., 2001).

Chamber-based methods are the most frequently used to estimate soil CO_2 efflux due to low cost and ease of use (Edwards, 1982; Norman et al., 1992; Fang and Moncrieff, 1996; Goulden and Grill, 1997; Rayment and Jarvis, 1997; Janssens and

Ceulemans, 1998). But these methods are criticized because of spatial variability and the so called "chamber effects" (Mosier, 1990). Chambers may disturb the soil environment and alter CO_2 and pressure gradients, turbulent fluctuations, and air flow. They may thus interfere with both production and transfer of CO_2. Modern chamber systems (Norman et al., 1992, 1997; Fang and Moncrieff, 1996; Iritz et al., 1997; Rayment and Jarvis, 1997; McGinn et al., 1998) have eliminated most of these effects, but mass flow across the soil surface, as well as the motion and pressure of air around and within the chamber still remain problems. However, Held et al. (1990) and Chan et al. (1994) found good agreement between BREB and chamber techniques.

The increase in atmospheric CO_2 concentration is an important forcing parameter of global warming (Intergovernmental Panel on Climate Change 1995). Estimating the magnitude of warming is therefore conditional on accurately estimating global source and sink strengths of atmospheric CO_2. The net CO_2 exchanged between agricultural system and the atmosphere is driven by primary production and soil respiration. The respiration component is a major source of uncertainty (Jensen et al., 1996). Quantifying soil carbon balance by measuring losses due to soil respiration and gains by straw and roots, is critical to the understanding of agriculture's contribution to the global warming and of the processes controlling soil organic matter dynamics (McGinn et al., 1998).

In this study, we used two Bowen ratio systems to measure energy fluxes (net radiation, latent heat and sensible heat) and CO_2 fluxes over a barley-fallow rotation in the growing seasons of 1996 and 1998 in Lethbridge. These measurements were part of the research project "Field Scale Estimates of Carbon Dioxide Exchange in a Fallow-Crop System", which was carried out by Agriculture and Agri-Food Canada, Lethbridge Research Center from 1994 to 2000. These measurements were used to test the modeled results of energy-, water- and carbon fluxes through an ecosystem model *"ecosys"* (Grant et al., 1999, 2001). We used these measured and modeled results to investigate changes of energy-, water- and carbon balance over a barley –fallow system in Lethbridge, southern Alberta.

2.2 Experimental site

The field experiments were conducted in the growing seasons of 1996 and 1998 in two adjacent dryland plots (area 200 m × 200 m each, one for barley, the other for fallow) in Lethbridge, Alberta (49° 42'N, 112° 47'W, elevation 899 m).

2.2.1 Topography

Located in south-west Alberta, Lethbridge is a gently rolling plain that generally slopes down from the Rocky Mountains to the northeast. The original vegetation was grassland with trees in river flood plains and near the foothills where increased rainfall occurs.

2.2.2 Soil

The soils were developed under native vegetations of tall and short grasses, with a high organic matter content, and is classified into Brown or Dark-Brown Chernozems (Agriculture and Agri-Food Canada, 1998). At soil surface layers (0-15 cm), the organic C and N contents are 16.8 g C kg^{-1} and 1.72 g N kg^{-1}, respectively, the pH in water paste is 7.6, and the average bulk density is 1.20 g cm^{-3}. Typically, the soil has a 10- to 15-cm A_p, a 15- to 27-cm B, and a calcareous C horizon (Bremer et al., 1994). The texture of the A horizon is a clay loam with 30% sand, 40% silt, and 30% clay, while B horizon has a clay texture with 28% sand, 30% silt, and 40 % clay. Ground water table is below 10 m.

2.2.3 Climate

The general climate of Southern Alberta is semi-arid continental climate with short, warm summers and long, cold winters. A prominent feature of the climate is the warm Chinook winds that moderate the winter air temperature, but also increase evaporation and soil erosion. The historical temperature extremes on an annual basis in Lethbridge range from +40 to -45°C, and range from +22.5 to -42.2 °C in February, and from +39.1 to 0.0 °C in July. Mean annual air temperature is 5.0°C, and the mean

monthly temperatures for January and July are -8.6°C and 18.0°C, respectively. The frost-free period averages 118 days (Agriculture and Agri-Food Canada, Lethbridge Research Center). Mean annual precipitation is 402 mm, with the greatest amounts of precipitation during May and June (32% falling in May and June). Potential evapotranspiration is 681 mm, resulting in a water deficit of 279 mm. Snow represents about 40% of the annual precipitation, but frequent Chinooks minimize the persistence of snow cover and its benefit for soil moisture replenishment.

2.3 Methods and materials

The project was conducted in 1996 and 1998 in two adjacent dryland plots in Lethbridge where a barley-fallow rotation cropping system was established from 1994. Prior to 1994, the plots were continuously cropped. The two plots then alternated between barley and summer fallow. Each field was 4 ha in area (200 m × 200 m) and the surrounding land was planted to small grain cereals, making for a large homogenous surface in all directions.

2.3.1 Crop management

Table 2.1   Crop planting information and flux measurement period

Year	Planting Date	Harvest Date	Plant density m^{-2}	Period of Bowen ratio measurement
1996	May 15 (DOY136)	Aug. 24 (DOY 237)	240	DOY 187-276
1998	May 10 (DOY130)	Aug. 24 (DOY 236)	240	DOY155-231

DOY: day of the year.

In 1996, barley was sown on May 15 (DOY 136) at a row spacing of 0.2 m with a planting density of 240 plant m^{-2}. It emerged on May 22 (DOY 143) and was harvested on August 24 (DOY 237) (Table 2.1). In 1998, barley was sown on May 10 (DOY 130) with the same planting pacing and planting density as in 1996, and was harvested on

42

August 24 (DOY 237) in 1998. In both years, only grain yields were removed from the field, and crop residues and straw was left in field. No irrigation and fertilizer were applied during the two years.

2.3.2 Soil management

After the crop was harvested in the cropped field, the field was left fallow in the next year, while barley was sown in the previous fallow field. Crop residues and straw were left in the fallow field where they underwent natural decomposition. During the growing season, all green vegetation was eliminated by herbicides in the fallow field. In both years, soils were managed under no tillage. No fertilizer or manure was applied during either growing or fallow seasons of the experimental years.

2.3.3 Bowen Ratio system setup

Two identical Bowen Ratio Systems were set up with one in barley and the other in fallow in the growing seasons of 1996 and 1998, to monitor the gradients of heat and water vapor at the center of each field. The systems were also modified to provide a measurement of CO_2 concentration gradients (McGinn and Akinremi, 2000). In 1996, the Bowen ratio flux measurements were initiated in the field on July 5 (DOY 187), and continued after the barley was harvested till October 2 (DOY 276). In 1998, the Bowen ratio systems were fully operational in the field on June 4 (DOY 155), and flux measurements were terminated on August 19 (DOY 231), 6 days before crop was harvested on August 24 (DOY 236) (Table 2.1, Fig. 2.1, 2.2).

Systematic errors between the two Bowen ratio systems were checked before they were set up in the barley and fallow field. This was done by comparing temperature, vapor and CO_2 gradients measured by the two sets of BREB instruments which were operated adjacent to each other in a field outside the BREB instrumentation laboratory. The Bowen ratio systems were checked and adjusted until the differences of temperature, vapor and CO_2 gradients between the two Bowen ratio systems were less than 5%. They were then installed in the experimental fields. During this testing period, measurements of net radiation, air temperature, vapor pressure etc., by Bowen ratio

systems were also ensured to be comparable to those from the Meteorological Station of Agriculture and Agri-Food Canada, Lethbridge Research Center, which is about 200 m away. Therefore, there was no systematic bias between the two BREB systems.
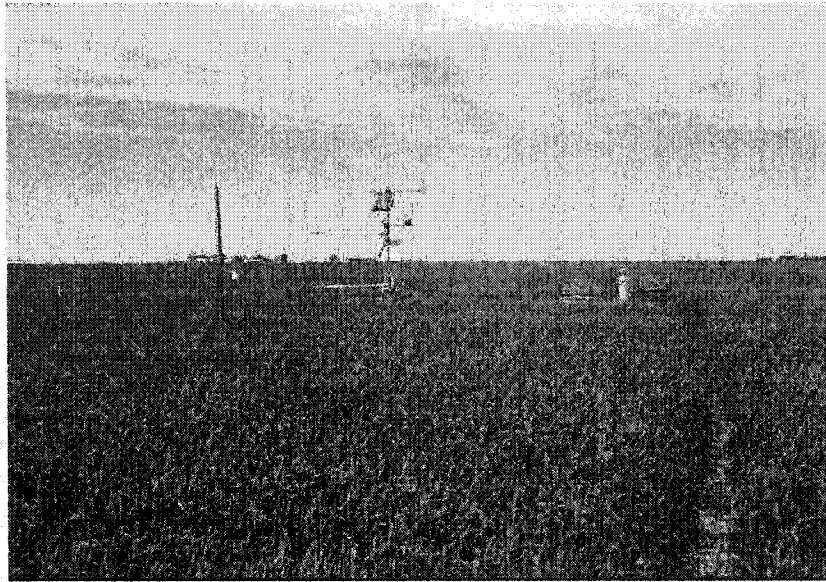
Fig. 2.1   The Bowen ratio system installed in the barley field, operating from DOY 187 to 276 in 1996, and from DOY 155 to 231 in 1998.
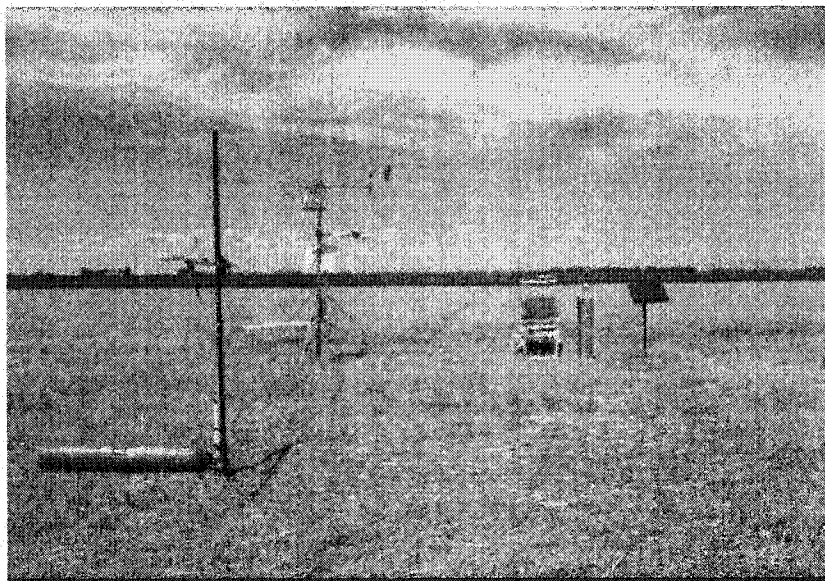
Fig. 2.2   The Bowen ratio system set up in the fallow field, operating from DOY 187 to 276 in 1996, and from DOY 155 to 231 in 1998.

2.3.4 Bowen ratio measurements

Bowen ratio systems recorded 15 measurements, based on which latent heat, sensible heat and CO_2 fluxes were calculated. Air temperature was measured at 0.5 and 1.5 m (the height at which the two arms of the BREB system were mounted and was adjusted as the crop grew) above surface using an exposed and unventilated 0.025-mm-diameter copper-constantan thermocouple junction (Omega Engineering Inc., model COCO-001), which was connected to a datalogger using shielded 22 gauge thermocouple wire. Dew point was measured at the same heights with a dew point hygrometer (cooled-mirror hygrometer) (General Easter Inc., model 100). The air at one height was passed through a dew point hygrometer and the outlet was ventilated to the atmosphere. The vapor pressure was calculated from the dew point for each reading. CO_2 concentration was measured with a CO_2 analyzer (LICOR Inc., model 6262). The air temperature, vapor concentration and CO_2 concentration were recorded every 5 seconds and the difference between intake levels was averaged every 30 minutes to calculate Bowen ratio, latent heat, sensible heat and CO_2 fluxes.

The average net radiation during each 30-minute period was measured with a net pyrradiometer (Middleton Inc., model CN-1) mounted at 1.5 m above the soil surface. Soil heat flux was measured with three soil heat flux plates (Thornthwaite Assoc., Model 610), which were wired in series and placed at a depth of 5 cm. Soil temperature at 2.5 cm was measured using three 24-gauge thermocouples (wired in parallel) in which each junction was encased in a sealed 10cm long copper tube. In addition, surface canopy temperature was monitored with an infrared thermometer (Everest Interscience Inc., model 4000 with 15° view) mounted 2 m above the soil surface on a 45° angle. Soil moisture at 5 cm was measured gravimetrically every day, values of which were used in calculating the surface soil heat flux density (G).

Wind speed was measured with two 3-cup anemometers, one on each of the Bowen ratio systems at about 4 m above the soil surface. A wind direction vane was also set up at the top of each tower to record wind direction. Precipitation was measured with a tipping bucket raingauge installed in the crop field. All the measurements were recorded every 5 seconds and were averaged every 30 minutes using a datalogger.

2.4 Data processing and flux calculation

All the half-hour measurements discussed above were downloaded from the datalogger and were processed with a computer program written in SAS language, to calculate the half-hour fluxes of sensible heat (H), latent heat (LE) and CO_2 fluxes. The SAS program was based on the theory discussed below.

2.4.1 Calculation of Energy Flux

The partition of energy between sensible (H) and latent (LE) heat fluxes can be obtained by the Bowen ratio-energy balance method by means of the Bowen ratio (β):

$$\beta = \frac{H}{LE} \qquad (2.1)$$

The Bowen-ratio is used with the energy balance, which for a uniform surface can be simplified to:

$$Rn = H + LE + G \qquad (2.2)$$

yielding the following expression for LE and H:

$$LE = \frac{Rn - G}{1 + \beta} \qquad (2.3)$$

$$H = \frac{\beta}{1 + \beta}(Rn - G) \qquad (2.4)$$

where Rn, H, LE, and G are the flux densities of net radiation, sensible heat, latent heat, and soil heat, respectively, all in (W m^{-2}).

Over an averaging period t (20-60 min), and using the flux-gradient approach, empirical relationships between fluxes and vertical gradients can be formulated as (Perez et al., 1999):

$$H = \rho_a C_p K_h \frac{\partial T}{\partial Z} \qquad (2.5)$$

$$LE = \frac{\rho_a C_p}{\gamma} K_v \frac{\partial e}{\partial Z} \qquad (2.6)$$

where ρ_a is air density (kg m^{-3}); C_p is the specific heat of air (J kg^{-1} °C^{-1}); T is the temperature (°C); e is vapor pressure (Pa); Z is the vertical height (m); $\partial e/\partial Z$ (Pa m^{-1}) and $\partial T/\partial Z$ (°C m^{-1}) are the gradients of vapor pressure and air temperature, respectively; K_h and K_v are the eddy diffusivities for heat and vapor, respectively (m^2 s^{-1}); γ =$C_p P/(L\varepsilon)$ is the psychrometric constant (Pa °C^{-1}); P is the atmospheric pressure (Pa); ε is the ratio between the molecular weights of water vapor and dry air (0.622); L is the latent heat of vaporization (J kg^{-1}).

In general, K_v and K_h are not known but under specific conditions they can be assumed equal and the ratio of H and LE can be used to partition available energy at the surface into sensible and latent heat flux (Verma et al., 1978). By measuring the temperature and vapor pressure gradients between two levels (0.5 m and 1.5 m) within the adjusted surface layer, and assuming $(\partial T/\partial Z)/(\partial e/\partial Z) \approx \Delta T/\Delta e$, β can be obtained from Equations (2.5) and (2.6) as:

$$\beta = \gamma \frac{\partial T / \partial Z}{\partial e / \partial Z} = \gamma \frac{\Delta T}{\Delta e} \qquad (2.7)$$

where ΔT and Δe are the vertical differences of temperature and vapor pressure, respectively.

Soil heat flux (G) was determined as the sum of (1) changes in soil heat storage in the upper 5 cm of the soil profile, and (2) soil heat flux at 5 cm (Equation 2.8). The first

term was calculated from: 1) change in soil temperature at 2.5 cm depth using three 24-gauge thermocouples, 2) soil heat capacity determined from the fraction of mineral, organic and water content in the 0-5 cm soil layer (Equation 2.9) (Hillel, 1982). The second term was calculated from the heat flux from the three soil heat flux plates at a depth of 5 cm.

$$G=SHF+C\times Z\times \Delta T/\Delta t \qquad (2.8)$$

$$C =f_m C_m+f_o C_o+f_w C_w \qquad (2.9)$$

where C is the volumetric heat capacity of soil (J cm^{-3} °C^{-1}); f_m, f_o, f_w are the volume fractions of minerals, organic matter and water respectively; C_m, C_o, C_w are the volumetric heat capacities of minerals, organic matter and water, respectively (J cm^{-3} °C^{-1}); SHF is the soil heat flux from the flux plate measurement at 5 cm depth (W m^{-2}); Z (cm) is the depth of soil layer; ΔT (°C) is the change of soil temperature between two measuring periods; and Δt (s) is the time step.

The convention used for the signs of energy fluxes is positive when these fluxes were towards the surface and negative when these fluxes were away from the surface. The unit for each flux is in W m^{-2}.

2.4.2 Calculation of CO_2 Flux

According to Fick's Law, carbon dioxide flux density (Fc) can be calculated as:

$$Fc = K_c \times \frac{\Delta C}{\Delta Z} \qquad (2.10)$$

where Fc is CO_2 flux density, K_c is the eddy diffusivity for CO_2, ΔC is the change of CO_2 concentration, ΔZ is the change of vertical height.

Assuming the transfer coefficients (eddy diffusivities) for heat and carbon dioxide are equal (Rosenberg et al., 1983), the following expression can be obtained by re-expressing equation (2.5) in terms of K_h and combining it with equation (2.10):

$$Fc = \frac{1}{\rho_a C_P} \times H \times \frac{(\Delta C / \Delta Z)}{(\Delta T / \Delta Z)} \qquad (2.11)$$

where, Fc is CO_2 flux (kg m^{-2} s^{-1}); $\Delta C/\Delta Z$ is the CO_2 concentration gradient (kg m^{-3} m^{-1}); $\Delta T/\Delta Z$ is the temperature gradient (°C m^{-1}); H is sensible heat flux (W m^{-2}); ρ_a (kg m^{-3}) is the air density; C_p is the specific heat of air (J kg^{-1} °C^{-1}). The unit of Fc values calculated from Equation 2.11 were converted from kg m^{-2} s^{-1} to µmol m^{-2} s^{-1} by multiplying by $\frac{10^9}{44}$ (44 is the molecular weight of CO_2).

The value of Fc is positive when the flux is towards the surface (downward, typical of a crop surface at midday), and it is negative when the flux was away from the surface (upward, typically of a crop surface at night).

2.4.3 Quality checking of the measured fluxes

Many researchers have discussed the accuracy of the calculated values of latent (LE) and sensible heat (H) fluxes using the BREB method (Perez et al., 1999; Bertela, 1989; Angus and Watts, 1984; Fuchs and Tanner, 1970; Ohmura, 1982; Sinclair et al., 1975). The partitioning of available energy between sensible (H) and latent heat (LE) depends on the accuracy of the Bowen ratio (β), which in turn depends on the accuracy of the measurements. In some work in which the BREB methods were used, to avoid serious errors in the estimation of the fluxes, the data within the instrumental errors of the Bowen ratio system were excluded. For cases in which the β values are close to -1, some authors eliminate β value lower than -0.75, or values in the range -1.3<β< -0.7 (Ortega-Farias et al., 1996; Unland et al., 1996). Perez et al. (1999) found that if sensible heat advection is considered negligible, the BREB method is able to determine correctly the surface flux partitioning or the flux values when certain conditions, consistent with the flux-gradient relationship, are fulfilled.

However, there were some gaps of measured fluxes during the growing season of 1996 and 1998, due to: 1) systems turned off during dew point hygrometer checking

and when the magnesium perchlorate column in the CO_2 analyzer needed to be replaced; 2) systems turned off during CO_2 analyzer calibration. This was done by checking CO_2 analyzer zero and span using CO_2-free air and a known CO_2 standard which was close to the ambient concentration. All these checks were done each morning between 8:00 to 10:00 am in the field, which caused a data gap of one to two hours. These missing fluxes were filled by interpolation using the adjacent values. 3) data gaps which were due to Bowen ratio approaching -1, thus no fluxes could be calculated. In order to avoid serious error in estimation of the fluxes, in our study, LE and hence dependent fluxes were estimated using adjacent values (McGinn and Akinremi, 2000). 4) large gaps due to systems failure. No attempt was made to fill a large gap. These missing data take up about 5% (1996) and 10 % (1998) of the data series.

When errors in measurements of available energy (Rn-G), or ΔT, Δe and β are sufficiently large, situations may arise where values of (LE+H) are not equal to (Rn-G), and therefore the energy at the surface is not balanced (McGinn, 1988). McGinn (1988) summarized 6 situations in which measurement errors caused sign of $\Delta T/\Delta Z$ and $\Delta e/\Delta Z$, and the magnitude of $|\beta|$ inconsistent with the energy gain (Rn-G>0) or loss (Rn-G<0), thus resulting in the imbalance of the energy at the surface. These measurement errors did not occur often and data during those periods were excluded from the final flux calculations.

Measured fluxes were also checked for energy balance closure, which allows a comparison of energy fluxes measured with the BREB systems (the sensible heat flux H, and the latent heat flux LE) with fluxes obtained by independent methods (net radiation Rn, soil heat flux G). The energy balance equation is written as:

$$LE + H = Rn - G \qquad\qquad (2.12)$$

A comparison between half-hourly measurements of Rn-G and LE+H was made. In both years, a strong relation is found (r^2 is 0.9986 for 1996 and 0.9988 for 1998). The slope and intercept for regression line in 1996 are 0.99 and 0.22 W m^{-2}, respectively, and 0.99 and 0.34 W m^{-2} in 1998, respectively. Only few data showed non-closure of the energy balance, and this was probably caused in data gap filling by interpolation.

However, the data in both years showed a good closure of the energy balance. Energy balance closure is usually not a problem for BREB method, since LE and, hence H (through Bowen ratio), were calculated based on the energy balance equation (Equation 2.2) (Rosenberg et al., 1983). However, non-closure of the energy balance is a common feature for eddy covariance measurements in that the sum of the eddy fluxes (LE+H) is systematically lower than the available energy (Rn-G) (Anthoni et al., 1999; Aubinet et al., 2001).

2.5 Soil and crop measurements

2.5.1 Soil water content

Soil moisture was measured daily in the 0-5 cm layer using a gravimetric method at six random locations in each field in 1996 and 1998. The soil moisture was used to calculate the surface soil heat flux (G) (see Equation 2.9).

Table 2.2 The regression results for calibrating the neutron probe reading

Soil layer	Regression equation	r^2	No. of observation
0-20 cm	Y=0.0021X-0.0023	0.99	34
20-45 cm	Y=0.0021X-0.0121	0.99	34
45-75 cm	Y=0.0021X-0.0159	0.99	34
75-105 cm	Y=0.0021X-0.0283	0.99	34
105-135 cm	Y=0.0021X-0.0686	0.99	34

Note: Y is the soil water content (m^3 m^{-3}), X is the counts from the neutron probe reading.

During the 1996 growing season, soil moisture was also measured with a neutron probe every week at depths of 0-20, 20-45, 45-75, 75-105, and 105-135 cm, respectively. The counts from the neutron probe at each depth were calibrated by regressing counts on soil water content measured in 1994. The regression results are shown in Table 2.2. The regression equations were used to calculate the volumetric water content using the count readings of neutron probe in 1996.

51

2.5.2 Leaf area

Leaf area was measured weekly during the crop growing season with a LI-300 Area Meter (LICOR, Inc., Lincoln, Nebraska, USA) at four random locations of 0.25 m^2 plot. From each sampling location, 12 plants were taken randomly and their leaves were removed to be measured in the Area Meter. After measuring the leaf area, leaves were returned to the plant samples for determining the above ground biomass. Since leaf area was based on 12 plants, leaf area was divided by 12 to obtain leaf area per plant, and then multiplied by mean plant population (plant counts/sampling area) to obtain leaf area index in $m^2 m^{-2}$.

2.5.3 Biomass

Both aboveground biomass and root biomass were measured weekly by removing and drying (at 60 °C for 48 hours in oven) all materials in a 0.25 m^2 plot at random locations in 1996 (six locations) and 1998 (four locations). This was done through the following steps: 1) two rows of plant were isolated within a ¼ m^2 quadrant; 2) all plants in the quadrant were carefully excavated with as much of the root as possible (60-80 cm depth), then the number of plants was recorded; 3) plant material was put in a bag and transported to the lab, and soil rinsed off the root. 4) roots were cut off at the soil surface and roots and shoots were put into separate bags for biomass measurements. The excavation could recover most root material at the early stage of the growing season (shallow roots), but was expected to underestimate root biomass at later stages of crop growth.

2.5.4 Yield

Grain yields were measured at harvest date for the entire field each year. Yields in kg m^{-2} were converted to g C m^{-2} in order to compare those from model output.

2.6 Summary

In the field experiments, two Bowen ratio systems were used to measure energy fluxes (net radiation, latent heat and sensible heat) and CO_2 fluxes over a barley-fallow rotation in the growing seasons of 1996 and 1998 in Lethbridge, southern Alberta. All the above measurements, together with other auxiliary measurements including soil water content, leaf area, biomass and grain yields, were used to test the modeled results of energy-, water- and CO_2 fluxes through the *ecosys* model. These results are presented in the **chapter 4** and **5** of the thesis.

References

Agriculture and Agri-Food Canada, 1998. The Canadian System of Soil Classification. Third Edition. NRC Research Press, Ottawa.

Agriculture and Agri-Food Canada, Lethbridge Research Center, 2000. Meteorological Data at the Agriculture and Agri-Food Canada, Lethbridge Research Center. Lethbridge, Alberta. http://www.res2.agr.ca/lethbridege/weather.

Angell, R.F., Svejcar, T., Bates, J., Saliendra, N.Z., Johnson, D.A., 2001. Bowen ratio and closed chamber carbon dioxide flux measurements over sagebrush steppe vegetation. Agric. For. Meteorol. 108, 153-161.

Angus, D.E., Watts, P.J., 1984. Evapotranspiration-how good is the Bowen ratio method? Agric. Water Manage. 8, 133-150.

Anthoni, P.M., Law B.E., Unsworth, M.H., 1999. Carbon and water vapor exchange of an open-canopied ponderosa pine ecosystem. Agric. For. Meteorol. 95, 151-168.

Aubinet, M., Chremanne, B., Vandenhaute, M., Longdoz, B., Yernaux, E., Laitat, E., 2001. Long term carbon dioxide exchange above a mixed forest in the Beigian Ardennes. Agric. For. Meteorol. 108, 293-315.

Baldocchi, D.D., S.B. Verma, and N.J. Rosenberg, 1981. Mass and energy exchange of a soybean canopy under various environmental regimes. Agron. J. 73, 706-710.

Bertela, M., 1989. Inconsistent surface flux partitioning by the Bowen ratio method. Bound. Layer Meteorol. 46, 149-167.

Blad, B.L., Rosenberg, N.J., 1974. Lysimetric calibration of the Bowen ratio/energy balance method for evapotranspiration estimation in the central Great Plains. J. Appl. Meteorol. 13, 227-236.

Bremer, E., Janzen, H.H., Johnston, A.M., 1994. Sensitivity of total, light fraction and mineralizable organic matter to management practices in a Lethbridge soil. Can. J. Soil Sci. 74, 131-138.

Chan, A.S.K., Pruger, J.H., Parkin, T.B., 1994. Comparison of gas flux measurement methods: Bowen ratio method vs. closed-chamber method. Agron. Abstr. 271. American Society of Agronomy Annual Meeting, Seattle, Washington.

Dabberdt, W.F., Lenschow, D.H., Horst, T.W., Zimmerman, P.R., Oncley, S.P., Delany, A.C., 1993. Atmosphere-surface exchange measurements. Science 260, 1472-1481.

Denmead, O.T., Dunin, F.X., Wong, S.C., Greenwood, E.A.N., 1993. Measuring water use efficiency of eucalypt trees with chambers and micrometeorological techniques. J. Hydrol. 150, 649-664.

Dugas, W.A., 1993. Micrometeorological and chamber measurements of CO_2 flux from bare soil. Agric. For. Meteorol. 67, 115-128.

Dugas, W.A., Fritschen, L.J., Gay, L.W., Held, A.A., Matthias, A.D., Reicosky, D.C., Steduto, P., Steiner, J.L., 1991. Bowen ratio, eddy correlation, and portable chamber measurements of sensible and latent heat flux over irrigated spring wheat. Agric. For. Meteorol. 56, 1-20.

Dugas, W.A., Heuer, M.L., Mayeux, H.S., 1999. Carbon dioxide fluxes over bermudagrass, native prairie and sorghum. Agric. For. Meteorol. 93, 121-139.

Edwards, N.T., 1982. The use of sola-lime for measuring respiration rates in terrestrial ecosystems. Pedobiologia 23, 321-330.

Fang, C., Moncrieff, J.B., 1996. An improved dynamic chamber technique for measuring CO_2 efflux from the surface of soil. Funct. Ecol. 10, 297-305.

Fritschen, L.J., Simpson, J.R., 1989. Surface energy balance and radiation systems: general description and improvements. J. Appl. Meteorol. 28, 680-689.

Fuchs, M., Tanner, C.B., 1970. Errors analysis of Bowen ratios measured by differential psychrometry. Agric. Meteorol. 7, 329-334.

Goulden, M.L., Grill, P.M., 1997. Automated measurements of CO_2 exchange at the moss surface of a black spruce forest. Tree Physiol. 17, 537-542.

Grant, R.F., Juma, N.G., Robertson, J.A., Izaurralde, R.C., McGill, W.B., 2001. Long-term changes in soil carbon under different fertilizer, manure, and rotation: testing the mathematical model *ecosys* with data from the Breton plots. Soil Sci. Soc. Am. J. 65, 205-214.

Grant, R.F., Wall, G.W., Kimball, B.A., Frumau, K.F.A., Pinter Jr., P.J., Hunsaker, D.J., Lamorte, R.L., 1999. Crop water relations under different CO_2 and irrigation: Testing of *ecosys* with the free air CO_2 enrichment (FACE) experiment. Agric. For. Meteorol. 95, 27-51.

Held, A.A., Steduto, F.O., Matista, A., Hsiao, T.C., 1990. Bowen ratio/energy balance technique for estimating crop net CO_2 assimilation, and comparison with a canopy chamber. Thoer. Appl. Climatol. 42, 203-2113.

Hillel, D., 1982. Introduction of soil physics. Academic Press.

Iritz, Z., Lindrot, A., Gardenas, A., 1997. Open ventilated chamber system for measurements of H_2O and CO_2 fluxes from soil surface. Soil Technol. 10, 169-184.

Janssens, I.A., Ceulemans, R., 1998. Spatial variability in forest soil CO_2 efflux assessed with a calibrated soda lime technique. Ecol. Lett. 1, 95-98.

Janssens, I.A., Kowalski, A.S., Ceulemans, R., 2001. Forest floor CO_2 fluxes estimated by eddy covariance and chamber-based model. Agric. For. Meteorol. 106, 61-69.

Jensen, L.S., Mueller, T., Tate, K.R., Ross, D.J., Magid, J. and Nielsen, N.E., 1996. Soil surface CO_2 flux as an index of soil respiration in situ: A comparison of two chamber methods. Soil Biol. Biochem. 28, 1297-1306.

Malek, E., Bingham, G.E., 1993. Comparison of the Bowen ratio energy balance and the water balance methods for the measurement of evapotranspiration. J. Hydrol. 146, 209-220.

McGinn, S.M. and Akinremi, O.O., 2000. Carbon dioxide balance of a crop-fallow rotation in western Canada. Can. J. Soil Sci. 81, 121-127.

McGinn, S.M. and Akinremi, O.O., McLean, H.D., Ellert, B., 1998. An automated chamber system for measuring soil respiration. Can. J. Soil Sci. 78, 573-579.

McGinn, S.M., 1988. Heat, water vapor and CO_2 exchange above alfalfa and maize. Ph.D. thesis, University of Guelph.

Mosier, A.R., 1990. Gas flux measurement techniques with special reference to techniques suitable for measurements over large ecologically uniform areas. In: Bouwman, A.F., (Ed.), Soils and the Greenhouse Effect. Willey, Chichester, 99, 289-301.

Norman, J.M., Garcia, R., Verma, S.B., 1992. Soil surface CO_2 fluxes and the carbon budget of a grassland. J. Geophys. Res. 97, 18845-18853.

Norman, J.M., Kucharik, C.J., Gower, S.T., Baldocchi, D.D., Grill, P.M., Rayment, M., Savage, K., Striegl, R.G., 1997. A comparison of six methods for measuring soil-surface carbon dioxide fluxes. J. Geophys. Res. 102, 28771-28777.

Ohmura, A., 1982. Objective criteria for rejecting data for Bowen ratio flux calculation. J. Appl. Meteorol. 21, 595-598.

Ortega-Farias, S.O., Cuenca, R.H., Ek, M., 1996. Daytime variation of sensible heat flux estimated by the bulk aerodynamic method over a grass canopy. Agric. For. Meteorol. 81, 131-143.

Perez, P.J., Castellvi, F., Ibanez, M., Rosell, J.I., 1999. Assessment of reliability of Bowen ratio method for partitioning fluxes. Agric. For. Meteorol. 97, 141-150.

Prueger, J.H., Hatfield, J.L., Aase, J.K., Pikul, J.L., 1997. Bowen ratio comparisons with lysimeter evapotranspiration. Agron. J. 89, 730-736.

Rayment, M.B., Jarvis, P.G., 1997. An improved open chamber system for measuring soil CO_2 effluxes of a Boreal black spruce forest. J. Geophys. Res. 102, 28779-28784.

Rosenberg, N.J., Blad, B.L., and Verma, S.B., 1983. Microclimate: the biological environment. John Wiley & Sons, Inc. New York.

Sinclair, T.R., Allen, L.H., Lemon, E.R., 1975. An analysis of errors in the calculation of energy flux densities above vegetation by a Bowen ratio profile method. Bound. Layer Meteorol. 8, 129-139.

Steduto, P., Hsiao, T.C., 1998. Maize canopies under two soil water regions - IV. Validity of Bowen ratio - energy balance technique for measuring water vapor and carbon dioxide fluxes at 5-min intervals. Agric. For. Meteorol. 89, 215-228.

Swindbank, W.C., 1951. The measurements of vertical transfer of heat and water vapor by eddies in the lower atmosphere. J. Meteorol. 8, 135-145.

Tanner, C.B., 1960. Energy balance approach to evapotranspiration from crops. Soil Sci. Soc. Am. Proc. 24, 1-9.

Todd, R.W., Evett, S.R., Howell, T.A., 2000. The Bowen ratio-energy method for estimating latent heat flux of irrigated alfalfa evaluated in a semi-arid, advective environment. Agric. For. Meteorol. 103, 335-348.

Unland, H.E., Horser, P.R., Shuttleworth, W.J., Yang, Z.L., 1996. Surface flux measurement and modeling at a semi-arid Sonoran Desert site. Agric. For. Meteorol. 82, 119-153.

Verma, S.B., 1990. Micrometeorological methods for measuring surface fluxes of mass and energy. In: Goel, N.S., Norma, J.M., (eds.), Remote Sensing Reviews: Instrumentation for Studying Vegetation Canopies for Remote Sensing in Optical and Thermal Infrared Regions. Vol. 5. Harwood, New York, pp. 99-115.

Verma, S.B., Rosenberg, N.J., 1975. Accuracy of lysimetric, energy balance, and stability corrected aerodynamic methods of estimating above-canopy flux of CO_2. Agron. J. 67, 699-704.

Verma, S.B., Rosenberg, N.J., Blad, B.L., 1978. Turbulent exchange coefficients for sensible heat and water vapor under advective conditions. J. Appl. Meteorol. 17, 330-338.

Chapter 3   Model development

3.1 Introduction

Apart from the direct measurements discussed in **Chapter 2**, modeling provides another effective way to study energy and carbon exchange in any ecosystem. Model method is considered important because it provides the opportunities to test future scenarios, to separate various component processes and to study their interactions, and its results can be used as a reference for measurements in the field (Ehleringer and Field, 1993; Van Gardingen et al., 1997; Cernusca et al., 1998). Moreover, a simulation model may provide a further framework for analysis of the effect of climate change on energy balance, crop growth, carbon exchange, and soil carbon dynamics. These models can be generally classified into two types: statistical or empirical models and process-based models. Statistical or empirical models usually employ statistical regression with specific climatic parameters such as temperature, soil moisture, radiation, precipitation, etc. (Rajvanshi and Gupta, 1986; Grahammer et al., 1991; Bridgham and Richardson, 1992; Peterjohn et al., 1994; Thierron and Laudelout, 1996). For example, Raich and Schlesinger (1992) reviewed the data in the literature and derived a statistical model to predict global variation of soil respiration. The model reflected the global trend of annual soil CO_2 efflux with temperature and precipitation and indicated that global variation of soil respiration is mostly accounted for by the variation of temperature. Hanson et al. (1993) developed an empirical model to predict CO_2 efflux by relating it to soil temperature, soil water content and the percentage of soil coarse fraction. A modeling study using aggregated mean monthly and yearly air temperatures was conducted by Kicklighter et al. (1994) to estimate regional soil CO_2 efflux from temperate forests. They found that the statistical model provide good estimates of annual soil CO_2 effluxes for different sites around the world regardless of forest types. Akinremi et al. (1999) developed a statistical model using daily soil temperature and soil moisture as the main parameters to estimate soil respiration in a barley-fallow system. This model was shown to account for 76 to 80% of the variation of soil

respiration. However, the lack of physiological and biological bases in statistical and empirical models, makes it difficult to explain processes that take place in the ecosystem. Therefore, their applications are greatly restricted to the conditions under which they are parameterized.

As their name implies, process-based models are built based on the physiological and biological theories that control the component processes, such as energy exchange, carbon fixation, carbon respiration, evapotranspiration, nutrient uptake, crop growth, etc. At the first stage of development, these process-based models were usually focused on a single component or process of the ecosystem, such as plant growth (Goudriaan, 1977; Penning de Vries and Laar, 1982; Penning de Vries et al., 1989); photosynthesis (de Wit et al., 1978; Farquhar et al., 1980); soil respiration; stomatal behavior (Ball et al., 1987); water balance and transpiration (Stroosnijder, 1982; Stewart and Gay, 1989); microbial decomposition (Juma and Paul, 1981); nutrient uptake (Barber and Cushman, 1981; Keulen and Seligman, 1987); and salinity (Grant, 1995a).

At the second stage of development, these process-based models scaled a single process, such as photosynthesis (Kull et al., 1995; Amthor, 1994; de Pury and Farquhar, 1997; Ehleringer and Field, 1993), water vapor and carbon dioxide exchange (Baldocchi, 1993; Thorgeirsson and Soegaard, 1999; Soegaard, 1999), or stomatal behavior and transpiration (Jarvis and McNaughton, 1986; Leuning et al., 1995), from a leaf to canopy and regional levels, and even to global levels, or scaled a single process to a multi-processes, multi-layer approach. The first approach (i.e. scaling a single process from a leaf to canopy and regional levels, and even to global levels) is referred to "big leaf approach", since it treats the vegetation as if it was a single "big leaf" (Raupach and Finnigan, 1988). Farquhar (1989) proposed a "big leaf approach" to scale photosynthesis from leaves to canopies. The underlying assumption for scaling of carbon dioxide fixation using this approach is that as radiation is attenuated with depth in the canopy, photosynthetic capacity in the leaves is also reduced. When these assumptions are met, methods or measurements of leaf photosynthesis can be used to represent canopy photosynthesis (Sellers et al., 1992; Kull and Jarvis, 1995). The latter approach (i.e. scaling a single process to a multi-processes, multi-layer approach) is often referred to as "multi-layer model" in that it retains the vertical profile of canopy

and soil structure and calculates micrometeorology and fluxes separately from each layer (Wohlfahrt et al., 2001; Tappeiner and Cernusca, 1998). These models can be useful tools for analyzing the details of canopy and soil carbon, energy exchange among the Soil-Plant-Atmosphere Continuum (SPAC).

One of the current trends of the process-based modeling is to couple them with General Circulation Models (GCMs) to study the ecosystem behavior under climate change and its feedback to global change. With the proliferation of climate change studies using GCMs, the construction and refinement of the process-based ecosystem models to generate land surface schemes suitable for coupling to GCMs has received increasing attention. Over the past decade, with the advent of larger and faster computers and the increase of GCM spatial resolutions, many process-based ecosystem models with varying complexities have been developed to provide various land surface schemes to be coupled with GCMs. These models include the soil-vegetation-atmosphere transfer schemes (SVATs) (Enrique et al., 1999), in which vegetation is treated as a separate layer. Soil in SVATs is divided into different layers and soil heat and moisture movement is simulated dynamically between these layers. The key surface calculations in most of the current land surface schemes generated from these models include energy fluxes, canopy temperature, canopy conductance, aerodynamic resistance, albedo, transpiration, canopy water potential, water holding capacity and runoff (Wang, 2000). These land surface models include the Biosphere-Atmosphere Transfer Scheme (Dickinson et al., 1986, 1992), the simple Biosphere Scheme (SiB) (Sellers et al., 1986), Goddard Institute for Space Studies (GISS) (Abramopoulos et al., 1988), the Bare Essentials of Surface Transfer (BEST) (Pitman, 1988; Pitman et al., 1991; Yang, 1992), the Interaction Soil-Biosphere-Atmosphere model (ISBA) (Noilhan and Planton, 1989), and the Canadian Land Surface Scheme (CLASS) (Verseghy, 1991; Verseghy et al., 1993).

In recent years, the lack of dynamic biological processes in soil and vegetation, and the climate feedback on these processes has been recognized to be the biggest limitation in these process-based models, and in GCMs (Dickinson, 1995). Much work has been carried out at the interface of climatology, geophysics, environmental physics and ecology aiming to understand such processes and climate feedbacks and including

them in process-based models and GCMs (Shackley et al., 1998; Bounoua et al., 1999). For instance, in a new version of CLASS (Wang, 2000), water, carbon and nitrogen processes have been added, creating a carbon coupled soil-vegetation-atmosphere water transfer model, with a plant module for simulating the plant carbon and nitrogen processes and a soil module for simulating the plant litterfall and soil organic matter transformation processes. These improvements enable the study of the exchanges and interactions of greenhouse gas, carbon and nitrogen between the earth's terrestrial ecosystem and the atmosphere.

Ecosys is a process-based model that combines the soil-vegetation-atmosphere transfer schemes (SVATs), which can simulate the transport and transformation of energy, water, carbon, oxygen, nitrogen, phosphorous, and ionic solutes through soil-plant-atmosphere systems with the atmosphere as the upper boundary layer and soil parent material as the lower boundary layer (Grant et al., 1999b). With its spatial scales ranging from mm to km in 1, 2, and 3 dimensions, *ecosys* allows the scaling up of microscale phenomena to landscape, region and global scale (Grant et al., 2001a). *Ecosys* also allows options to introduce a full range of management practices into model simulation, including tillage, fertilizer, irrigation, planting and harvest. Options are also provided in *ecosys* to introduce change in atmosphere boundary conditions (incremental and step changes in CO_2 concentration, temperature, precipitation, humidity, wind speed, and changes in chemical composition of precipitation). These options allow the effects of a wide range of disturbances to be simulated when studying disturbance effects on ecosystem function (Grant and Nalder, 2000; Grant, 2001). Therefore, *ecosys* was selected in this study to simulate energy, water and CO_2 exchange through the soil-plant-atmosphere continuum of a barley-fallow system in Lethbridge, and it was also used with the outputs from the Canadian Regional Climate Model (CRCM-II) to study the effect of climate change on long-term soil carbon dynamics.

3.2 Model development

The ecosystem model *ecosys* is a comprehensive mathematical model of natural and managed terrestrial ecosystems, which simulates the transport and transformation of heat, carbon, oxygen, nitrogen, phosphorus and ionic solutes through soil-plant-atmosphere systems with the atmosphere as the upper boundary layer and soil parent material as the lower boundary layer (Grant et al., 1999a). It also simulates ecosystem behavior under different management practices (tillage methods, fertilizer and irrigation application) and environmental conditions (soils, climates, and land use practices) (Grant et al., 1999a, 2001a, b).

Ecosys includes 6 modules relevant to this study: energy exchange, canopy water relations, canopy C fixation, canopy respiration and senescence (autotrophic respiration), plant growth, and soil microbial decomposition (heterotrophic respiration). Components of *ecosys* relevant to the objectives of this study are briefly described below with references to equations and variables in the Appendix. Further information can be found in the cited literature authored by R.F. Grant.

3.2.1 Energy exchange

Energy exchanges in *ecosys* are simulated between the atmosphere and vegetation, and between the atmosphere and ground surfaces (soil, crop residue and snow) (Grant et al., 1999b). Total energy exchange is calculated as the sum of exchanges with the canopy and ground surfaces using first-order closure (Equation 3.1, 3.2). Net radiation (Rn) is calculated from the absorption, reflection, and transmission of shortwave and longwave radiation by canopy and soil surfaces (Equation 3.3, 3.4). Latent heat (LE) is calculated from the vapor pressure difference between atmosphere and canopy and soil surfaces (Equation 3.5, 3.6, 3.7). If precipitation is not intercepted by canopy surfaces, latent heat flux is calculated from transpiration (Equation 3.5) determined by the canopy-atmosphere vapor density gradient and aerodynamic (r_{Ai}) (Eq. 3.10) and stomatal (r_{Ci}) (Eq. 3.11, 3.12) resistances. If intercepted precipitation is present, evaporation takes precedence over transpiration in the calculation of latent heat flux which is determined by aerodynamic resistance (r_{Ai}) (Equation 3.6). Sensible heat (H) is calculated from the temperature difference between atmosphere and canopy and soil surfaces (Equation 3.8, 3.9). Change in heat storage in canopy and soil surfaces is

calculated from temperature change in time and in depth (Equation 3.13, 3.14, 3.15). Surface energy exchanges are coupled to subsurface conductive, convective and latent heat transfers using a forward differencing scheme (Equation 3.16) with heat capacities and thermal conductivities calculated from de Vries (1963).

3.2.2 Water relations

Soil-plant and plant-atmosphere water transfers are coupled by calculating stomatal conductance (r_{Ci}) from an hourly two-stage convergence solution for the transfer of water and heat through a multi-layered, multi-population soil-root-canopy system. The first stage of this solution requires convergence to a canopy temperature for each plant population at which the first-order closure of the canopy energy balance (Eq. 3.1) is achieved. In the second stage, a value for the canopy water potential is sought at which the difference between canopy transpiration from the energy balance (Eq. 3.5) and total water uptake from all rooted soil layers (Eq. 3.19-3.24) equals the difference between canopy water contents from the previous and current hours. The canopy water potential determines transpiration by setting the osmotic (Eq. 3.18) and hence turgor (Eq. 3.17) potential which affects stomatal conductance (r_{Ci}) (Eq. 3.11) and thereby canopy temperature through its effect on vapor pressure (Eq. 3.5) (Grant et al., 1999b). The canopy water potential also determines water uptake in each rooted soil layer by setting the canopy-root potential gradient (Eq. 3.20, 3.25), which is determined by soil-root and root-canopy hydraulic conductance in each rooted soil layer (Eq. 3.21-3.24)(Grant et al., 1999b). In addition, the canopy water potential determines the canopy water content according to plant water potential–water content relationships. Soil-root conductance is calculated from root length given by a root growth sub-model driven by shoot-root C transfer (Grant, 1993a, b; Grant 1998, Grant and Robertson, 1997), and from soil-root hydraulic conductivity for radial water uptake calculated according to Cowan (1965) for an assumed horizontally uniform root distribution in each soil layer (Eq. 3.21). Root-canopy conductance is calculated from radial and axial root conductance (Reid and Huck, 1990) and from lengths of primary and secondary root (Eq. 3.22-3.24) (Grant, 1998).

3.2.3 Gross primary productivity (GPP)

Because leaf CO_2 fixation rate partly determines leaf conductance to water vapor, the accurate simulation of leaf CO_2 fixation is an important requirement of ecosystem models (Grant et al., 1999b). Leaf CO_2 fixation is determined by carboxylation, which is controlled by irradiance, temperature, and leaf CO_2 concentration, and by diffusion, which is controlled by the atmosphere-leaf CO_2 concentration gradient and leaf conductance. The coupling of leaf carboxylation and diffusion in *ecosys* allows the calculation of a leaf CO_2 fixation rate, which is then aggregated to the canopy level.

Carboxylation rates are calculated for each leaf surface of multi-specific plant canopies as the lesser of dark (Eq. 3.26-3.29) and light (Eq. 3.30-3.34) reaction rates according to Farquhar et al. (1980) (Eq. 3.35). These rates are driven by irradiance (R_P in Eq. 3.31), canopy temperature (T_i in Eq. 3.33), and canopy CO_2 concentration (C_C in dark reaction Eq. 3.26, light reaction Eq. 3.34). Maximum dark or light reaction rates used in these functions are determined by specific activities and surficial concentrations of rubisco (V_i' and R_{C_i} in Eq. 3.28) or chlorophyll (J_i' and E_{C_i} in Eq. 3.32), respectively. These activities and concentrations are determined by environmental conditions (CO_2 concentration, radiation, temperature, water, N and P uptake) and assimilation during leaf growth. Photosynthesis is used here for gross photosynthesis and includes photorespiration (Eq. 3.27), an intensive process in C_3 plants that is intimately coupled with photosynthesis itself.

Carbon dioxide diffusion rates (V_G in Eq 3.36) are calculated for each leaf surface by first calculating the leaf stomatal conductance required to maintain a set $C_i:C_a$ ratio from the leaf carboxylation rate (V_B in Eq. 3.35) and the CO_2 concentration difference between the canopy atmosphere and the mesophyll at zero canopy water potential (Eq. 3.36). CO_2 concentration in canopy air (C_B) depends on net soil and canopy CO_2 fluxes (V_S and V_N in Eq. 3.37) and boundary layer resistance (r_{A_i} in Eq. 3.37). Stomatal conductance is then reduced according to an exponential function of canopy turgor (Ψ_{T_i} in Eq. 3.38) generated from the convergence solution for canopy water potential at which the difference between transpiration (Eq. 3.5) and root water uptake (Eq. 3.19) is equal to the difference between canopy water content at previous and current water

potentials. A convergence solution is then sought for C_i and its aqueous equivalent at which diffusion equals carboxylation (V_X in Eq. 3.40). Values of V_X of all leaf surfaces in the canopy are added to give a value for canopy gross primary productivity (GPP).

3.2.4 Autotrophic respiration (R_a)

Autotrophic respiration (including canopy and root respiration) has two components: maintenance respiration, required to maintain the biological integrity of the plant, and growth respiration, required to form new plant material. The product of CO_2 fixation V_X from Eq. 3.40 is added to a C storage pool from which C is oxidized to meet requirements for maintenance and growth respiration (Grant et al., 1999a) using a first-order function of storage C (X in Eq. 3.41). Crop maintenance respiration (Q_M) is calculated from total crop N and temperature using a value for specific maintenance respiration from Grant et al. (1993a) (Eq. 3.42). Crop growth respiration (Q_G in Eq.3.43) is reduced from storage pool C oxidation by maintenance respiration and by turgor (Ψ_{Ti} in Eq. 3.17). If the C storage pool is depleted, the C oxidation rate may be less than the maintenance respiration requirement, in which case the difference is made up through respiration of remobilizable C in leaves, stems and other supporting organs (Q_S in Eq 3.44). Upon exhaustion of the remobilizable C, the remaining C is dropped from the branch and added to residue at the soil surface as litterfall (Q_D in Eq. 3.45). Environmental constraints such as nutrient, heat or water stress that reduce the C fixation and hence C storage, will therefore accelerate the loss of leaf C from the plant, causing senescence and litterfall of associated non-remobilizable C. When the storage C oxidation exceeds maintenance respiration requirements, the excess is used for growth respiration (Q_G in Eq. 3.43), which drives the formation of new biomass ($M_{i,j}$ in Eq. 3.45)(Grant et al., 2001). Net canopy CO_2 fixation (V_N) is calculated as the difference between aggregated leaf carboxylation rates (V_X from Eq. 3.40) and the sum of canopy maintenance, growth and senescence respiration (Eq. 3.46). This is the canopy net primary productivity (NPP). Growth and maintenance respiration from crop roots, which is calculated in the same way for the canopy as described above, is also subtracted from net canopy CO_2 fixation (V_N), thus giving the NPP of the entire plant.

3.2.5 Heterotrophic respiration (R_h)

1) Decomposition: Soil organic matter in *ecosys* is resolved into four substrate-microbe complexes (plant residue, animal manure, particulate organic matter and non-particulate organic matter) within each of which C, N and P may move among five organic states: solid substrate, sorbed substrate, soluble hydrolysis products, including acetate, microbial communities, and microbial residues (Table 1 in Grant, 1999). Each organic state in each complex is resolved into structural components of differing vulnerability to hydrolysis and into elemental fractions C, N and P within each structural component. Microbial communities are also resolved into functional type including obligate aerobes, facultative anaerobes (denitrifiers), obligate anaerobes (fermenters), methanogens, diazotrophs and autotrophs (nitrifiers and CH_4 oxidizers).

Litterfall described in *Autotrophic Respiration* above (Q_D in Eq. 3.45) is added to the plant residue complex and partitioned into carbohydrate, protein, cellulose and lignin structural components according to Broder and Wagner (1988). Rates of component hydrolysis (D_S and D_Z in Equations 3.47, 3.48) are the product of the active biomass ($M_{i,a,c}$ in Equations 3.47, 3.48) and specific activity ($D'_{S_{i,j,c}}$ and $D'_{Z_{i,j,c}}$ in Equations 3.47-3.48) of each microbial functional type within each complex (Eq. 3.47-3.48) (Grant et al., 1993b; Grant and Rochette, 1994). The active biomass of each functional type is determined by its growth vs. decomposition described under *Microbial Growth* below. Specific microbial activity is determined by substrate concentration [$S_{i,c}$] and [$Z_{i,c}$] in soil, by microbe concentration [$M_{i,a,c}$] in water (Equations 3.49-3.50) (Grant et al., 1993a; Grant and Rochette, 1994), and by soil and surface residue temperatures (Arrhenius kinetics, Eq. 3.51) (Sharpe and DeMichelle, 1977). Values of [$M_{i,a,c}$] are determined by water contents of surface residue and a spatially resolved soil profile (Grant, 1997; Grant and Rochette, 1994; Grant et al., 1998). A fraction of the hydrolysis products of lignin are coupled with those of protein and carbohydrate (F_H in Eq. 3.54) according to the stoichiometry proposed by Shulten and Schnitzer (1997) and the resulting compound is transferred to the solid substrate of the particulate organic matter complex. Rates of particulate organic matter formation

66

($H_{S_{i,j,c}}$ in Eq. 3.54) are thus determined by substrate lignin content and heterotrophic microbial activity (Eq. 3.54).

   2) Microbial growth: Microbial growth in *ecosys* relies on substrate oxidization through growth and maintenance respiration. The concentration of the soluble hydrolysis products from *Decomposition* above ($[Q_{i,c}]$) determines rates of C oxidation by each heterotrophic population $R_{i,c}$ in (Eq. 3.55), the total of which gives the heterotrophic respiration (R_h) that drives CO_2 emission from the soil surface. This oxidation is coupled to the reduction of O_2 by all heterotrophic aerobic populations (Grant et al., 1993a,b; Grant and Rochette, 1994), to the sequential reduction of NO_3^-, NO_2^- and N_2O by heterotrophic denitrifiers (Grant et al., 1993c,d; Grant and Pattey, 1999) and to the reduction of organic C by fermenters and of their acetate product by heterotrophic methanogens (Grant, 1994, 1998). Some of the total C oxidation ($R_{i,c}$ in Eq. 3.55) is required for maintenance respiration determined from microbial N (Eq. 3.56) and soil temperature (Eq. 3.57), and the remainder is used for growth respiration ($R_{g_{i,c}}$ in 3.58) that drives microbial biosynthesis ($M_{i,j,c}$ in Eq. 3.59) from uptake of decomposition products (Eq. 3.60). The energetics of these oxidation-reduction reactions vs. energy requirements for biosynthesis determine microbial growth and hence the active biomass of each heterotrophic functional type from which its decomposer activity is calculated as described in *Decomposition* above (Eq. 3.47-3.48). In addition, autotrophic nitrifiers conduct NH_4^+ and NO_2^- oxidation and N_2O evolution (Grant, 1995b; Grant and Hesketh, 1992), autotrophic methanogens conduct CO_2 reduction, and autotrophic methanotrophs conduct CH_4 oxidation (Grant, 1999), the energetics of which determine autotrophic growth and hence biomass and activity. Microbial populations in the model seek to maintain steady-state ratios of biomass C:N:P by mineralizing or immobilizing NH_4^+, NO_3^- and $H_2PO_4^-$ (Eq. 3.61), thereby regulating solution concentrations that drive N and P uptake by roots and mycorrhizae (Grant and Heaney, 1997). Microbial populations undergo first order decomposition (Eq. 3.62, 3.63), products of which are partitioned between microbial residues within the same substrate-microbe complex, and the solid substrate of the non-particulate organic matter complex (H_M) according to soil clay content (F_H in Eq. 3.64) (Grant et

al., 1993a,b). Rates of non-particulate organic matter formation from H_M in equation 3.64 are thus determined by rates of microbial decay and by soil clay content.

3.3 Model input and output data

3.3.1 Model input

Model input are the data or parameters that drive the model to run on/under a specific purpose/condition. The input data which are needed for *ecosys* to simulate energy and carbon dioxide fluxes in a barley-fallow system in southern Alberta can generally be classified into six categories: meteorological data, soil attributes, crop attributes, soil management information, crop management information and site information. Key model inputs are listed here.

1) Meteorological data: hourly solar radiation (W m^{-2}), air temperature (°C), wind speed (m s^{-1}), relative humidity (%) or vapor pressure (kPa) and precipitation (mm). Hourly meteorological data from 1990 to 2000 used in this study were provided by Lethbridge Research Center, Agriculture and Agri-Food Canada, which were converted to the format required by the model to set the boundary conditions.

2) Soil attributes: bulk density, field capacity, wilting point, saturated hydraulic conductivity, soil texture, organic C, N, P content, depth of soil layer. Soil attributes of a Dark-Brown Chernozem in Lethbridge are shown in Table 3.1, 3.2.

3) Crop attributes: crop attributes used to represent barley in *ecosys* are shown in Table 3.2, variables of which are described in the Appendix glossary.

4) Soil management information: Crop rotation, tillage (date, tillage type, and depth), fertilizer application (date, fertilizer type, amount and depth), irrigation application (date, time, amount, depth and water quality). In this study, soils were managed under no tillage, no fertilizer and no irrigation conditions.

5) Crop management information: planting date, depth of planting (m), planting density (m^{-2}), harvest date, type of harvest (none, grain, whole plant), height of harvest cut (m), fraction of population harvested, efficiency of harvest removal.

6) Site and topographic information: latitude, longitude, altitude (m), average annual air temperature (°C), solar noon (h), depth of water table (m), aspect, slope, surface roughness, concentration of atmospheric components, boundary conditions (permeability, runoff).

Table 3.1   General soil characteristics of a Dark-Brown Chernozem at the experimental site in Lethbridge

Depth (cm)	BD	FC	WP	K_{sat}	SC	SiC	OC	ON	pH
0.0-1.0	1.24	0.33	0.18	3.5	28.8	40	15.9	1.58	7.1
1.0-5.0	1.24	0.33	0.18	3.5	28.8	40	15.9	1.58	7.1
5.0-10	1.24	0.33	0.18	3.5	28.8	40	15.9	1.43	7.1
10-25	1.24	0.38	0.24	2.2	27.4	43	14.1	1.43	7.1
25-45	1.27	0.38	0.24	2.2	27.4	43	13.8	0.79	6.9
45-60	1.32	0.32	0.19	2.9.	33	33.3	8.69	0.29	6.9
60-75	1.32	0.32	0.19	2.9	33	33.3	3.17	0.28	7.4
75-90	1.30	0.35	0.20	2.9	26	38.3	3.03	0.19	7.4
90-105	1.37	0.28	0.15	5.4	38.5	36.5	2.06	0.13	7.6
105-120	1.40	0.27	0.13	6.8	41	37	1.38	0.06	7.5
120-135	1.40	0.27	0.13	7.0	41	37	0.69	0	7.5

Note: BD-bulk density (g cm^{-3}); FC-field capacity (m^3 m^{-3}); WP-wilting point (m^3 m^{-3}); K_{sat}-saturated hydraulic conductivity (mm h^{-1}); SC-sand content (%), SiC-silt content (%); OC-organic C (g C kg^{-1}), ON- organic N (g N kg^{-1}). Data for bulk density, sand and silt content, organic matter concentration were estimated from the Agricultural Region of Alberta Soil Inventory Database AGRASID (Agriculture and Agri-Food Canada, 2001), and from Bremer et al. (1994) and Janzen et al. (1997). Field capacity, wilting point and saturated hydraulic conductivity were calculated from Saxton (2001) by inputting soil sand and silt content.

Table 3.2 Key parameters of crop and soil characteristics used by the model *ecosys*

Variable	Equation	Value	Unit	Reference
		Crop		
r_{C_i}'	3.11	50	s m^{-1}	Grant et al., 1995
$r_{C\,max}$	3.11	2000	s m^{-1}	Grant et al., 1995
Ψ_{π_i}'	3.18	-1.25	MPa	Grant et al., 1995
K_{C_i}'	3.27	12.5	μM	Douglas and Ogren, 1984
K_{O_i}'	3.27	500.0	μM	Douglas and Ogren, 1984
V_i'	3.28	25.0	μmol g^{-1} s^{-1}	Kozlowski and Pallardy, 1997
R_{C_i}	3.28	0.25	g g leaf protein^{-1}	Grant et al., 2001c
Q	3.31	0.5	μmol e$^-$ μmol quanta^{-1}	Evans and Farquhar, 1991
α	3.31	0.8	unitless	Evans and Farquhar, 1991
J_i'	3.32	500	μmol e$^-$ g^{-1} s^{-1}	Evans and Farquhar, 1991
E_{C_i}	3.32	0.02	g g leaf protein^{-1}	Evans and Farquhar, 1991
A	3.33	18.02	Unitless	Sharpe and DeMichelle, 1977
R	3.33	8.31	J mol^{-1} K^{-1}	Sharpe and DeMichelle, 1977
S	3.33	710.0	J mol^{-1} K^{-1}	Sharpe and DeMichelle, 1977
H$_a$	3.33	57.5	KJ mol^{-1}	Farquhar et al., 1980
H$_{dl}$	3.33	190.0	KJ mol^{-1}	Farquhar et al., 1980
H$_{dh}$	3.33	214.0	KJ mol^{-1}	Farquhar et al., 1980
$F_{x_{i,j}}$	3.45	0.64 (leaf)	g C g C^{-1}	McCree, 1988
	3.45	0.76(stalk, grain)	g C g C^{-1}	McCree, 1988
		Soil		
P$_{Si,j,c}$	3.49	1.0 (Protein)	g C g C^{-1} h^{-1}	Grant et al., 2001c
	3.49	1.0 (Carbohydrate)	g C g C^{-1} h^{-1}	Grant et al., 2001c
	3.49	0.15 (Cellulose)	g C g C^{-1} h^{-1}	Grant et al., 2001c
	3.49	0.025 (Lignin)	g C g C^{-1} h^{-1}	Grant et al., 2001c
	3.49	0.025 (Active OM))	g C g C^{-1} h^{-1}	Grant et al., 2001c
	3.49	0.005 (Humus)	g C g C^{-1} h^{-1}	Grant et al., 2001c
$K_{mSi,c}$	3.49	75	g C Mg^{-1}	Grant and Rochette, 1994c
$K_{mZi,c}$	3.50	150	g C Mg^{-1}	Grant and Rochette, 1994c
K_{mPc}	3.55	0.35	g C m^{-3}	Grant and Rochette, 1994c
$R_{gi,c}'$	3.55	0.25	g g^{-1} h^{-1}	Ridge, 1976; Shields et al., 1974
R$_m$	3.56	0.015	g C g N^{-1} h^{-1}	Grant and Rochette, 1994c
C_{N_j}	3.61	0.125	g N g C^{-1}	Grant and Rochette, 1994c

3.3.2 Model output

All model outputs were given in two types of file, plant files and soil files, both of which were given in daily and hourly time steps. The energy and carbon exchanges were calculated as the sums of those from plant and soil files. The model outputs related to this study include:

1) Energy exchange: net radiation (W m^{-2}) (Eq. 3.3, 3.4), latent heat (W m^{-2}) (Eq. 3.5-3.7), sensible heat (W m^{-2}) (Eq. 3.8, 3.9), ground heat storage (W m^{-2}) (Eq. 3.13-3.15), canopy temperature (°C).

2) Water relations: crop transpiration (mm h^{-1}), soil evaporation (mm h^{-1}), canopy water potential (MPa), canopy turgor (MPa), boundary layer resistance (s m^{-1}), canopy stomatal resistance (s m^{-1}).

3) CO_2 exchange: CO_2 fixation of leaf and canopy (μmol m^{-2} s^{-1}) (Eq. 3.40), autotrophic respiration (μmol m^{-2} s^{-1}) (Eq. 3.41-3.44), heterotrophic respiration (μmol m^{-2} s^{-1}) (Eq. 3.55).

4) Crop growth: biomass accumulation (shoot and root) (g C m^{-2}) (Eq. 3.45), leaf area (m^2 m^{-2}), grain yield (g C m^{-2}), canopy height (m).

5) Soil: soil temperature (°C), soil water content (m^3 m^{-3}), soil water potential (MPa).

3.4 Model test

3.4.1 Diurnal energy and CO_2 exchange

The model was first initialized with the site information, soil attributes (Table 3.1), crop attributes (Table 3.2), soil management information, crop management information from the field experimental site (see Field Experiment in **Chapter 2**). The model was then run with meteorological data recorded from 1990 to 2000 under two barley-fallow rotations that followed those at the field site in Lethbridge (Table 3.3). The barley-fallow system at Lethbridge was established after 1993, prior to which the

experimental fields were continuously cropped. In order to simulate energy and carbon exchange over this cropping system, the model was run under continuous barley before 1993, and then under barley-fallow afterwards. Comparison of modeled versus measured Rn, LE, H, and CO_2 fluxes were made during the selected periods with different soil water levels in 1996 and 1998 (see **Chapter 4, 5**).

3.4.1.1 Energy flux comparison

Hourly net radiation (W m^{-2}) (Eq. 3.3, 3.4), latent heat (W m^{-2}) (Eq. 3.5-3.7), and sensible heat (W m^{-2}) (Eq. 3.8, 3.9) fluxes from model output for crop and soil were added to give the energy fluxes of the soil-plant-atmosphere continuum in the barley-fallow system. These fluxes were compared with the measured half-hourly fluxes (Eq. 2.3, 2.4) from the BREB methods.

3.4.1.2 CO_2 flux comparison

Modeled hourly CO_2 fluxes include CO_2 fixation of leaf and canopy (μmol m^{-2} s^{-1}) (Eq. 3.40), autotrophic respiration (μmol m^{-2} s^{-1}) (Eq. 3.41-3.44), heterotrophic respiration (μmol m^{-2} s^{-1}) (Eq. 3.55). The algebraic sums of these fluxes give the CO_2 fluxes. These modeled CO_2 fluxes were compared with those from the measurements by BREB methods (Equation 2.11).

Table 3.3 The cropping system scenarios of the simulation study at Lethbridge

1990	1991	1992	1993	1994	1995	1996	1997	1998	1999	2000
Barley	Barley	Barley	Barley	Barley	Fallow	Barley	Fallow	Barley	Fallow	Barley
Barley	Barley	Barley	Barley	Fallow	Barley	Fallow	Barley	Fallow	Barley	Fallow

3.4.2 Seasonal CO_2 exchange and annual carbon balance

Comparison of modeled versus measured daily net CO_2 exchanges, season phytomass accumulation, annual GPP (gross primary productivity), NPP(net primary productivity), NEP(net ecosystem productivity) and NBP (net biome primary

productivity) were made in 1996 and 1998 to examine the seasonal CO_2 exchange and annual carbon balance.

3.4.2.1 Daily net CO_2 exchange

The comparison of modeled and measured seasonal CO_2 exchange was achieved by comparing the daily net CO_2 exchanges. Daily net CO_2 exchanges were obtained by aggregating half-hourly (measured) and hourly (simulated) CO_2 fluxes into daily totals. Detailed comparison can be found in **Chapter 5**.

3.4.2.2 Annual carbon balance

Modeled values of V_X of all leaf surfaces (Eq. 3.40) in the canopy were added to give a value for canopy gross primary productivity (GPP). Autotrophic respiration (R_a) (including canopy and root respiration) (Eq. 3.41-3.44) were subtracted from GPP to get a value for net primary productivity (NPP). To calculate the net ecosystem productivity (NEP), heterotrophic respiration (R_h) (Eq. 3.58) was subtracted from NPP. Grain yield removal was subtracted from NEP to calculate net biome productivity (NBP). These fluxes were compared with those estimated from the measurements with the BREB methods, to evaluate annual carbon balance of the barley-fallow system in 1996 and 1998.

The following equations were used to calculate annual carbon balance:

$$NPP = GPP - R_a \tag{3.65}$$

$$NEP = NPP - R_h \tag{3.66}$$

$$NBP = NEP - Harvest \tag{3.67}$$

where harvest is harvested grain yield which is removed from the ecosystem. The unit for all items in above Equations is $g\ C\ m^{-2}$.

3.4.2.3 Biomass accumulation

73

Modeled biomass accumulation (time integral of Eq. 3.45) (including above ground and below ground) and leaf area index (LAI) were compared with the biomass data measured weekly in the field.

3.4.2.4 Soil water content

Soil water content in *ecosys* was calculated using the water balance equation (Eq. 3.68), and was compared with the soil moisture measured with the gravimetric method and with a neutron probe during the growing season in 1996 and 1998.

Soil water contents were calculated in the model as:

$$\Delta W = P - (ET + R_O + D_R + U_i) \tag{3.68}$$

where ΔW is change in soil water content; ET is evapotranspiration (calculated from LE_i, LV_i and LE_g in Eq. 3.5-3.7); R_O is runoff; D_R is drainage; U_i is root uptake (Eq. 3.19).

3.5 Model prediction of long-term soil carbon dynamics

Land use practices that involve soil disturbance and removal of vegetation have been widely observed to cause losses of soil carbon to the atmosphere. However, the effect of the land use on soil carbon over a long period and under future climate conditions is still uncertain. To predict soil carbon dynamics of the crop-fallow system over a long period and under future possible climates, the model was run for 100 years (from 1991 to 2090) under current climate versus climate change scenarios.

The model was run under a current climate scenario by repeating the current 10-year meteorological data (from 1991 to 2000) 10 times to get the modeled fluxes in 100 years (from 1991 to 2090). The climate change scenario was developed from the results of CRCM-II (Canadian Regional Climate Model) (Laprise et al., 1998) under the IS92a emissions scenario in which atmospheric CO_2 concentration was assumed to double in 100 years (Table 3.4). This rise in CO_2 concentration caused rises in seasonal temperatures that varied from $0.015\,^{\circ}C\ yr^{-1}$ during October to December to $0.041\,^{\circ}C\ yr^{-1}$

from January to March, and changes in seasonal precipitation that varied from -0.17% yr^{-1} from July to September, to 0.23% yr^{-1} from April to June. Relative humidity did not change, and wind speed decreased by 9.5% only during October to December. These changes were implemented hourly to create gradual climate change during 10 cycles of 1991-2000 climate data, to obtain a 100-year model run. Results for soil C storage under this climate change scenario were compared with those modeled under the current climate scenario.

Table 3.4 The change of temperature, precipitation, wind speed, CO_2 concentration under climate change scenario from CRCM-II

Period	Max. temperature ($^\circ$C yr.$^{-1}$)	Min. temperature ($^\circ$C yr.$^{-1}$)	Precipitation (yr^{-1})	Wind speed (yr.$^{-1}$)	CO_2 concentration (yr.$^{-1}$)
Jan.—Mar.	0.039	0.041	1.000	1.000	1.007
Apr.—Jun.	0.032	0.031	1.002	1.000	1.007
July—Sep.	0.031	0.038	0.998	1.000	1.007
Oct.—Dec.	0.028	0.015	1.001	0.999	1.007

Note: values for temperature represent amount of increase per year; values for precipitation, wind speed, and CO_2 concentration represent the fractional rates of increases.

3.6 Summary

In the study, a process-based model *ecosys* was selected to simulate energy, water and CO_2 exchange through the soil-plant-atmosphere continuum of a barley-fallow system in Lethbridge, and it was also used with the outputs from the Canadian Regional Climate Model (CRCM-II) to study the effect of climate change on long-term soil carbon dynamics under a crop-fallow rotation. The boundary conditions of the model run were determined by meteorological, site and topographic conditions, which were represented in a meteorological file, a site file and a topographic file, respectively. Meteorological data provided by Lethbridge Research Center, Agriculture and Agri-Food Canada, were converted to a meteorological file in a format required by the model

to set the meteorological conditions. A soil file was created to represent the soil characteristics of the experimental site (Table 3.1), and a crop file was built to represent the crop physiological and phonological attributes (Table 3.2). Agricultural activities including soil and crop management were represented by a soil management and a crop management file, respectively, which were created according to the filed experiments (see **Chapter 2**). Simulated results from the model *ecosys* are presented in the following two Chapters.

References

Abramopoulos, F., Rosenzweig, C., Choudhury, B., 1988. Improved ground hydrology calculation for global climate change models (GCMs): Soil water movement and evapotranspiration. J. Climate 1, 921-941.

Akinremi O.O., McGinn S.M., McLean, H.D.J., 1999. Effects of soil temperature and moisture on soil respiration in barley and fallow plots. Can. J. Soil Sci. 79, 5-13.

Amthor, J.S., 1994. Scaling CO_2 – photosynthesis relationships from the leaf to the canopy. Photosynth. Res. 39, 321-350.

Baldocchi, D.D., 1993. Scaling water vapor and carbon dioxide exchange from leaves to canopy: rules and tools. In: Ehleringer, J.R., Field, C.B., (Eds.), Scaling Photosynthesis Processes, Leaf to Global. Academic Press. San Diego, USA.

Ball, J.T., Woodrow, I.E., Berry, J.A., 1987. A model predicting stomatal conductance and its contributions to the control of photosynthesis under different environmental conditions. In: Biggens, J. (Ed.), Progress in Photosynthesis Research, vol. IV, Martinus Nijhoff, Dordrecht, The Netherlands, 221-225.

Barber, S.A., Cushman, J.H., 1981. Nitrogen uptake model for agronomic crops. In: Iskandar, I.K. (ed.), Modeling wastewater renovation-land treatment. Wiley-Interscience, New York.

Bounoua, L., Collatz, G.J., Sellers, P.J., Randall, D.A., Dazlich, D.A., Los, S.O., Berry, J.A., Fung, J., Tucker, C.J., Field, C.B., Jensen, T.G., 1999. Interactions between

vegetation and climate: radiative and physiological effects of doubled atmosphere CO_2. Journal of Climate. 12, 309-324.

Bremer, E., Janzen, H.H., Johnston, A.M., 1994. Sensitivity of total, light fraction and mineralizable organic matter to management practices in a Lethbridge soil. Can. J. Soil Sci. 74, 131-138.

Bridgham, S.D., Richardson, C.J., 1992. Mechanisms controlling soil respiration (CO_2 and NH_4) in southern peatlands. Soil Biol. Biochem. 27, 279-286.

Broder, M.W., Wagner, G.H., 1988. Microbial colonization and decomposition of corn, wheat and soybean residue. Soil Sci. Soc. Am. J. 52, 112-117.

Cernusca, A., Bahn, M., Chemini, C., Graber, W., Siegwolf, R., Tappeiner, U., Tenhunen, J., 1998. ECOMONT: a combined approach of field measurements and process-based modelling for assessing effects of land-use changes in mountain landscape. Ecol. Model. 113, 167-178.

Collatz, G.J., Ball, J.T., Grivet, C., Berry, J.A., 1991. Physiological and environmental regulation of stomatal conductance, photosynthesis and transpiration: A model that includes a laminar boundary layer. Agric. For. Meteorol. 54, 107-136.

Cowan, I.R., 1965. Transport of water in the soil-plant-atmosphere system. J. Appl. Ecol. 2, 221-239.

de Pury, D.G.G., Farquhar, G.D., 1997. Simple scaling of photosynthesis from leaves to canopies without the errors of big-leaf models. Plant Cell Environ. 20, 527-557.

de Vires D.A., 1963. Thermal properties of soils. In: R. van Wijk (ed.), Physics of Plant Environment. North Holland Publishing, Amsterdam, The Netherlands, 210-235.

de Wit, C.T., 1978. Simulation of assimilation, respiration and transpiration of crops. John Wiley &Sons, New York.

Dickinson, R.E., 1995. Land surface processes and climate modeling. Bulletin of the American Meteorological Society, Vol. 76, 1445-1448.

Dickinson, R.E., Henderson-Sellers, A., Kennedy, P.J., Giorgi, F., 1992. Biosphere-Atmosphere Transfer Scheme (BATS) version 1e as coupled to the NCAR Community Climate Model, Center for Atmosphere Research, Boulder, CO, Tech Note.

Dickinson, R.E., Henderson-Sellers, A., Kennedy, P.J., Wilson, M.F., 1986. Biosphere-Atmosphere Transfer Scheme (BATS) for the NCAR Community Climate Model, National Center for Atmosphere Research, Boulder, CO, Tech Note/TN-275+STR.

Douglas, B.J., Ogren, W.L., 1984. The CO_2/O_2 specificity of ribulose 1, 5-bisphosphate carboxylase/oxygenase. Planta, 161, 308-313.

Ehleringer, J.R., Field, C.B., (Eds.), 1993. Scaling photosynthesis processes, leaf to global. Academic Press. San Diego, USA.

Enrique, G., Braud, I., Jean-Louis, T., Michel, V., Pierre, B., Jean-Christophe, C., 1999. Modelling heat and water exchanges of fallow land covered with plant-residue mulch. Agric. Forest Meteorol. 97, 151-169.

Evans, J.R., Farquhar, G.D., 1991. Modeling canopy photosynthesis from the biochemistry of C_3 chloroplast. In: Boote, K.J., Loomis, R.S., (Eds.), Modeling crop photosynthesis from biochemistry to canopy. CAAS special publication number 19, 1-15.

Farquhar, G.D., 1989. Models of integrated photosynthesis of cells and leaves. Phil. Trans. Soc. Lond. B. 323, 357-367.

Farquhar, G.D., von Caemmerer, S., 1982. Modeling of photosynthetic response to environment. In: Encyclopedia of plant physiology. Lange, O.L., et al. (Eds.), new Ser. Vol. 12 B. Physiological Plant Ecology II. Spring-Verlag, Berlin. 549-587.

Farquhar, G.D., von Caemmerer, S., and Berry, J.A., 1980. A biological model of photosynthetic CO_2 assimilation in leaves of C_3 species. Planta 149, 78-90.

Goudriaan, J., 1977. Crop micrometeorology: a simulation study. Centre for Agriculture Publishing and Documentation, Wageningen, the Netherlands.

Grahammer, K., Jawson, M.D., Skopp, J., 1991. Day and night soil respiration from a grassland. Soil Biol. Biochem. 23, 77-81.

Grant, F.R., 1999. Simulation of methanotrophy in the mathematical model *ecosys*. Soil Biol. Biochem. 31, 287-297.

Grant, R.F, Nalder, I.A., 2000. Climate change effects on net carbon exchange of a boreal aspen-hazelnut forest: Estimates from the ecosystem model *ecosys*. Global Change Biol. 6, 183-200.

Grant, R.F., 1993a. Simulation model of soil compaction and root growth. (1). Model development. Plant Soil 150, 1-14.

Grant, R.F., 1993b. Simulation model of soil compaction and root growth. (2). Model testing. Plant Soil 150, 15-24.

Grant, R.F., 1994. Simulation of ecological controls on nitrification. Soil Biol. Biochem. 26, 305-315.

Grant, R.F., 1995a. Salinity, water use and yield of maize: testing of the mathematical model *ecosys*. Plant Soil 172, 309-322.

Grant, R.F., 1995b. Mathematical modeling of nitrous oxide evolution during nitrification. Soil Biol. Biochem. 27, 1117-1125.

Grant, R.F., 1997. Changes in soil organic matter under different tillage and rotation: Mathematical modeling in *ecosys*. Soil Sci. Soc. Am. J. 61, 1159-1174.

Grant, R.F., 1998. Simulation in *ecosys* of root growth response to contrasting soil water and nitrogen. Ecol. Model. 107, 237-264.

Grant, R.F., 2001. A review of the Canadian ecosystem model-*ecosys*. CRC press.

Grant, R.F., Garcia, R.L., Pinter, P.J. Jr., Hunsaker, D., Wall, G.W., Kimball, B.A., LaMorte, R.L., 1995. Interaction between atmospheric CO_2 concentration and water deficit on gas exchange and crop growth: Testing of *ecosys* with data from the Free Air CO_2 Enrichment (FACE) experiment. Global Change Biology 1, 443-454.

Grant, R.F., Black, T.A., den Hartog, G., Berry, J.A., Neumann, H.H., Blanken, P.D., Yang, P.C., Russell, C., Nalder, I.A., 1999a. Diurnal and annual exchanges of mass and energy between an aspen-hazelnut forest and the atmosphere: Testing the mathematical model *ecosys* with data from the BOREAS experiment. J. Geophys. Res. 104, 27699-27717.

Grant, R.F., Heaney, D.J., 1997. Inorganic phosphorus transformation and transport in soils: mathematical modelling in *ecosys*. Soil Sci. Soc. Am. J. 61, 752-764.

Grant, R.F., Hesketh, J.D., 1992. Canopy structure of maize (*Zea mays* L.) at different population: Simulation and experimental verification. Biotronics 21, 11-24.

Grant, R.F., Juma, N.G., McGill, W.B., 1993a. Simulation of carbon and nitrogen transformations in soils: I. Mineralization. Soil Biol. Biochem. 27, 1317-1329.

Grant, R.F., Juma, N.G., McGill, W.B., 1993b. Simulation of carbon and nitrogen transformations in soils: II. Microbial biomass and metabolic products. Soil Biol. Biochem. 27, 1331-1338.

Grant, R.F., Juma, N.G., Robertson, J.A., Izaurralde, R.C., McGill, W.B., 2001a. Long-term changes in soil carbon under different fertilizer, manure, and rotation: testing the mathematical model ecosys with data from the Breton plots. Soil Sci. Soc. Am. J. 65, 205-214.

Grant, R.F., Kimball, B. A., Brooks, T.J., Wall, G.W., Pinter, P.J., Hunsaker, D.J., Adamsen, F.J., Lamore, R.L., Leavitt, S.W., Thompson, T.L., Matthias, A.D., 2001b. Modeling the interactions among carbon dioxide, nitrogen, and climate on energy exchange of wheat in a free air carbon dioxide experiment. Agron. J. 93, 638-649.

Grant, R.F., Jarvis, P.G., Massheder, J.M., Hale, S.E., Moncrieff, J.B., Rayment, M., Scott, S.L., Berry, J.A., 2001c. Controls on carbon and energy exchange by a black spruce-moss ecosystem: Testing the mathematical model Ecosys with data from the BOREAS experiment. Global Biogeochemical Cycles 15, 129-147.

Grant, R.F., Nyborg, M., Laidlaw, J., 1993c. Evolution of nitrous oxide from soil. I. Model development. Soil Sci. 156, 259-265.

Grant, R.F., Nyborg, M., Laidlaw, J., 1993d. Evolution of nitrous oxide from soil. II. Experimental results and model testing. Soil Sci. 156, 266-277.

Grant, R.F., Pattey, E., 1999. Mathematical modeling of nitrous oxide emissions from an agricultural field during spring thaw. Global Biogeochemistry Cycles. 13, 679-694.

Grant, R.F., Robertson, J.A., 1997. Phosphorus uptake by root systems: mathematical modelling in ecosys. Plant Soil 188, 279-297.

Grant, R.F., Rochette, P., 1994. Soil microbial respiration at different water potentials and temperatures: theory and mathematical modeling. Soil Sci. Soc. Am. J. 58, 1681-1690.

Grant, R.F., Wall, G.W., Kimball, B.A., Frumau, K.F.A., Pinter Jr., P.J., Hunsaker, D.J., Lamorte, R.L., 1999b. Crop water relations under different CO_2 and irrigation:

Testing of *ecosys* with the free air CO_2 enrichment (FACE) experiment. Agric. For. Meteorol. 95, 27-51.

Hanson P.J., Wullschleger, S.D., Bohlman, S.A, Todd, D.E., 1993. Seasonal and topographic patterns of forest floor CO_2 efflux from an upland oak forest. Tree Physiology 13, 1-15.

Janzen, H.H., Johnston, A.M., Carefoot, J.M., Lindwall, C.W., 1997. Soil organic matter dynamics in long-term experiments in Southern Alberta. CRC Press, Inc..

Jarvis, P.G., McNaughton, K.G., 1986. Stomatal control of transpiration: Scaling up from leaf to region. Adv. Ecol. Res. 15, 1-49.

Juma, N.G., Paul, E.A., 1981. Use of tracers and computer simulation techniques to assess mineralization and immobilization of soil nitrogen. In: Simulation of nitrogen behavior of soil-plant system- papers of a workshop models for the behavior of nitrogen in soil and uptake by plant. Wageningen, the Netherlands.

Keulen, H. van, Seligman, N.G., 1987. Simulation of water use, nitrogen nutrition and growth of a Spring wheat. Simulation Monographs. Pudoc, Wageningen.

Kicklighter, D.W., Melillo, J.M., Peterjohn, W.T., Rastetter, E.B., McGuire, A.D., Steudler, P.A., 1994. Aspects of spatial and temporal aggregation in estimating regional carbon dioxide fluxes from temperate forest soils. J. Geophys. Res. 99(D1), 1303-1315.

Kozlowski, T.T., Pallardy, S.G., 1997. Physiology of woody plants. Academic Press, San Diego.

Kull, O., Jarvis, P., 1995. The role of nitrogen in a simple scheme to scale up photosynthesis from leaf to canopy. Plant Cell and Environ. 18, 1174-1182.

Laprise, R., D. Caya, M. Giguere, G. Bergeron, H. Cote, J.-P. Blanchet, G.J. Boer, and N.A. McFarlane, 1998. Climate and Climate Change in Western Canada as simulated by the Canadian Regional Climate Model. Atmos. Oc. 36, 119-167.

Leuning, R., Kelliher, F.M., de Pury, D.G.G., Schulze, E.D., 1995. Leaf nitrogen, photosynthesis, conductance and transpiration: scaling from leaves to canopies. Plant Cell Environ. 18, 1183-1200.

McCree, K.J., 1988. Sensitivity of sorghum grain yield to ontogenetic changes in respiration coefficients. Crop Sci. 28, 114-120.

Monteith, J.L., 1973. Principles of Environmental Physics. Edward Arnold, London.

Noilhan, J., Planton, S., 1989. A simple parameterization of land surface processes for meteorological model. Mon. Wea. Rev. 117, 536-549.

Penning de Vries, F.W.T., Jansen, D.M., ten Berge, H.F.M., Bakema, A., 1989. Simulation of ecophysiological processes of growth in several annual crops. Pudoc, Wageningen.

Penning de Vries, F.W.T., Laar, H.H. van (Eds.), 1982. Simulation of plant growth and crop production. Centre for Agriculture Publishing and Documentation, Wageningen, the Netherlands.

Peterjohn, W.T., Melillo, J.M., Steudler, P.A., Newkirk, K.M., Bowles, F.P., Aber, J.D., 1994. Response of trace gas fluxes and N availability to experimentally elevated soil temperature. Ecol. Appl. 4, 617-625.

Pitman, A.J., 1988. The development and implementation of a new land surface scheme for use in general circulation models. Ph.D. thesis, University of Livepool.

Pitman, A.J., Yang Z.-L., Cogley, J.G., and Henderson-Sellers, A., 1991. Description of Bare Essentials of Surface Transfer for the Bureau of Meteorology Research Center AGCM, BMRC Research Report No. 32, Melbourne, Victoria.

Raich, J.W., Schlesinger, W.H., 1992. The global carbon dioxide flux in soil respiration and its relationship to climate. Tellus 44B, 81-99.

Rajvanshi, R., Gupta, S.R., 1986. Soil respiration and carbon balance in a tropical Dalbergia sissoo forest ecosystem. Flora 178, 251-260.

Raupach, M.R., Finnigan, J.J., 1988. Single-layer models of evaporation from plant canopies are incorrect but useful, whereas multilayer models are correct but useless: discuss. Aust. J. Plant Physiol. 15, 705-716.

Reid, J.B., and Huck, M.G., 1990. Diurnal variation of crop hydraulic resistance: a new analysis. Agron. J. 82, 827-834.

Ridge, E.H., 1976. Studies on soil fumigation. II. Effects on bacteria. Soil Biol. Biochem. 8, 249-253.

Saxton, K.E., 2001. Soil texture triangle, hydraulic properties calculator. http://www.bsyse.wsu.edu/saxton/soilwater.

Sellers, P.J., Berry, J.A., Collatz, G.J., Field, C.B., Hall, F.G., 1992. Canopy reflectance, photosynthesis, and transpiration. III. A reanalysis using improved leaf models and a new canopy integration scheme. Remote Sens. Environ. 42, 187-216.

Sellers, P.J., Mintz, Y., Sud, Y.C., Dalcher, A., 1986. A simple biosphere model (SiB) for use within general circulation models. J. Atmos. Sci. 43, 505-531.

Shackley, S., Young, P., Parkison, S., Wynne, B., 1998. Uncertainty complexity and concepts of good science in climate change modeling: Are GCMs the best tools? Climate Change 38, 159-205.

Sharpe, P.S.H., and DeMichelle, D.W., 1977. Reaction kinetics of poikilothermic development. J. Theor. Biol. 64, 649-670.

Sharpe, P.S.H., DeMichelle, D.W., 1977. Reaction kinetics of poikilothermic development. J. Theor. Biol. 64, 649-670.

Shields, J.A., Paul, E.A., Lowe, W.E., 1974. Factors influencing the stability of labelled microbial materials in soils. Soil Biol. Biochem. 6, 31-37.

Shulten, H.R., Schnitzer, M., 1997. Chemical model structures for soil organic matter and soils. Soil Sci. 162, 115-130.

Soegaard, H., 1999. Fluxes of carbon dioxide, water vapor and sensible heat in a boreal agricultural area of Sweden-scaled from canopy to landscape level. Agric. Forest Meteorol. 98-99, 463-478.

Stewart, J.B., Gay, L.W., 1989. Preliminary modeling of transpiration from the FIFE site in Kansas. Agric. Forest Meteorol. 48, 305-315.

Stroosnijder, L., 1982. Simulation of the soil water balance. In: Penning de Vries F.W.T., van Laar, H.H. (Eds.): Simulation of plant growth and crop production. Centre for Agriculture Publishing and Documentation, Wageningen, 175-193.

Tappeiner, U., Cernusca, A., 1998. Model simulation of spatial distribution of photosynthesis in structurally differing plant communities in the Central Caucasus. Ecol. Model. 113, 201-223.

Thierron, V., Laudelout, H., 1996. Contribution of root respiration to total CO_2 efflux from the soil of a deciduous forest. Can. J. For. Res. 26, 1142-1148.

Thorgeirsson, H., Soegaard, H., 1999. Simulated carbon dioxide exchange of leaves of barley scaled to the canopy and compared to measured canopy flux. Agric. Forest Meteorol. 98-99, 479-489.

Van Gardingen, P.R., Foody, G.M., Curran, P.J., (Eds.), 1997. Scaling-up: From Cell to Landscape. Society of experimental Biology Seminar Series 63. Cambridge University Press, Cambridge.

Verseghy, D.L., 1991. CLASS-A Canadian land surface scheme for GCMs. I. Soil model. International Journal of Climatology 11, 111-113.

Verseghy, D.L., McFarlane, N.A., Lazare, M., 1993. CLASS-A Canadian land surface scheme for GCMs. II. Vegetation model and coupled runs. International Journal of Climatology 13, 347-370.

Wang, S., 2000. Modeling water, carbon, and nitrogen dynamics in CLASS-Canadian Land Surface Scheme. Ph.D. dissertation, University of Alberta.

Wohlfahrt, G., Bahn, M., Tappeiner, U., Cernusca, A., 2001. A multi-component, multi-species model of vegetation-atmosphere CO_2 and energy exchange for mountain grasslands. Agric. Forest Meteorol. 106, 261-287.

Yang, Z.L., 1992. Land surface processes in 3-dimentaional climate model. Ph.D. thesis, Macquarie University.

Chapter 4 Energy exchange

4.1 Introduction

Energy exchange is among the most important processes in agricultural ecosystems, because it affects variables such as temperature, water transport, plant development and growth, CO_2 fixation and crop productivity (Ham et al., 1991). Calculation of the energy exchange between any ecosystem and atmosphere is one of the major objectives in process-based ecosystem models to be coupled with GCMs. The general equation that sets boundary layer conditions to soil-plant-atmosphere continuum is the energy balance equation of the surface (Larcher, 1995):

$$Rn+LE+H+G+Q_M+Q_P=0 \qquad (4.1)$$

where Rn is net radiation, LE and H are the latent and sensible heat fluxes, respectively, G is soil heat flux, Q_M is turnover in metabolic processes, and Q_P is heat storage by the phytomass, all in W m^{-2}. The convention commonly used for the signs of energy fluxes is positive if directed towards the surface, and negative if directed away from the surface. Despite the significance of metabolism to the plants, the share Q_M of in the overall energy turnover is negligibly small, of the order of 1-2% (Larcher, 1995). The share of Q_P is also comparatively small. For a 3°C h^{-1} change in plant temperature, the sensible heat storage in phytomass Q_P is only 3.2 W m^{-2}. Therefore, in this study, the last two items in equation (4.1) were ignored because of their negligible effects in surface energy balance, yielding a simplified form of the energy balance equation at vegetated surface (Rosenberg et al., 1983; Berge, 1990):

$$Rn+LE+H+G=0 \qquad (4.2)$$

The equation implies that the surface itself has no heat capacity, i.e. no energy can be stored in it. The same assumption is made for canopy volume and phytomass. Also

photochemical energy is not considered. Although these terms are comparatively small, these assumptions may cause errors in estimating H and LE from available energy (Rn-G) by BREB method. Since BREB measures G as only soil heat flux, ignoring changes in thermal storage in vegetation and biomass, which will cause an overestimate of available energy (Rn-G) and a proportional overestimate of sensible heat (H) (Fritschen and Simpson, 1989; Copper et al., 1998), as discussed later in 4.2. However, a number of investigators have compared the sensible heat flux measured with Bowen ration and eddy correlation over rough canopies of forested sites (McNeil and Shuttleworth, 1975; Spittlehouse and Black, 1979, 1980; Shuttleworth et al., 1984; Denmead and Bradley, 1985). Agreement between Bowen ratio and eddy correlation over forested sites was generally found to be within the experimental error of the systems.

There is a strong feedback between energy fluxes and surface properties and environmental conditions. Net radiation, the sum of incoming and outgoing radiation terms, is the fundamental quantity of energy available at the earth's surface to drive the processes of evaporation, air and soil heating and photosynthesis. Rn is affected by soil moisture content, temperature, crop cover and crop development stage, which influence soil albedo, emissivity and emittance. The atmospheric latent and sensible heat fluxes are governed by surface temperature and humidity, and by air temperature and an exchange coefficient. The latter coefficient depends on the magnitude of the sensible heat flux itself (stability), on wind speed, and on surface roughness. The soil heat flux is determined by thermal conductivity and heat capacity of the soil, both of which are functions of soil moisture content (Berge, 1990).

The energy balance is closely linked to ecosystem carbon dioxide exchange because it determines soil and canopy water potentials, which influence stomatal behavior. Stomata control 95%, or more, of the CO_2 and water vapor exchange between the leaf and the atmosphere, which therefore control rates of photosynthesis and transpiration (LE) by the plant (Willmer, 1983). In semi-arid regions where precipitation is limited, soil water status is an important factor regulating stomatal behavior, which in turn determines the energy partitioning between latent and sensible heat. Therefore, understanding energy balance is important to understanding the physiological and biological processes in agriculture ecosystems. In this chapter, we

discuss the daily and seasonal variations of energy exchange of a barley-fallow system, using the framework of the surface energy balance equation (Eq. 4.2).

4.2 Testing modeled energy fluxes

The ecosystem model *ecosys* was used to simulate hourly fluxes of energy (net radiation Rn, latent heat LE, sensible heat H) under measured hourly shortwave radiation, air temperature, humidity, wind speed and precipitation from January 1, 1990 to December 31, 2000. The ability of model *ecosys* to adequately simulate the energy exchange within the SPAC system was assessed by comparing model predictions with independent above-canopy measurements. For this purpose, simulated fluxes were tested against the fluxes measured from two Bowen Ratio systems during the growing seasons of 1996 and 1998 by regressing modeled on measured fluxes. For statistical analysis, half-hourly measured fluxes were aggregated into hourly averages, which were then matched with hourly fluxes computed from the model. An objective test of agreement between modeled and measured fluxes was accomplished by evaluating regression parameters (slope, intercept, correlation coefficient, and standard error of the means) from a linear regression of modeled versus measured fluxes. The results are shown in Table 4.1 and in Fig. 4.1, 4.2. Regression results show that the regressions between measured and modeled fluxes were highly significant.

The accuracy of net radiation (Rn) simulation is very important in computing realistic latent and sensible heat and CO_2 flux densities (Baldocchi and Harley, 1995). A comparison between measured and modeled net radiation flux density (Fig. 4.1a, 4.2a) reveals that net radiation was slightly overestimated by the model at lower values, but was fairly well simulated at higher values, as also indicated by the large intercepts in the linear regression analysis in Table 4.1. In both years, the average of net radiation was overestimated by about 25-30 W m^{-2}, which is in the same range as the typical accuracy of net radiation measurements (Halldin and Lindroth, 1992; Smith et al., 1997). Overestimation of net radiation by the model indicates that either simulated canopy temperatures, and hence the long-wave radiation (emission), or the reflected short-wave radiation (i.e. albedo) are too low. Overall, the slope and intercept obtained from the

least-squares linear regression are 0.95 and 24.91 W m^{-2}, respectively, in 1996, and 0.98 and 28.28 W m^{-2}, respectively, in 1998. The correlation coefficients between modeled and measured Rn are 0.96 and 0.97 in 1996 and 1998, respectively. The standard differences are 39.06 W m^{-2} and 37.10 W m^{-2} in 1996 and 1998, respectively (Table 4.1).

Table 4.1 Results of a linear regression analysis of modeled versus measured fluxes of net radiation (Rn), latent heat (LE), sensible heat (H) and CO_2 fluxes in 1996 and 1998

		Year: 1996			
Parameter	Slope	Intercept (W m^{-2})	r^2	Standard error (W m^{-2})	No. of observations
Rn (W m^{-2})	0.95±0.01	24.91±1.86	0.96	39.06	2137
LE (W m^{-2})	1.19±0.02	-5.28±1.72	0.89	34.28	2020
H (W m^{-2})	0.84±0.01	-19.48±1.39	0.90	28.89	2021
		Year: 1998			
Rn (W m^{-2})	0.98±0.01	28.28±2.23	0.97	37.10	1527
LE (W m^{-2})	1.03±0.02	-21.53±2.94	0.86	47.14	1470
H (W m^{-2})	0.75±0.01	-12.10±2.27	0.80	39.85	1470

Model performance was evaluated by the slope and intercept of a regression line through modeled versus measured fluxes, and by correlation coefficient and standard error of the means.
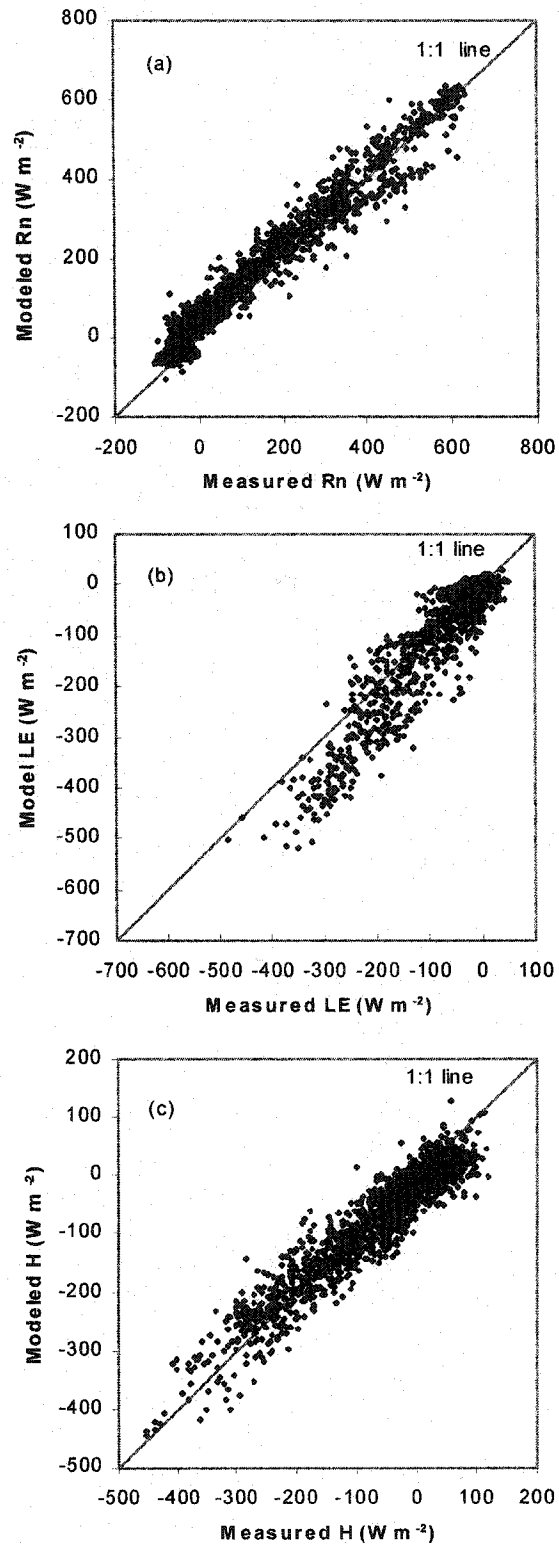
Fig. 4.1 Comparison of measured and modeled: (a) net radiation (Rn), (b) latent heat (LE) and (c) sensible heat (H) from a barley field in 1996.
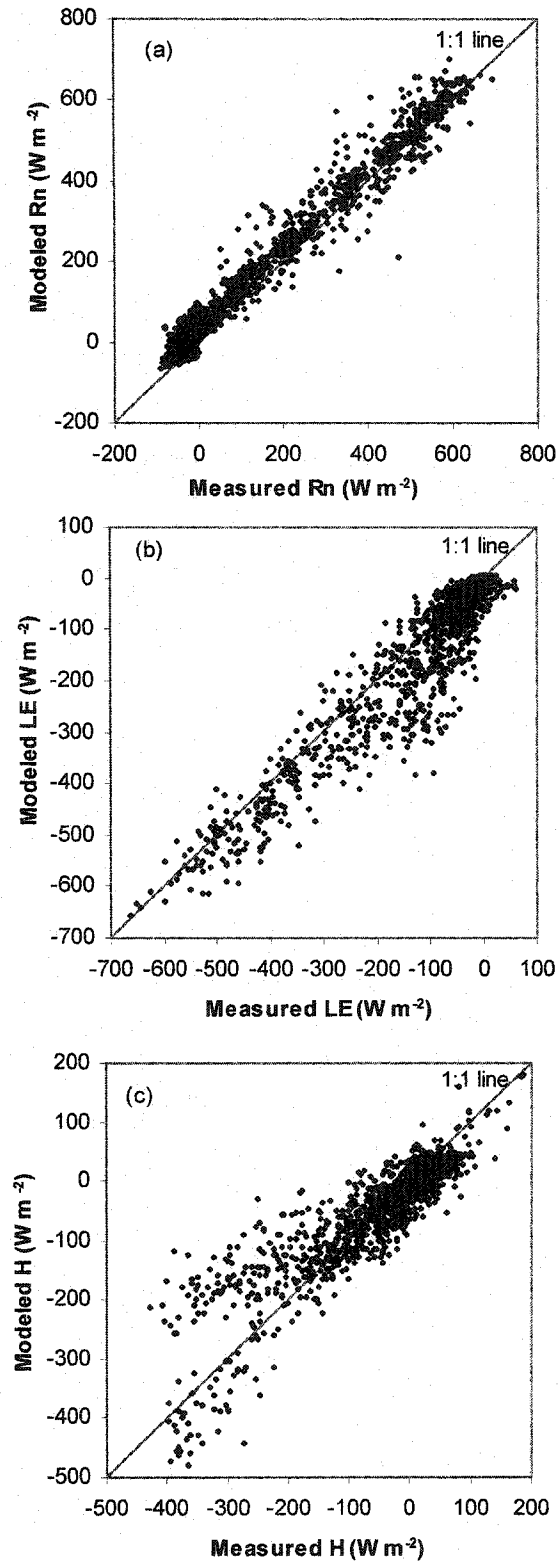
Fig. 4.2 Comparison of measured and modeled: (a) net radiation (Rn), (b) latent heat (LE) and (c) sensible heat (H) from a barley field in 1998.

The latent heat fluxes were slightly overestimated while sensible heat fluxes were slightly underestimated by the model for both years (Fig. 4.1, 4.2, Table 4.1). The average latent heat was overestimated by the model by about 20%, which is equivalent to an absolute difference of 30-40 W m^{-2}. Baldocchi et al. (1988) reported that, due to a range of possible sources of error in sensor responses or in the basic assumptions (uniform fetch, little or no slope, etc.) estimates of LE by the Bowen ratio techniques carry potential errors of 15-20%. Given this measurement accuracy of Bowen ratio techniques, it can be concluded that the model predicted LE within the range of measurement error of BREB. On the other hand, sensible heat fluxes were underestimated by the model at an average of 25-35 W m^{-2}. These modeled results are consistent with the conclusion drawn from field experiments of energy flux measurements, that latent heat was underestimated while sensible heat was overestimated by the Bowen ratio method (Verma et al., 1978; Motha et al., 1979; Rosenberg et al., 1983; Dugas et al., 1991; Cooper et al., 1998). This may be explained by the following:

1) Inequality of heat and water vapor eddy diffusivities (K_v and K_h in Equation 2.5-2.6) under stable atmospheric conditions. Blad and Rosenberg (1974) reported that sensible heat advection caused an inequality of K_v and K_h. Further studies by Verma et al. (1978) and Motha et al. (1979) showed that the eddy diffusivities for heat (K_h) was greater than that for water vapor (K_v) when conditions of regional sensible heat advection prevail. This could result in an underestimation of latent heat flux by BREB measurement. Dugas et al. (1991) compared sensible heat flux measured with Bowen ratio and eddy correlation and found that sensible heat H from Bowen ratio measurements were often larger (more negative) than that from eddy correlation measurements under sensible heat advection. Blad and Rosenberg (1974) observed an underestimation of latent heat fluxes of alfalfa by BREB methods compared with lysimeters in eastern Nebraska under sensible heat advection.

2) Systematic overestimation of available energy (Rn-G). Since BREB measures heat storage G as only soil heat flux, ignoring changes in thermal storage in vegetation and biomass. This will cause a slight overestimate of available energy (Rn-G) and a

proportional overestimate of sensible heat (H) (Fritschen and Simpson, 1989; Cooper et al., 1998). Cooper et al. (1998) compared sensible heat fluxes measured with BREB and eddy correlation system over winter wheat in southern Arizona and found that sensible heat measured by Bowen ratio was systematically larger (more negative) than that by eddy correlation. The Bowen ratio and eddy correlation estimates of sensible heat were closely related over a range of +180 W m^{-2} to -450 W m^{-2}. The best statistical agreement between the two systems occurred when the plant-soil environment was dry and sensible heat flux was larger. In a moist environment, the absolute differences between the two systems were small but the percentage error was large. Cooper et al. (1998) concluded that the unmeasured heat storage gains in the morning hours caused an overestimate of available energy and a proportional overestimate of H by BREB with respect to H by eddy correlation.

Based on the discussion above, we conclude that the underestimation of latent heat and the overestimation of sensible heat fluxes by Bowen ratio method, would therefore cause an apparent overestimation of latent heat (LE) and an apparent underestimation of sensible heat (H) fluxes by the model. These results also indicated that the enclosure of energy balance was achieved in *ecosys*. The slope and intercept from a linear regression line through modeled versus measured LE are 1.19 and -5.28 W m^{-2}, respectively, in 1996, and 1.03 and -21.53 W m^{-2}, respectively, in 1998. The correlation coefficients between modeled and measured LE are 0.89 and 0.86 in 1996 and 1998, respectively. The standard differences are 34.28 W m^{-2} and 47.14 W m^{-2} in 1996 and 1998, respectively (Table 4.1). For the statistical analysis of sensible heat, the slope and intercept of a regression line through modeled versus measured fluxes are 0.84 and -19.48 W m^{-2}, respectively, in 1996, and 0.75 and -12.10 W m^{-2}, respectively, in 1998. The correlation coefficients between modeled and measured H are 0.90 and 0.80 in 1996 and 1998, respectively. The standard differences are 28.89 W m^{-2} and 39.85 W m^{-2} in 1996 and 1998, respectively (Table 4.1).

4.3 Energy exchange

Energy dynamics are discussed using the half-hourly fluxes measured by Bowen ratio systems and hourly fluxes simulated by *ecosys*. These fluxes include net radiation (Rn), latent heat (LE) and sensible heat (H). Although ground heat storage G was measured by BREB and simulated in *ecosys*, this flux was comparatively small and can be regarded as the residue of Rn, LE and H, so it was not included in the following discussion. In the growing seasons of 1996 and 1998, representative periods in which soil water status changed from wet to dry were selected to investigate the dynamics of energy exchange and the corresponding model behavior under different soil water conditions.

4.3.1 Environmental conditions

The years 1996 and 1998 provide two different meteorological conditions, a dry year (1996) and a wet year (1998), respectively (Table 4.2, Fig. 4.3). During 1996, annual precipitation was 269 mm, which was 67% of the average. Precipitation was particularly limited during the growing season with only 90 mm from May to August, which was only about 33% of the annual precipitation in that year, and was about 40% of the growing season average (Table 4.2). By contrast, 1998 was a wetter year with an annual precipitation of 435 mm, which was 109% of the annual average. Moreover, precipitation during the growing season was 315 mm, which was 73% of the annual precipitation in that year, and was about 150% of the growing season average (Table 4.2). Erratic rainfall and drought periods are common to this semi-arid region even though annual precipitation may be near to or exceed long-term average. Relative humidity was similar for both years with higher values during winter and lower values during the crop growing seasons (Fig. 4.3).

93

Table 4.2 The general meteorological conditions in 1996 and 1998

	Mean shortwave Radiation (W m^{-2})	Monthly mean Temperature (°C)	Precipitation (mm) Year	Precipitation (mm) May-August
1996	154	4.0	269	90
1998	162	6.8	435	315
Annual average		5.2	400	212
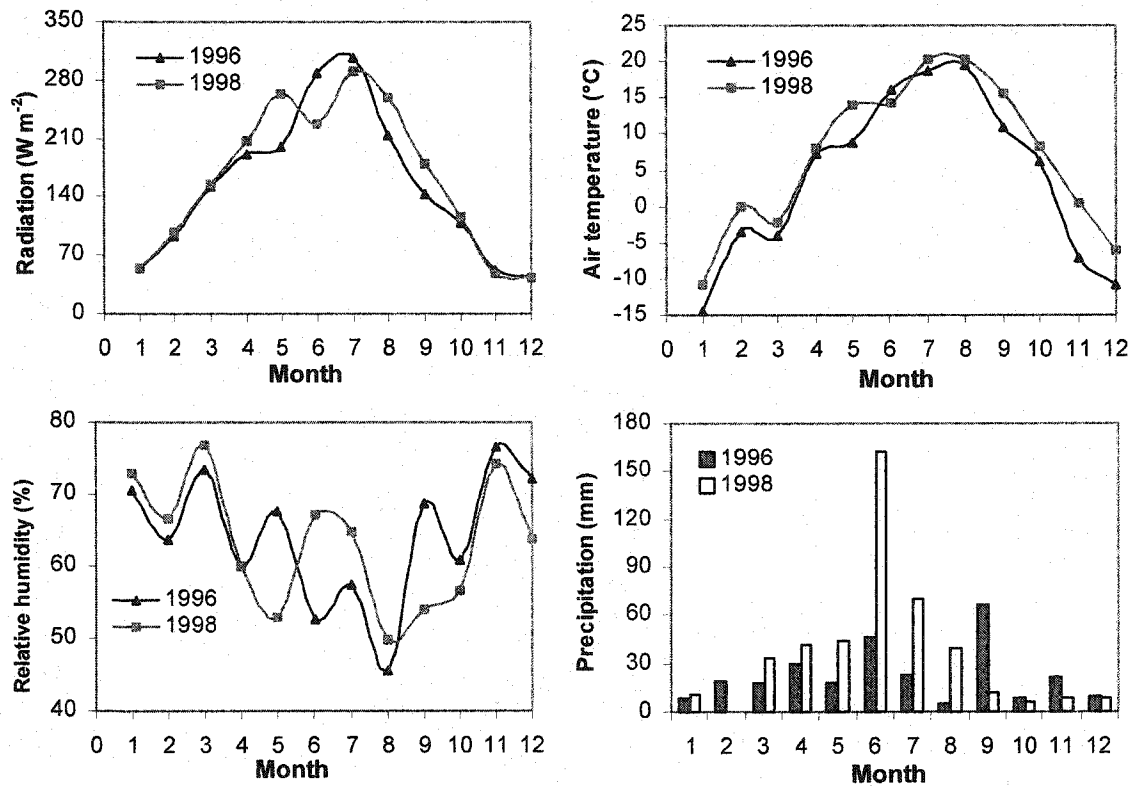
Fig. 4.3 Mean monthly shortwave radiation, air temperature, relative humidity and precipitation in 1996 and 1998.

94
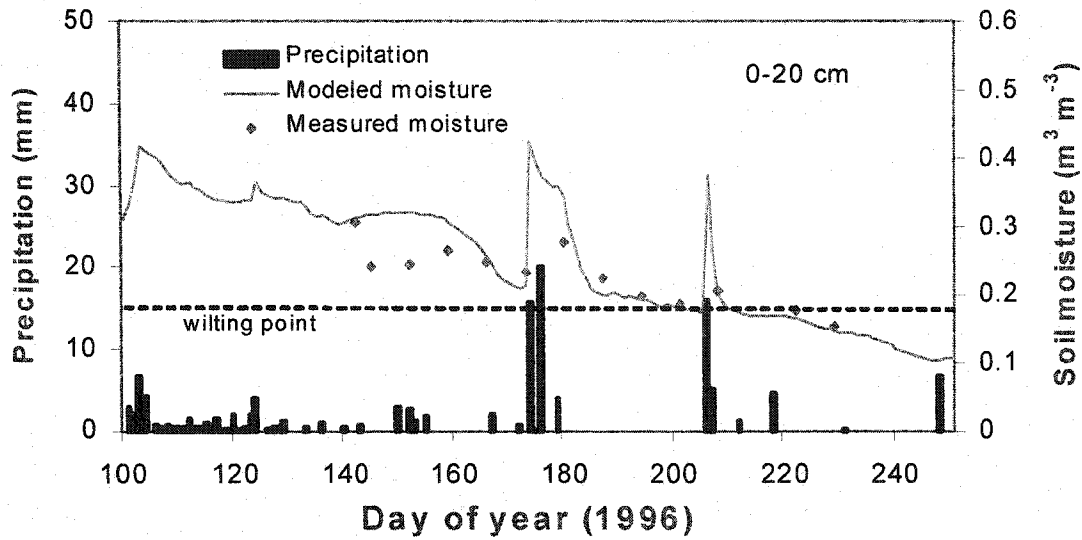
Fig. 4.4 Simulated (lines) and measured (symbols) surface soil moisture in a barley field during the growing season of 1996. Precipitation during corresponding period is shown in column.
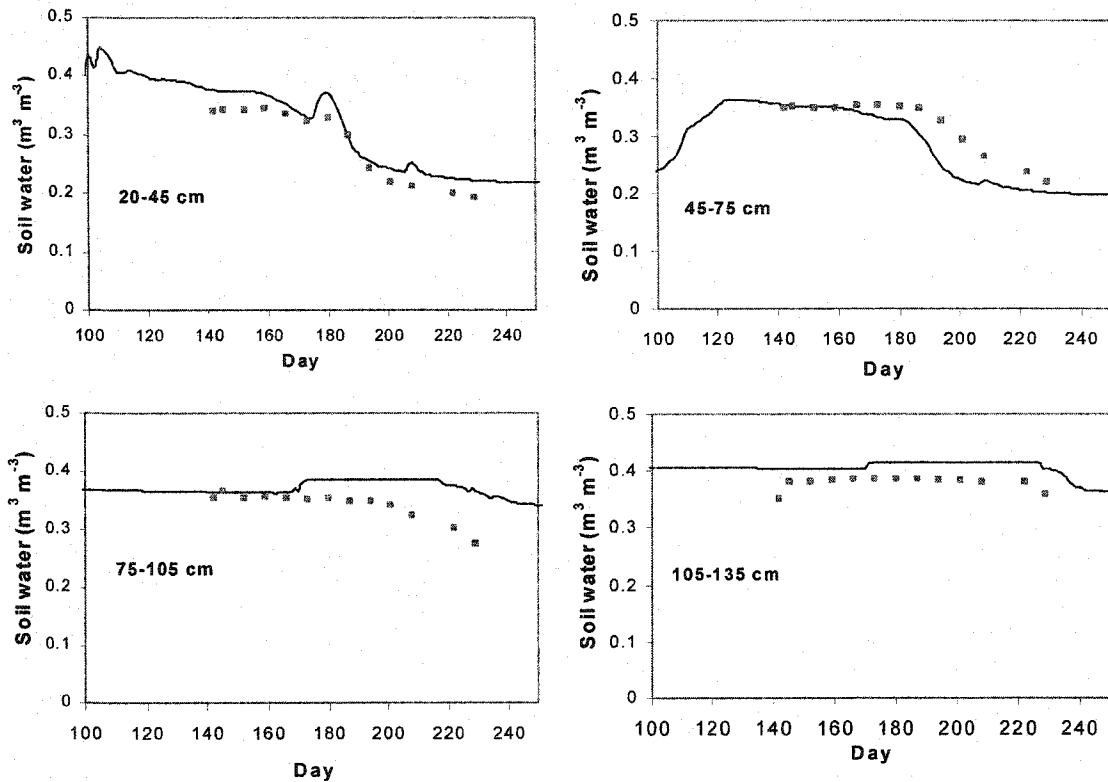
Fig. 4.5 Simulated (lines) and measured (symbols) soil moisture content at different soil layers in a barley field during the growing season of 1996.
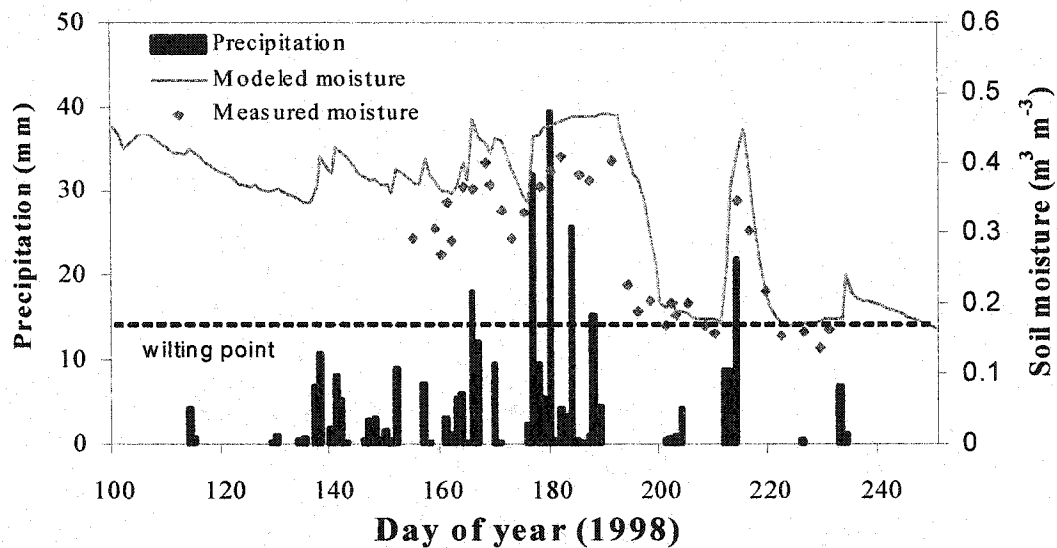
Fig. 4.6 Simulated (lines) and measured (symbols) soil moisture content at surface soil layer (0-5 cm) in a barley field during the growing season of 1998. Precipitation during corresponding period is shown in column.

Mean shortwave radiation was higher in 1998 than that in 1996. Mean monthly shortwave radiation was 154 W m^{-2} in 1996 and 162 W m^{-2} in 1998. Minimum air temperature was -39°C and -36°C in 1996 and 1998, respectively, and maximum air temperature was 34°C and 35°C in 1996 and 1998, respectively. Mean air temperatures were lower than annual average in 1996 and higher in 1998 (Table 4.2, Fig. 4.3). In 1996, mean monthly air temperature ranged from -14.5°C in January to a high of 19.6°C in August, and it ranged from -10.7°C in January to 20.4°C in July and August in 1998.

Fig. 4.4 - 4.6 show the measured and modeled soil water content during the growing seasons of 1996 and 1998. During the crop growing season, soil water content was higher in 1998 than in 1996. In 1996, water stress developed at late July (DOY 210) when soil water content in the upper 20 cm layer was approaching the wilting point (about 0.17 m^3 m^{-3}) (Fig. 4.4). After DOY 210, soil water was taken up from the deeper soil layers (20-105 cm) for crop growth, causing decreases in soil water contents (Fig. 4.5). Below 105 cm soil moisture almost remained stable, indicating it was not

used for crop growth. The soil water status for 1998 was much better (Fig. 4.6), which maintained above the wilting point almost throughout the early and mid-growing seasons. Rainfall in late July caused the water stress to develop later in the growing season (after about DOY 220) when surface soil water content (0-5 cm) declined below the wilting point (Fig. 4.6).

4.3.2 Diurnal energy exchange in 1996

Three periods with different soil water levels in 1996 were selected in order to study the model behavior and variation of energy exchanges during a drying period (from DOY 200 to 230). DOY 200-210 occurred before water stress when the mean soil water content at 0-20 cm layer was 0.21 m^3 m^{-3} (Table 4.3, Fig. 4.4). The surface boundary conditions during this period are plotted in Fig. 4.7. During DOY 200 to 210, solar radiation was very high with daily maximum above 800 W m^{-2}. Both air temperature and relative humidity were rising and precipitation occurred between DOY 206-207. The continuous measured half-hourly fluxes versus simulated hourly fluxes of Rn, LE and H are shown in Fig. 4.8. During this period, both measured and simulated results showed that the radiative energy received by the canopy during daytime was dissipated more as latent heat than as sensible heat (Fig. 4.8, Table 4.3). At this stage, modeled leaf area index was above 3.0, indicating crop fully covered field (Fig. 4.9). Soil moisture rose after rainfall on DOY 206 (Fig. 4.4, 4.7b). During this period, since hydraulic conductivity was simulated exponential to soil water content, high soil water content caused a high hydraulic conductivity (Eq. 3.21), and high soil and root water potential, which resulted in a high canopy potential (Eq. 3.17), and hence high stomatal conductance (Eq. 3.11) that allowed a high transpiration rate to be sustained by the canopy (Eq. 3.5). Therefore, evapotranspiration (LE) was larger than sensible heat (H) (Fig. 4.8). Both modeled and measured results for average energy fluxes showed that during DOY 200-210, about 70% of the net radiation was consumed as latent heat, and 30% as sensible heat (Table 4.3).

Fig. 4.7 Meteorological conditions during DOY 200-210 of 1996.
(a): Shortwave radiation and air temperature; (b): Precipitation and relative humidity.

Fig. 4.8 Comparison of simulated (lines) and measured (symbols) net
radiation (Rn), latent heat (LE), sensible heat (H) from a barley field
before water stress (DOY 200-210) in 1996.

Table 4.3 Comparison of average energy fluxes from a barley field between before water stress, a transition to water tress, and during water stress in the growing season of 1996

Before water stress (DOY 200-210) (mean soil moisture: 0.21 m^3 m^{-3})

	Measured (W m^{-2})			Simulated (W m^{-2})		
	Rn	LE	H	Rn	LE	H
Average	152.7	-100.2	-52.8	196.6	-141.4	-53.9

Transition period (DOY 210-220) (mean soil moisture: 0.17 m^3 m^{-3})

	Measured (W m^{-2})			Simulated (W m^{-2})		
	Rn	LE	H	Rn	LE	H
Average	126.6	-80.5	-47.4	143.2	-78.5	-66.8

Water stress (DOY 220-230) (mean soil moisture: 0.15 m^3 m^{-3})

	Measured (W m^{-2})			Simulated (W m^{-2})		
	Rn	LE	H	Rn	LE	H
Average	107.5	-15.2	-83.7	124.8	-27.5	-90.6
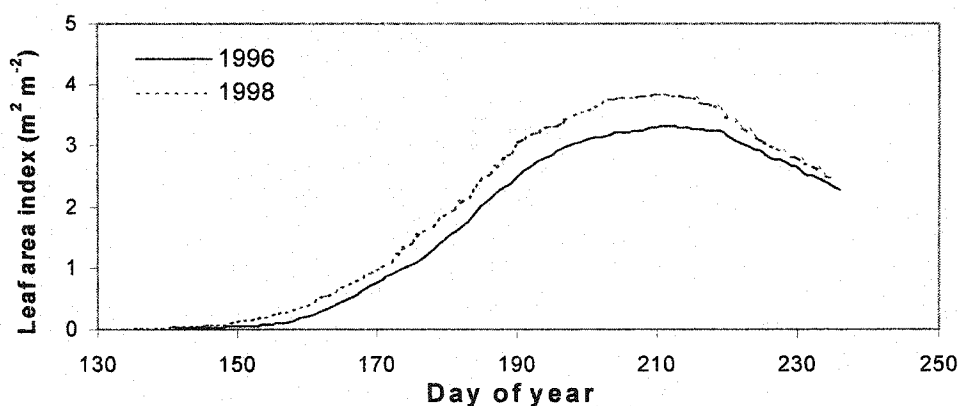
Fig. 4.9 Simulated leaf area index (LAI) of barley in 1996 and 1998.

Fig. 4.10 Meteorological conditions for DOY 210-220 of 1996. (a): Shortwave radiation and air temperature; (b): Precipitation and relative humidity.

Fig. 4.11 Comparison of simulated (lines) and measured (symbols) net radiation (Rn), latent heat (LE), sensible heat (H) from a barley field during a transition to water stress (DOY 210-220) in 1996.
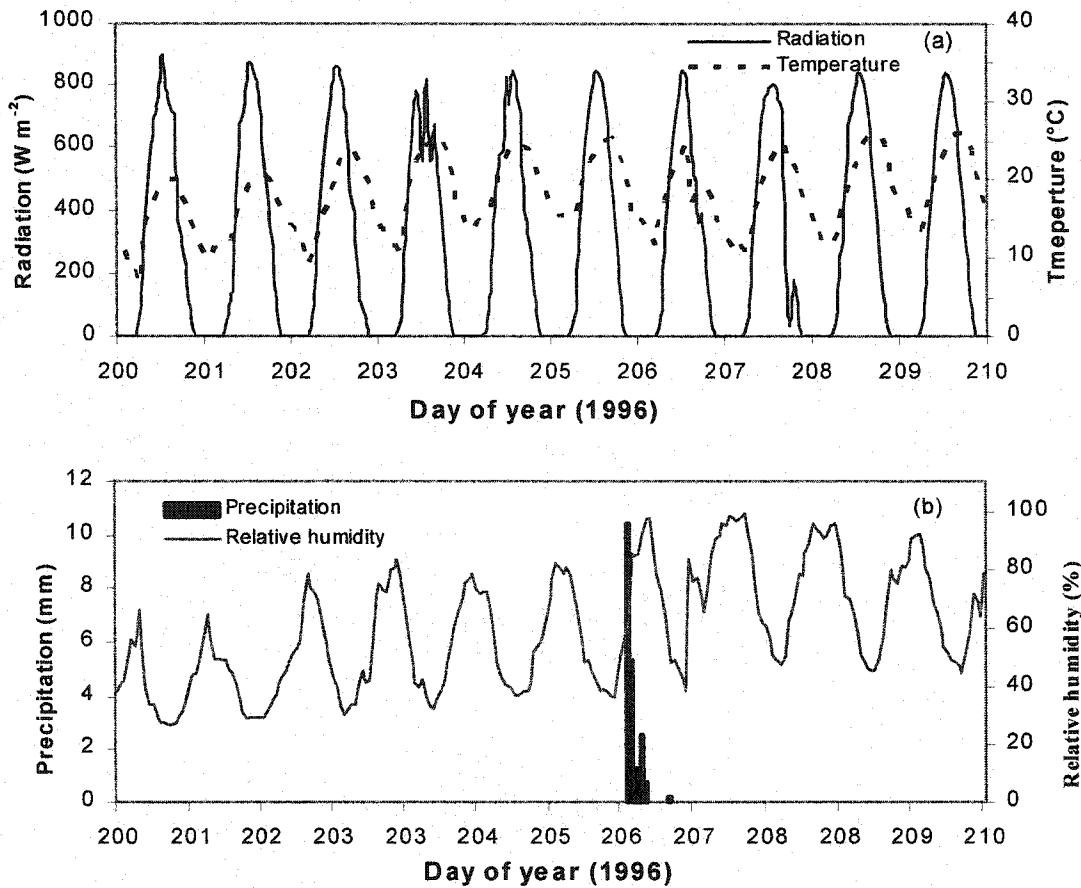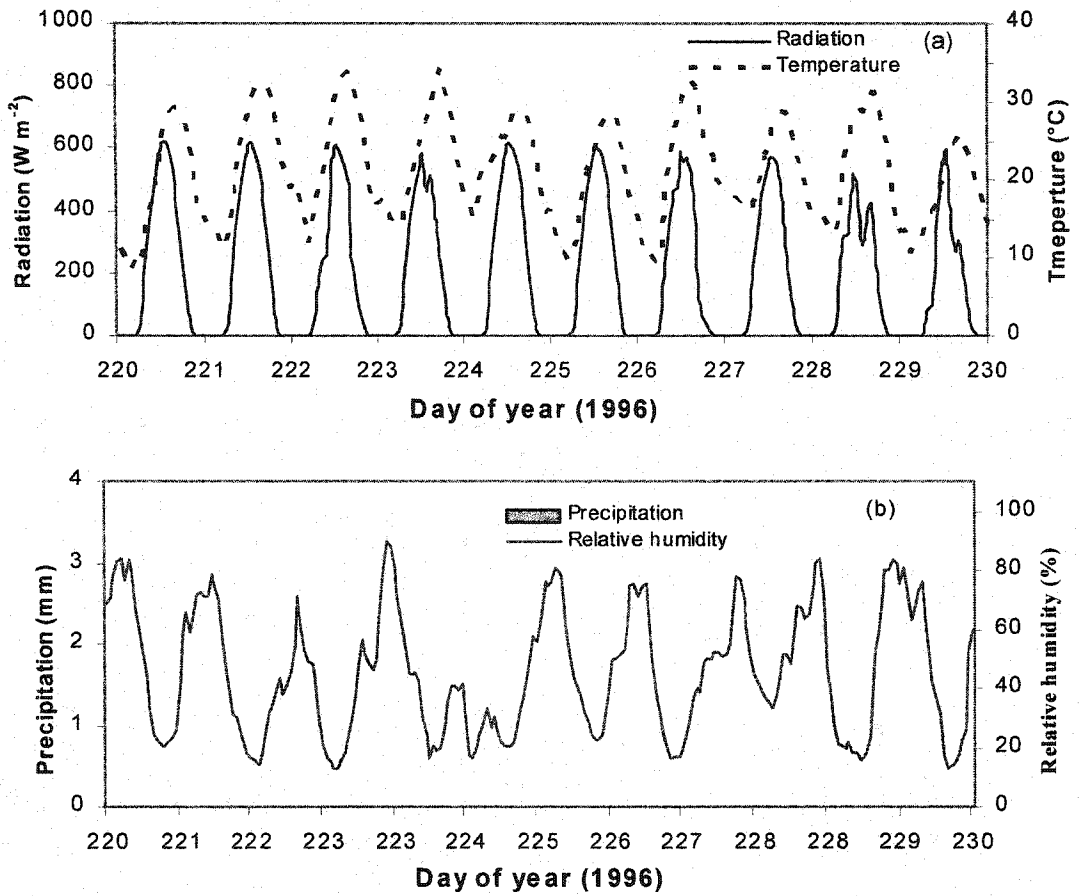
Fig. 4.12 Meteorological conditions for DOY 220-230 of 1996.
(a): Shortwave radiation and air temperature; (b): Precipitation and relative humidity.
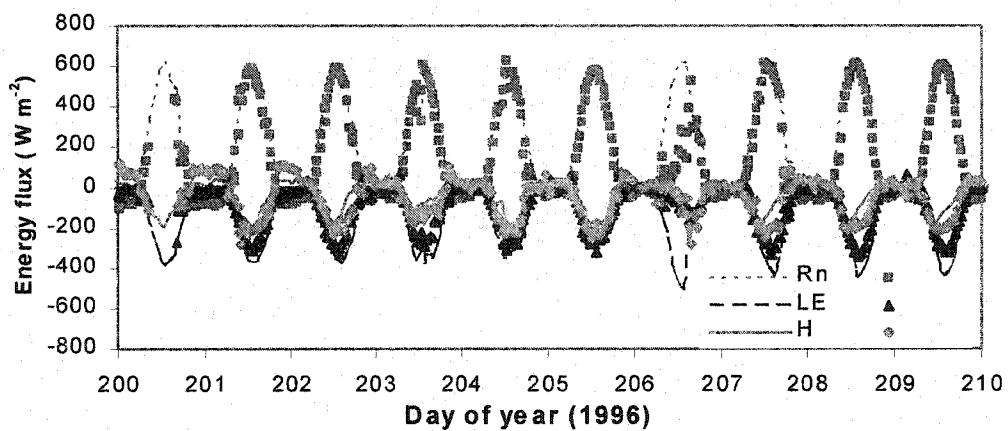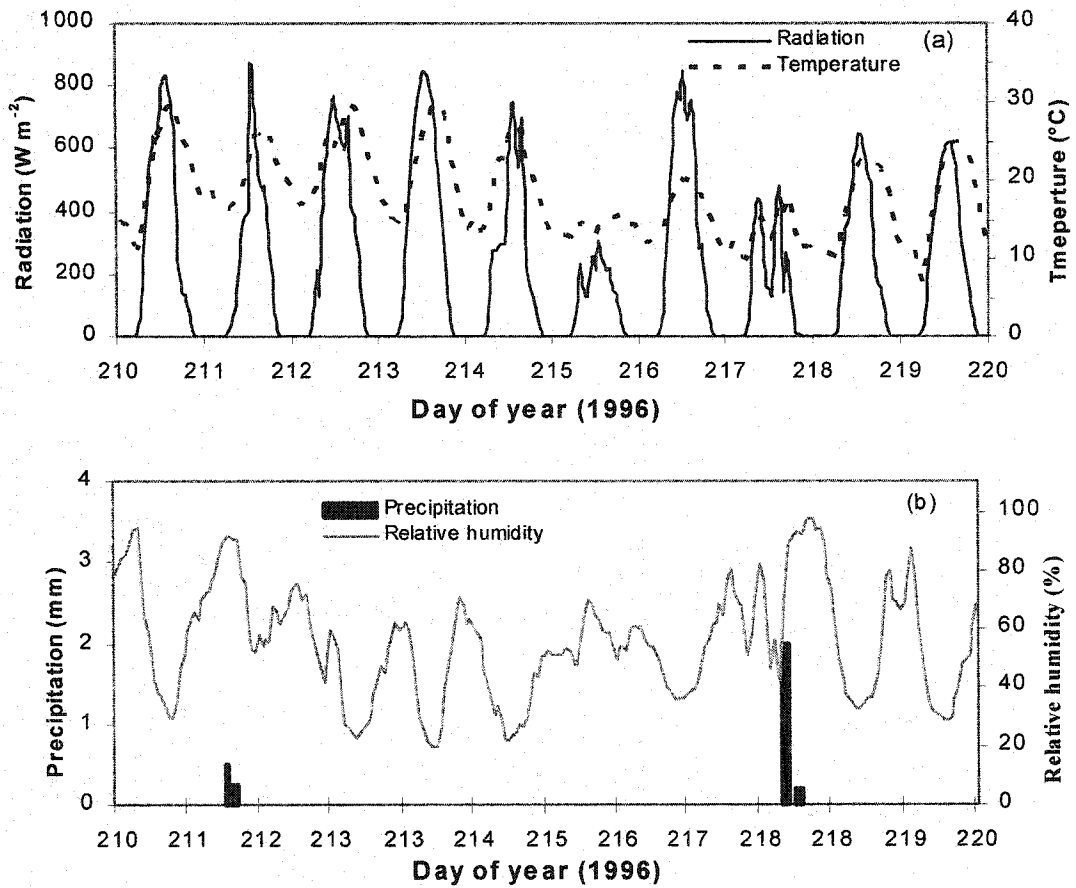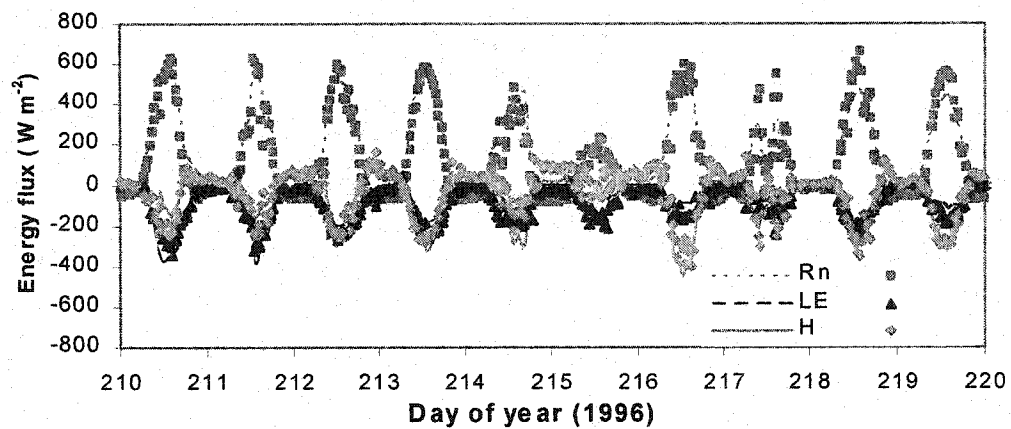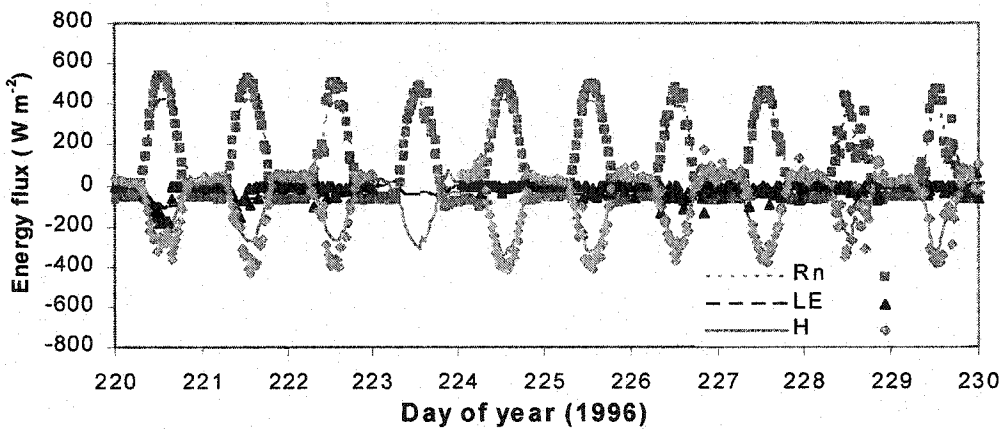

Fig. 4.13 Comparison of simulated (lines) and measured (symbols) net
radiation (Rn), latent heat (LE), sensible heat (H) from a barley field during
water stress (DOY 220-230) in 1996.

Without significant precipitation after DOY 206, soil water content decreased, which made DOY 210-220 a transition period to water stress when soil moisture content at surface soil layers (0-20 cm) approached the wilting point (Fig. 4.4, Table 4.3). The surface boundary conditions during this period are plotted in Fig. 4.10 and the continuous measured half-hourly fluxes versus simulated hourly fluxes of Rn, LE and H are shown in Fig. 4.11. Both solar radiation and air temperature were higher before DOY 215, while relative humidity was lower, causing a large vapor pressure difference between canopy and atmosphere that caused a large LE to be modeled (Eq. 3.5). Therefore, LE was generally larger than H during DOY 210-215 (Fig. 4.11). Both solar radiation and air temperature decreased and relative humidity was relatively higher after DOY 215. The vapor pressure difference between canopy and atmosphere thus declined, causing a lower LE to be modeled after DOY 215 (Eq. 3.5). Therefore LE was lower than H during 215 to 220 (Fig. 4.11). Overall, latent heat flux decreased while sensible heat flux increased during this period (Fig. 4.11). Modeled (measured) average energy fluxes showed that during day 210-220, about 55% (60%) of the net radiation was consumed as latent heat, and 45% (40%) as sensible heat (Table 4.3).

Water stress developed during DOY 220-230 when there was no precipitation and surface soil moisture (0-20 cm) was below the wilting point (Fig. 4.4, 4.12b). The surface boundary conditions during this period are plotted in Fig. 4.12, and the continuous measured half-hourly fluxes versus simulated hourly fluxes of Rn, LE and H are shown in Fig. 4.13. Because of higher temperatures and lower relative humidity (Fig. 4.12), soil water was lost rapidly by evaporation. Solar radiation received by the canopy during daytime was almost dissipated as H, causing very high H and very low LE to be measured (Fig. 4.13). In the model, as soil water content decreased, soil hydraulic conductivity and soil water potential decreased exponentially, forcing decreases in root and canopy water potentials to maintain water uptake (Eq. 3.20). Low canopy water potentials caused low turgor (Eq. 3.17) and thereby high stomatal resistance (Eq. 3.11) and low LE (Eq. 3.5). During this water stress period, average energy fluxes indicated that about 22% (modeled)/15% (measured) of net radiation was consumed as latent heat, while 72% (modeled)/78% (measured) as sensible heat (Table 4.3).

4.3.3 Diurnal energy exchange in 1998

Three comparison periods during a drying period in 1998 (DOY 200-230) were also selected for a study of model behavior and energy exchanges during different soil water levels.

DOY 200 to 210 was a wet period during the growing season of 1998. Precipitation prior to this period was very high, and soil water content at surface layer (0-5 cm) remained above the wilting point (Fig. 4.6), indicating water stress did not occur during this period. The surface boundary conditions during this period are plotted in Fig. 4.14, and the continuous measured half-hourly fluxes versus simulated hourly fluxes of Rn, LE and H are shown in Fig. 4.15. During this period, higher solar radiation and air temperature, and lower relative humidity (Fig. 4.14), together with higher soil water content (Fig. 4.6), caused a higher rate of evapotranspiration (LE). Therefore very high LE and very low H were measured (Fig. 4.15). As discussed above (under 4.3.2), high soil water content caused a high hydraulic conductivity, high soil, root and canopy water potentials, and hence low stomatal resistance. Thus high LE and low H were modeled (Fig 4.15). During this wet period, both measured and modeled results indicated that about 85% of average net radiation (Rn) was consumed as latent heat, and about 10% as sensible heat (Table 4.4).

Higher soil water content in 1998 versus 1996 delayed the onset of water stress. Therefore, DOY 210-220 in the growing season of 1998 was also a wet period with mean soil moisture at 0-5 cm soil layer 0.29 m^3 m^{-3} (Fig. 4.6, Table 4.4). The surface boundary conditions during this period are shown in Fig. 4.16, and the continuous measured half-hourly fluxes versus simulated hourly fluxes of Rn, LE and H are shown in Fig. 4.17. During this period, both solar radiation and air temperature were very high, except for DOY 213 and 214 when rainfall occurred. Relative humidity was also very high before DOY 214 and it decreased rapidly afterwards (Fig. 4.16). Lower radiative energy, lower air temperature, and higher relative humidity caused lower LE to be modeled during DOY 213-214 (Fig. 4.17). Rapid decrease in relative humidity after DOY 214, resulted in a large vapor pressure difference between canopy and atmosphere, together with the high solar radiation and air temperature, causing large LE

fluxes while small H fluxes to have been modeled during DOY 215-220 (Fig. 4.17). Latent heat fluxes started to decrease after DOY 218 mainly because of the increase in relative humidity (Fig. 4.16, 4.17). During the whole period (DOY 210-220), modeled average energy fluxes showed that about 88% of net radiation (Rn) was consumed as latent heat, and only about 12% as sensible heat (Table 4.4).

Table 4.4 Comparison of energy fluxes from a barley field between

dry and wet periods in the growing season of 1998

Before water stress (DOY 200-210) (mean soil moisture: 0.19 m^3 m^{-3})					
	Measured (W m^{-2})			Simulated (W m^{-2})		
Flux	Rn	LE	H	Rn	LE	H
Average	187.2	-157.2	-18.3	201.5	-177.3	-20.8

Transition to water stress (DOY 210-220) (mean soil moisture: 0.29 m^3 m^{-3})					
	Measured (W m^{-2})			Simulated (W m^{-2})		
Flux	Rn	LE	H	Rn	LE	H
Average	n/a	n/a	n/a	170.6	-150.4	-21.7

Water stress (DOY 220-230) (mean soil moisture: 0.17 m^3 m^{-3})					
	Measured (W m^{-2})			Simulated (W m^{-2})		
Flux	Rn	LE	H	Rn	LE	H
Average	136.4	-31.8	-105.4	165.7	-42.	-120.4

Note: n/a means that data are not available.

Fig. 4.14 Meteorological conditions during DOY 200-210 of 1998.
(a): Shortwave radiation and air temperature; (b): Precipitation and relative humidity.

Fig. 4.15 Comparison of simulated (lines) and measured (symbols) net
radiation (Rn), latent heat (LE), sensible heat (H) from a barley field
before water stress (DOY 200-210) in 1998.
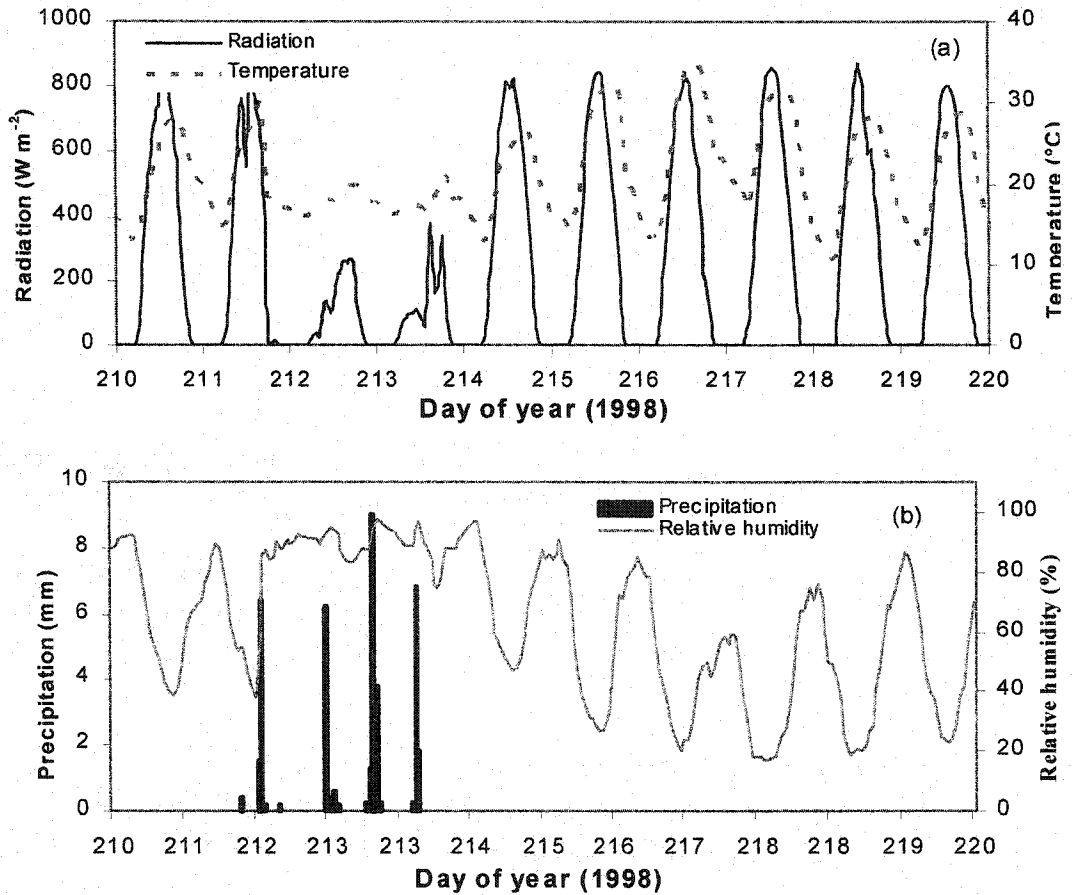
Fig. 4.16 Meteorological conditions for DOY 210-220 of 1998.
(a): Shortwave radiation and air temperature; (b): Precipitation and relative humidity.
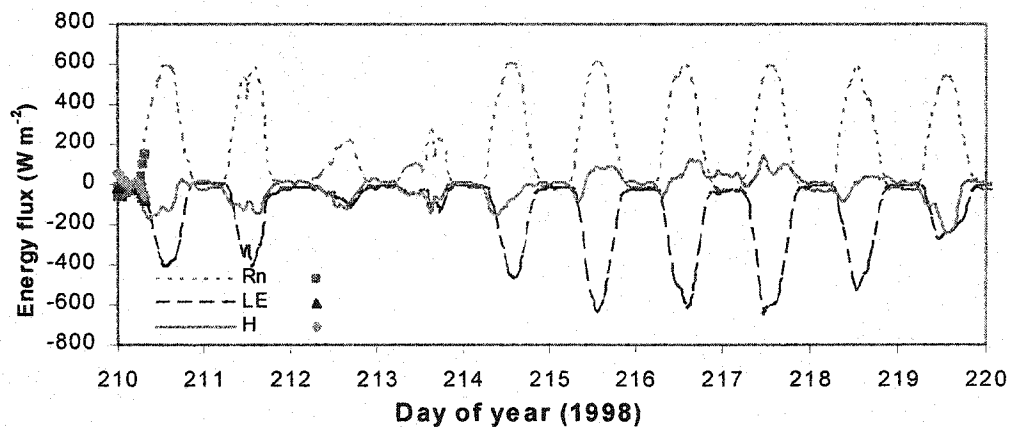
Fig. 4.17 Comparison of simulated (lines) and measured (symbols) net radiation (Rn), latent heat (LE), sensible heat (H) from a barley field during a transition to water stress (DOY 210-220) in 1998. Measured data are not shown because of system failure.
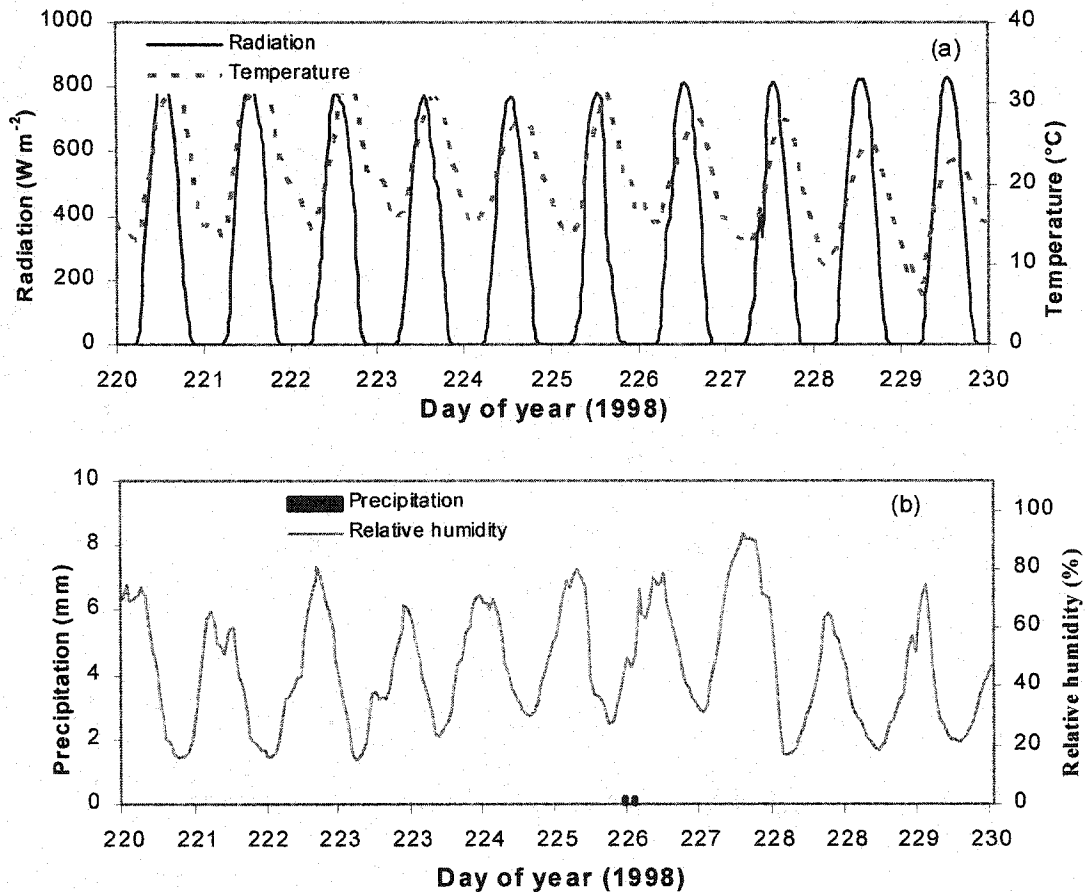
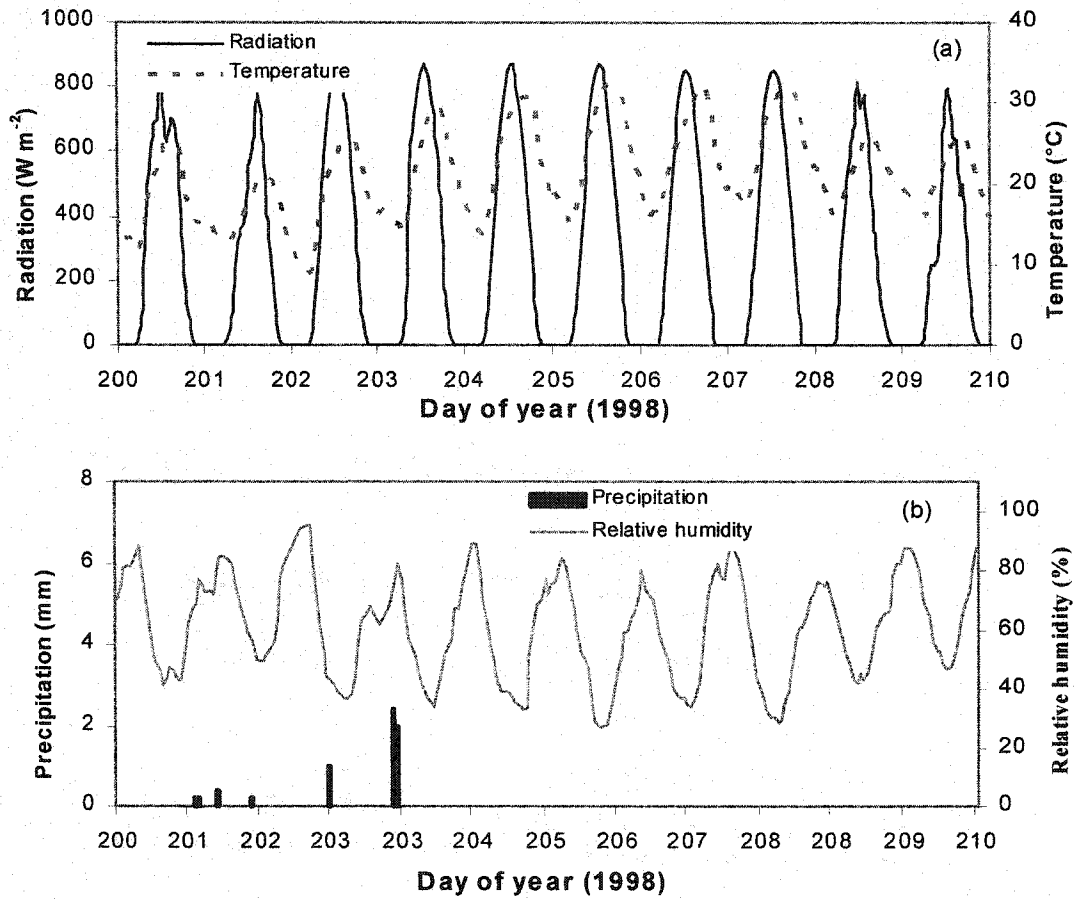Fig. 4.18 Meteorological conditions for DOY 220-230 of 1998.
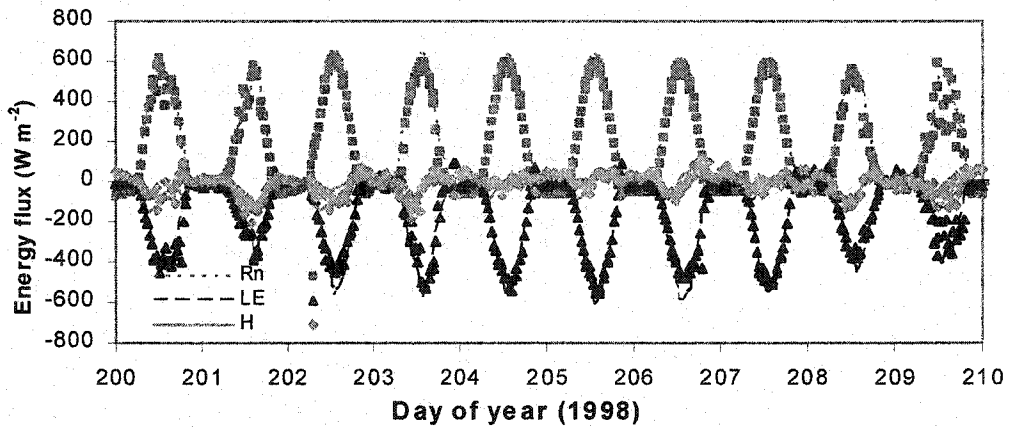(a): Shortwave radiation and air temperature; (b): Precipitation and relative humidity.
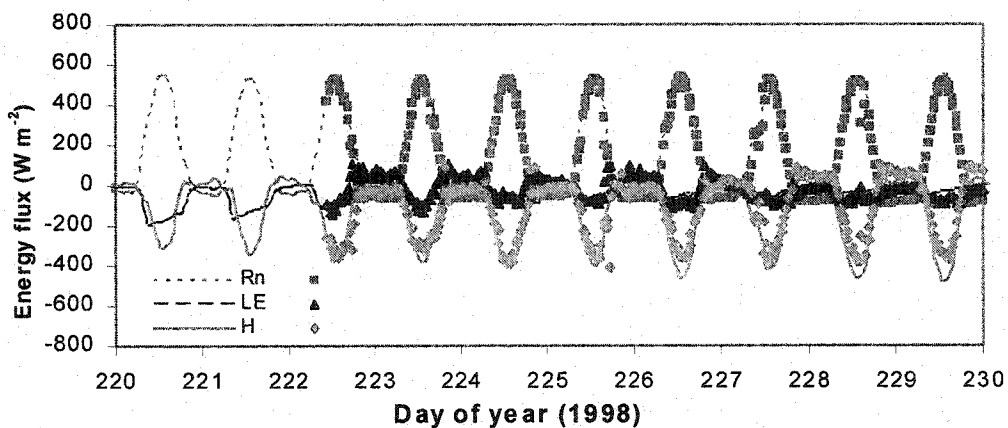
Fig. 4.19 Comparison of simulated (lines) and measured (symbols) net radiation (Rn), latent heat (LE), sensible heat (H) from a barley field during water stress (DOY 220-230) in 1998. Measured data of DOY 220-222 are not shown due to system failure.

107

Water stress developed during DOY 220-230 when there was nearly no rainfall and surface soil water content approached the wilting point (Fig. 4.6, 4.18). The surface boundary conditions during DOY 220 to 230 are plotted in Fig. 4.18, and the continuous measured half-hourly fluxes versus simulated hourly fluxes of Rn, LE and H are shown in Fig. 4.19. During this period, low precipitation, high radiation and high air temperature (Fig. 4.18), caused soil water to lose rapidly through evaporation. Therefore, very low LE and very high H were measured (Fig. 4.19). Under these conditions, transpiration rates were reduced by water stress (low soil water content resulted in low soil, root, canopy water potentials, and hence a higher canopy resistance). Thus lower LE was modeled, and large radiative energy was partitioned into H, causing H to be much larger than LE (Fig. 4.19). During this dry period, both measured and modeled results indicated that about 25% of average net radiation was consumed as latent heat and 70% as sensible heat (Table 4.4).

4.4 Discussion

By regulating the stomatal aperture, soil water conditions influenced the convective and radiative transfer within the ecosystem, and had a major impact on how the energy was partitioned into LE and H. During the crop growing season, latent heat flux (LE) was a major component, while sensible heat flux (H) was a minor component of energy budget before the water stress. During a period before water stress (DOY 200-210) in 1996, both modeled and measured results for average energy fluxes showed that about 70% of the net radiation was consumed as LE, and 30% as H (Table 4.3). The soil water status during the same period (DOY 200-210) in 1998 was much better, so that more available energy (Rn-G) was partitioned into LE (85%) and H only took up a low percentage of the available energy (10%) (Table 4.4). As soil moisture decreased from the wet period to the transition period, LE decreased while H increased. Modeled (measured) average energy fluxes showed that during the transition period of 1996 (DOY 210-220), about 55% (60%) of the net radiation was consumed as LE, and 45% (40%) as H (Table 4.3).

As water stress developed after the transition period, available energy was partitioned more in H than in LE. During the water stress period in 1996 and 1998 (DOY 220-230), both measured and modeled results showed that about 20% of net radiation was consumed as LE, while about 70% as H (Table 4.3, 4.4).

Stomatal behavior was also a major factor influencing the CO_2 transfers in the ecosystem, which will be discussed in **Chapter 5**.

References

Baldocchi, D.D., Harley, P.C., 1995. Scaling carbon dioxide and water vapor exchange from leaf to canopy in a deciduous forest. II. Model testing and application. Plant Cell Environ. 18, 1157-1173.

Baldocchi, D.D., Hicks, B.B., Meyers, T.P., 1988. Measuring biosphere-atmosphere exchanges of biologically related gases with micrometeorological methods. Ecology 69, 1331-1340.

Berge, H.F.M. ten, 1990. Heat and water transfer in bare topsoil and the lower atmosphere. Pudoc Wageningen.

Blad, B.L., Rosenberg, N.J., 1974. Lysimetric calibration of the Bowen ratio/energy balance method for evapotranspiration estimation in the central Great Plains. J. Appl. Meteorol. 13, 227-236.

Cooper, D.I., Alves, L.M., Matthias, A.D., and Gay, L.W., 1998. Comparison of Bowen ration and eddy correlation methods for sensible heat flux estimates.117-140.

Denmead, O.T., Bradley, E.F., 1985. Flux gradient relationships in a forest canopy. In: Hutchison, B.A., Hicks, B.B. (eds.), The Forest-Atmosphere Interaction. Riedel, Boston.

Dugas, W.A., Fritschen, L.J, Gay, L.W, Held, A.A., Matthias, A.D., Reicosky, D.C., Steduto, P., Steiner, J.L., 1991. Bowen ratio, eddy correlation, and portable chamber measurements of sensible and latent heat flux over irrigated spring wheat. Agric. For. Meteorol. 56, 1-20.

Fritschen, L.J., Simpson, J.R., 1989. Surface energy balance and radiation systems: general description and improvements. J. Appl. Meteorol. 28, 680-689.

Halldin, S., Lindroth, A., 1992. Errors in net radiometry: comparison and evaluation of six radiometer designs. J. Atmos. Ocean. Technol. 9, 762-783.

Ham, J.M., Heilman, J.L., Lascano, R.J., 1991. Soil and canopy energy balances of a row crop at partial cover. Agron. J. 83, 744-753.

Larcher, W., 1995. Physiological Plant Ecology. Springer, Austria.

McNeil, D.D., Shuttleworth, W.J., 1975. Comparative measurements of the energy fluxes over a pine forest. Boud.-layer Meteorol. 9, 297-313.

Motha, R.P., Verma, S.B., Rosenberg, N.J., 1979. Exchange coefficients under sensible heat advection determined by eddy correlation. Agric. Meteorol. 20, 273-280.

Rosenberg, N.J., Blad, B.L., Verma, S.B., 1983. Microclimate, the biological environment. John Wiley & Sons, Inc. New York.

Shuttleworth, W.J, Gash., J.H.C., Lloyd, C.R., Moore, C.J., Roberts, J., Filho, A.M., Fisch, G., Filho, V.P.S., Ribeiro., M.N.G., Molion, L.C.B., Sa, L.D.A., Nobre, J.C.A., Cabral, O.M., Patel, S.R., and Moraes, J.C., 1984. Eddy correlation measurements of energy partition for Amazonian forest. Quart. J. R., Soc. 110, 1143-1162.

Smith, E.A., Hodges, G.B., Bacrania, M., Cooper, H.J., Owens, M.A., Chappel, R., Kincannon, W., 1997. BOREAS net radiometer engineering study. NASA-Goddard Space Flight Center, Greenbelt, USA.

Spittlehouse, D.L., Black, T.A., 1979. Determination of forest evapotranspiration using Bowen ratio and eddy correlation measurements. J. Appl. Meteorol. 18, 647-653.

Spittlehouse, D.L., Black, T.A., 1980. Evaluation of the Bowen ratio/energy method for determining forest evapotranspiration. Atmos. –Ocean 18, 98-116.

Verma, S.B., Rosenberg, N.J., Blad, B.L., 1978. Turbulent exchange coefficients for sensible heat and water vapor under advective conditions. J. Appl. Meteorol. 17, 330-338.

Willmer, C.M., 1983. Stomata. Longman Inc., New York.

Chapter 5 Carbon dioxide exchange and Carbon Balance

5.1 Introduction

In agricultural ecosystems, CO_2 exchange involves a series of physiological and biological processes taking place in crops and soils. These processes include crop photosynthesis, photorespiration (light respiration), autotrophic respiration (respiration by plant tissues), and heterotrophic respiration (soil microbial respiration). Environmental factors affecting these processes were described in **Chapter 1**. In agricultural fields, CO_2 is provided to crops from three sources: the atmosphere above, the crop itself (autotrophic respiration), and the soil below (heterotrophic respiration). This CO_2 is fixed and converted into sugars and other compounds through photosynthesis, driven by absorbed solar radiation. Part of the products of photosynthesis are used for crop respiration, the rest is used for crop biomass accumulation and yield formation. Litterfall from biomass accumulation returns to the soil where it is used for heterotrophic respiration by soil microbial organisms. The CO_2 from autotrophic and heterotrophic respiration is released into atmosphere as CO_2 effluxes, where it will re-enter the agricultural ecosystems through crop photosynthesis, thus completing the carbon cycle in agricultural ecosystems. In this chapter, modeled CO_2 fluxes were first tested against measurements, followed by the diurnal and seasonal CO_2 exchange, and annual carbon balance over a barley-fallow rotation 1996 and 1998. The model was then used to predict the long-term soil carbon dynamics for a barley-fallow system under current climate and climate change. Analysis and discussion were given at the end of this chapter.

5.2 Testing modeled CO_2 fluxes

For simulating carbon dioxide fluxes, the same measured hourly weather data as those in the energy simulation were input into the model to set the boundary layer conditions. These weather data included shortwave radiation, air temperature, humidity, wind speed and precipitation measured at Lethbridge Research Center, Agriculture and Agri-Food Canada from 1990 through 2000. The model was run from January 1, 1990 to December 31, 2000 to simulate the carbon dioxide fluxes from the barley-fallow system. Simulated fluxes were tested against the fluxes measured from two Bowen Ratio systems during the growing seasons of 1996 and 1998 by regressing modeled on measured fluxes. For statistical analyses, half-hourly measured fluxes were aggregated into hourly averages, which were then matched with hourly fluxes computed from the model. Model accuracy was evaluated by slope, intercept of a regression line through simulated versus measured values (mean ± standard error), correlation coefficient (r^2), and standard error of the means. The results are shown in Table 5.1 and in Fig. 5.1.
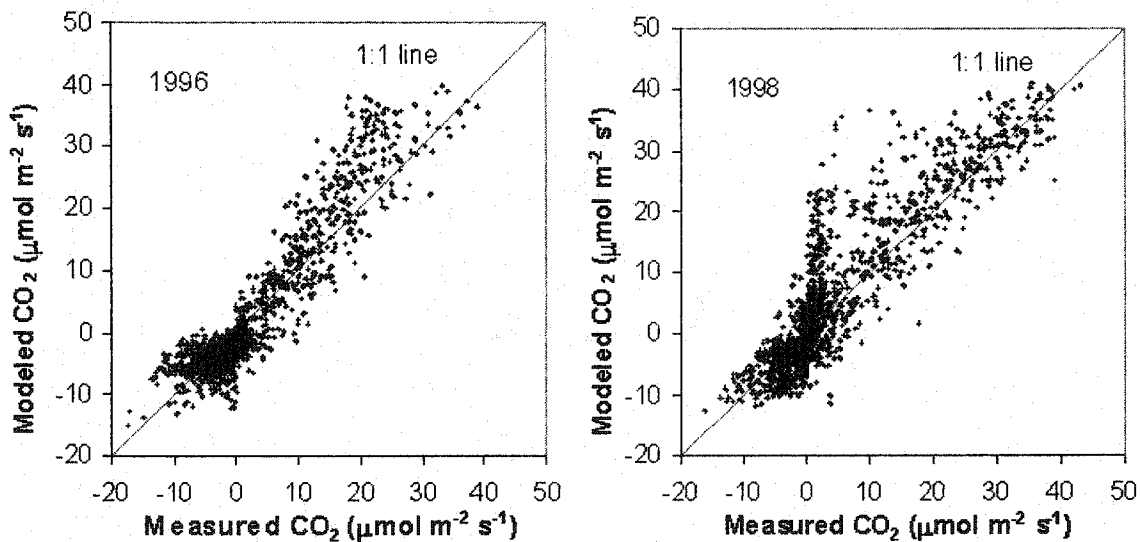
Fig. 5.1 Comparison of measured and modeled CO_2 fluxes from a barley field in the growing seasons of 1996 and 1998.

Table 5.1 Results of a linear regression analysis of modeled versus measured CO_2 fluxes in barley fields

Year	Slope	Intercept (μmol m^{-2} s^{-1})	r^2	Standard error (μmol m^{-2} s^{-1})	No. of observations
1996	1.14±0.02	-0.41±0.16	0.87	3.58	1963
1998	1.04±0.02	0.92±0.31	0.81	5.59	1500

Model performance was evaluated by the slope and intercept of a regression line through model versus measured fluxes, and by correlation coefficient and standard error of the means.

The model was well capable of predicting carbon fluxes of both years with correlation coefficients 0.87 and 0.81 for 1996 and 1998 respectively. The slopes and intercepts are close to 1 and 0, respectively, as well as p-values for the regression model are very small (<0.0001) (Table 5.1).

5.3 Diurnal carbon dioxide exchange

The same periods of the growing seasons in 1996 and 1998 as those in the discussion of energy exchange were selected to examine the effects of weather and soil water conditions on carbon dioxide exchange.

5.3.1 Diurnal CO$_2$ exchange in 1996

Fig. 5.2 shows the diurnal carbon dioxide variations before water stress (DOY 200 to 210) over the barley field in 1996, the corresponding meteorological conditions are shown in Fig. 4.7. During this period, solar radiation was high (maximum radiation above 800 W m^{-2}) (Fig. 4.7a), and soil moisture at 0-200 cm layer was 0.18-0.37 m^3 m^{-3} (Fig. 4.4). The mean net carbon fixation during DOY 200-210 was 8.6 and 10.4 μmol m^{-2} day^{-1} from measurements and modeled results, respectively (Table 5.2). Daytime peak carbon dioxide influxes (net carbon fixation) (Equation 3.35) ranged from 30-35 μmol m^{-2} s^{-1} (modeled) and 25-30 μmol m^{-2} s^{-1} (measured), and nighttime CO$_2$ effluxes

(soil respiration including root autotrophic respiration and microbial heterotrophic respiration) (Equation 3.55) were less than 5 μmol m^{-2} s^{-1} (modeled) and from 5 to 15 μmol m^{-2} s^{-1} (measured) (Fig. 5.2).

Table 5.2 Mean daily net carbon fixation for three periods with different soil water status in the growing season of 1996 and 1998 (unit: g C m^{-2} day^{-1})

Period	1996		1998	
	Measured	Modeled	Measured	Modeled
Before water stress (DOY 200-210)	8.6	10.4	7.7	8.2
Transition to water stress (DOY 210-220)	4.2	4.0	n/a	8.4
Water stress (DOY 220-230)	-0.8	-1.5	0.6	0.4

Note: n/a means that data are not available.

The diurnal carbon dioxide variations over barley during a transition to water stress (DOY 210-220) are shown in Fig. 5.3 and the corresponding meteorological conditions are shown in Fig. 4.10. The model predicted measurements quite well, except for a few scattered measured values. Both modeled and measured results showed a gradual decline in both daytime CO_2 influxes and nighttime CO_2 effluxes, but the decline in daytime CO_2 influxes was much larger than nighttime CO_2 effluxes, causing net CO_2 exchange to decline rapidly. During this period, mean net CO_2 fixation was 4.2 μmol m^{-2} day^{-1} (measured) and 4.0 μmol m^{-2} day^{-1} (modeled), which were about the half of the net CO_2 fixation in the previous period (Table 5.2). Both measured and modeled results showed that during this transition period, daytime peak CO_2 influxes deceased from about 28 μmol m^{-2} s^{-1} on DOY 210, to about 18 μmol m^{-2} s^{-1} on DOY 220, while the nighttime peak CO_2 effluxes decreased only 2-3 μmol m^{-2} s^{-1}. This is because soil microbial respiration is less sensitive to water stress than is crop photosynthesis (Equation 3.49, 3.50).

Water stress developed after about DOY 220 when soil moisture was below the wilting point (Fig. 4.4). The variations in diurnal CO_2 fluxes over barley during water stress (DOY 220-230) are shown in Fig. 5.4, and the corresponding meteorological conditions are shown in Fig. 4.12. During this period, both CO_2 influxes and effluxes

were quite small compared with previous periods, and again, the decline in daytime CO_2 influxes was much larger than that in nighttime CO_2 effluxes, causing the ecosystem to change from a net CO_2 sink to a net CO_2 source. The mean net CO_2 fixation during this period was -0.8 μmol m^{-2} day^{-1} (measured) and -1.55 μmol m^{-2} day^{-1} (modeled) (Table 5.2).

The diurnal changes in carbon dioxide influxes modeled from wet- to dry period were controlled by those in soil moisture. With the rainfall on DOY 206, soil water content was maintained above the wilting point during DOY 200-210 (Fig. 4.4). As discussed in **Chapter 4**, high soil water content caused a high hydraulic conductivity (Eq. 3.21), and high soil and root water potentials, which resulted in a high canopy potential (Eq. 3.17), and hence a high stomatal conductance (Eq. 3.11) that allowed a high CO_2 fixation rate to be sustained by the canopy (Eq. 3.36) under high radiation. As soil moisture decreased after DOY 210, soil water potential declined, causing canopy water potential (Equation 3.17), and canopy turgor potential (ψ_T) (Equation 3.17) to decrease, and hence stomatal resistance (Equation 3.11) to increase. Therefore, CO_2 fixation decreased (Equation 3.36).

The nighttime CO_2 effluxes also decreased from DOY 200-210 (before water stress) to DOY 220-230 (under water stress) (Fig. 5.2-5.4). During DOY 200-210, peak CO_2 effluxes ranged from 6-10 μmol m^{-2} s^{-1} (Fig. 5.2), while it ranged from 2-5 μmol m^{-2} s^{-1} during the period of water stress (DOY 220-230) (Fig. 5.4). Denmead (1976) stated that there is a strong suggestion that the evolution of CO_2 is linked with the rate of CO_2 assimilation in the crop. The reduction in CO_2 fixation resulted from water stress caused a decrease in microbial heterotrophic respiration (Equation 3.55), resulting a reduction in CO_2 effluxes. The fact that soil microbial function is inhibited under severe water stress (Equation 3.49, 3.50) can be another reason for the reduction of nighttime CO_2 effluxes.

Fig. 5.2 Measured (symbols) and modeled (lines) carbon dioxide fluxes over a barley field before water stress (DOY 200-210) in 1996.

Fig. 5.3 Measured (symbols) and modeled (lines) carbon dioxide fluxes from a barley field during a transition to water stress (DOY 210-220) in 1996.

Fig. 5.4 Measured (symbols) and modeled (lines) carbon dioxide fluxes from a barley field during water stress (DOY 220-230) in 1996.

5.3.2 Diurnal CO_2 exchange in 1998

Fig. 5.5, 5.6 and 5.7 show the CO_2 fluxes over barley varying from DOY 200-210 (before water stress), DOY 210-220 (transition to water stress), and to DOY 220-230 (under water stress), respectively, in the growing season of 1998. The corresponding meteorological conditions for these three periods are shown in Fig. 4.14, 4.16 and 4.18, respectively. Surface soil water content remained above the wilting point during DOY 200-210 (Fig. 4.6), indicating water tress did not develop. As discussed above, high soil water content allowed high stomatal conductance to be maintained in the model, together with high radiation (Fig. 4.14), causing a high rate of CO_2 fixation to be modeled (Equation 3.31). Both modeled and measured results showed that maximum net carbon fixation (CO_2 influxes) varied from 30-35 $\mu mol\ m^{-2}\ s^{-1}$, while the maximum soil respiration (CO_2 effluxes including root autotrophic and microbial heterotrophic respiration) varied from 10-15 $\mu mol\ m^{-2}\ s^{-1}$ (Fig. 5.5). The mean net carbon fixation during this period was 7.7 $\mu mol\ m^{-2}\ day^{-1}$ (measured) and 8.2 $\mu mol\ m^{-2}\ day^{-1}$ (Modeled) (Table 5.2).

With rainfall on DOY 213 and 214, soil water content was generally above the wilting point during the transition period to water stress (DOY 210-220), and it deceased after DOY 218 when soil moisture approached the wilting point (Fig. 4.6). Model results showed that daytime peak CO_2 influxes ranged from 30 to 35 $\mu mol\ m^{-2}\ s^{-1}$, and nighttime CO_2 effluxes varied from 5 to 10 $\mu mol\ m^{-2}\ s^{-1}$ (Fig. 5.6). Precipitation events and thus lower shortwave radiation on DOY 213-214 (Fig. 4.16), causing a lower CO_2 fixation to be modeled during DOY 213-214 with a peak CO_2 influx of 22-28 $\mu mol\ m^{-2}\ s^{-1}$ (Fig. 5.6). The mean net carbon fixation during the period was simulated to be 8.4 $\mu mol\ m^{-2}\ day^{-1}$ (Table 5.2).
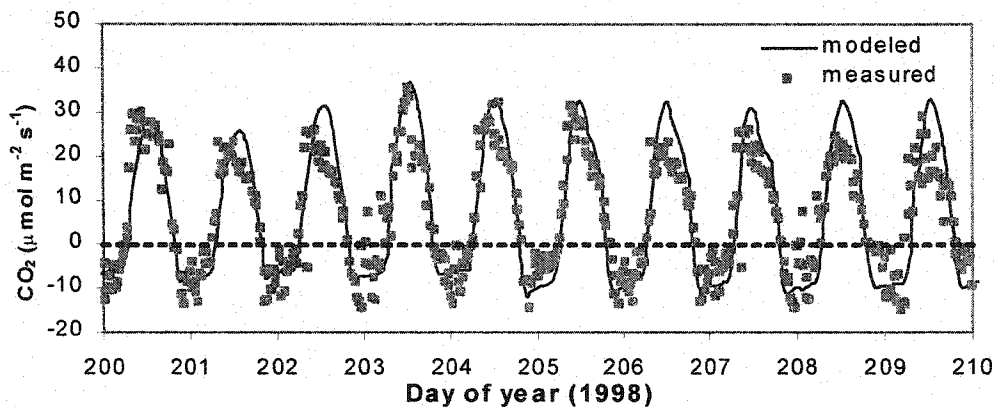
Fig. 5.5 Measured (symbols) and modeled (lines) carbon dioxide fluxes from a barley field before water stress (DOY 200-210) in 1998.
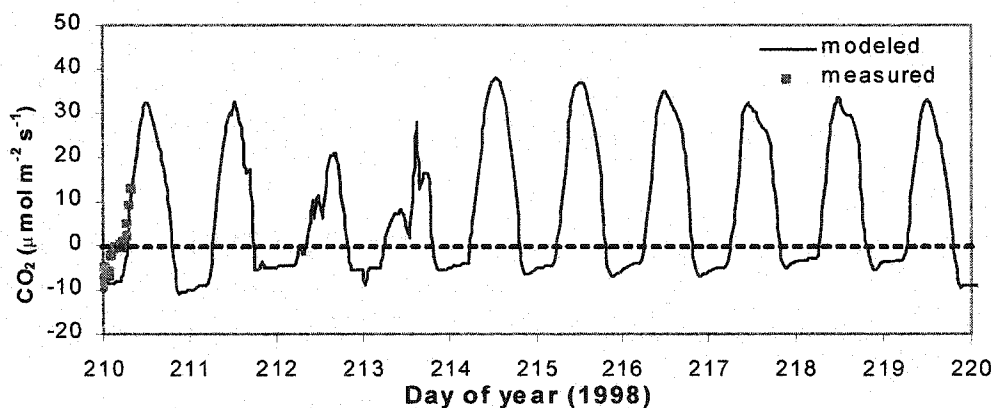
Fig. 5.6 Measured (symbols) and modeled (lines) carbon dioxide fluxes from a barley field during a transition to water stress (DOY 210-220) in 1998. Measured data are not shown due to system failure.
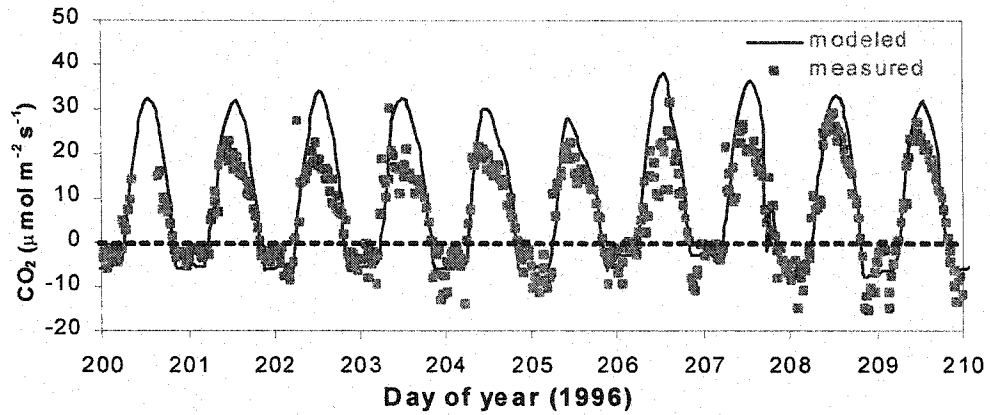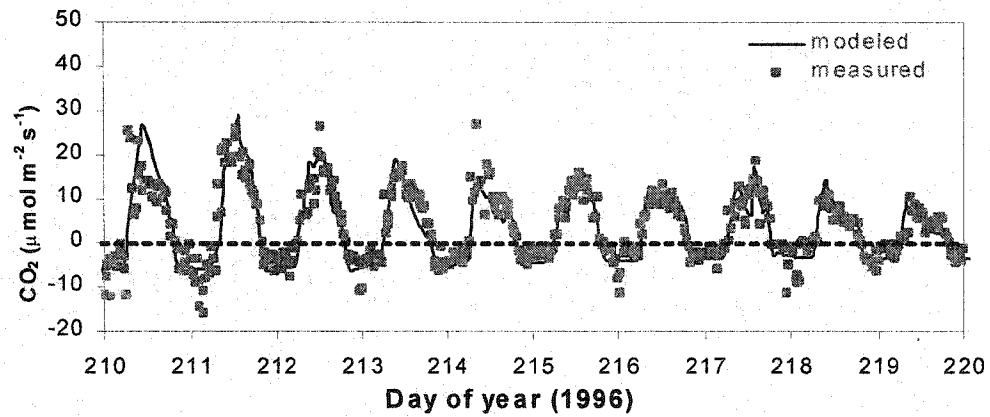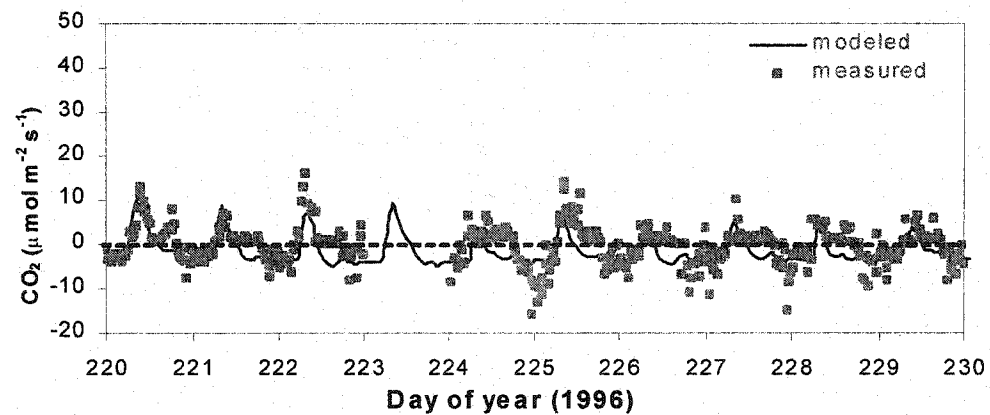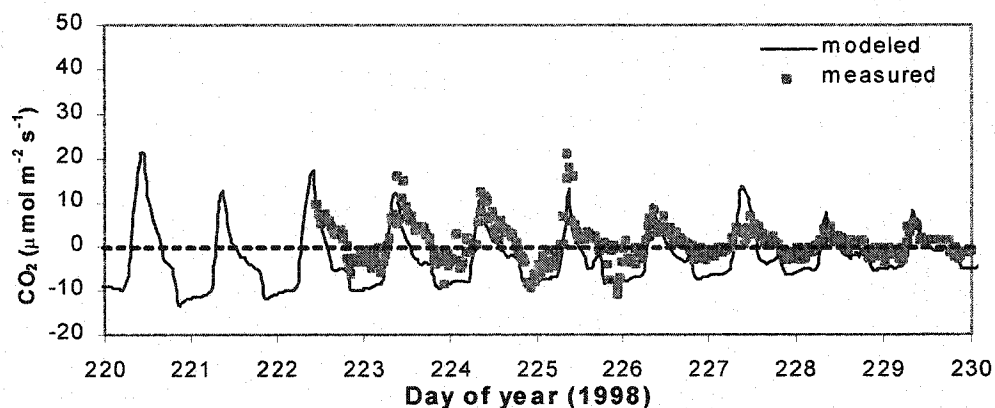

Fig. 5.7 Measured (symbols) and modeled (lines) carbon dioxide fluxes from a barley field during water stress (DOY 220-230) in 1998. Measured data of DOY 220-222 are not shown due to system failure.

Because of low precipitation, high radiation and high air temperature (Fig. 4.18), water stress developed late in the growing season (DOY 220-230) of 1998 when soil water content was below the wilting point (Fig. 4.6). Since CO_2 fixation and heterotrophic respiration are both suppressed by water stress, CO_2 influxes and effluxes were relatively small during the period. Both measured and modeled results showed that maximum CO_2 influxes varied from 10 to 15 $\mu mol\ m^{-2}\ s^{-1}$, and maximum CO_2 effluxes varied from 5 to 10 $\mu mol\ m^{-2}\ s^{-1}$ (Fig. 5.7). Mean net carbon fixation during this period was 0.6 $\mu mol\ m^{-2}\ day^{-1}$ (measured) and 0.4 $\mu mol\ m^{-2}\ day^{-1}$ (modelled), indicating the CO_2 influxes and effluxes were about in equilibrium.

The reduction in nighttime CO_2 effluxes from wet to dry period in 1998 followed the same pattern as in 1996 (Fig.s 5.5, 5.6, 5.7). The maximum nighttime CO_2 effluxes varied from about 10-15 $\mu mol\ m^{-2}\ s^{-1}$ during the wet period (Fig. 5.5-5.6), to about 5-10 $\mu mol\ m^{-2}\ s^{-1}$ during the dry period (Fig. 5.7). But the reduction in CO_2 efflux was smaller in 1998 than that in 1996, because the water stress was not as severe in 1998 as in 1996.

5.4 Seasonal carbon dioxide exchanges

5.4.1 Net carbon fixation

Seasonal carbon dioxide exchanges were evaluated from daily net CO_2 exchanges, which were obtained by aggregating half-hourly (measured) and hourly (simulated) CO_2 fluxes into daily totals. Since there were some gaps in measured CO_2 fluxes, due to BREB system failure, CO_2 analyzer calibration, data transfer or experimental errors, special attention was given to half-hourly data that seemed to be questionable, or to the filling of the gaps. The following methods were followed in gap filling and data quality checking: 1) short gaps, which were due to CO_2 analyzer calibration, or data transfer, of up to 6 h were filled by interpolation using the adjacent data (data immediately before and after the gap); 2) short gaps (less than 6 h), when the Bowen ratio approached -1, so that no fluxes could be calculated, were filled by setting the Bowen ratio to those of the

adjacent data to calculate sensible heat fluxes (H) and then CO_2 fluxes (Eq. 2.11) (McGinn and Akinremi, 2000). 3) Any day that had missing data more than 6 h was discarded in the daily CO_2 flux calculation. 4) Data larger than 50 μmol m^{-2} s^{-1} (influxes) or less than -25 μmol m^{-2} s^{-1} (effluxes) were assumed to be system error and therefore were removed (Anthoni et al., 1999). No attempt was made to fill a large gap, due to BREB breakdown, at daily scale (from DOY 211, 8:00 am to DOY 223, 10:00 am in 1998). Results of measured and modeled daily net carbon dioxide exchanges in 1996 and 1998 are shown in Fig. 5.8 and 5.9, respectively. Mean daily net carbon fixation for the three periods with different soil water status in the growing seasons of 1996 and 1998 is shown in Table 5.2.

The crop was seeded on DOY 136 and harvested on 240 in 1996 (Table 2.1). The barley field became a net carbon sink (positive value) after DOY 158 which lasted until DOY 220. Highest carbon fixation of 10-14 g C m^{-2} day^{-1} occurred during DOY 180 to DOY 205. The net carbon fixation decreased rapidly after DOY 210 when water stress began to develop (a transition to water stress) (Fig. 5.8, Table 5.2). This is because the net photosynthesis declined more than did soil respiration during the transition period to water stress (DOY 210-220) (Fig. 5.3). Net carbon fixation became negative (carbon source to the atmosphere) after DOY 220 when water stress developed (Fig. 5.8, Table 5.2).

In 1998, the crop was seeded on DOY 130 and harvested on DOY 240 (Table 2.1). Net carbon fixation was positive (net C sink) from DOY 155 to DOY 230 (Fig. 5.9, Table 5.2). Highest carbon fixation of 8-15 g C m^{-2} day^{-1} occurred from DOY 177 to DOY 204 and from DOY 215 to DOY 220. Rapid decline in net carbon fixation was only observed after DOY 220 when water stress began to develop (Fig. 5.9, Table 5.2). Greater reduction in net carbon fixation than in soil respiration caused net carbon fixation and soil respiration to be about in equilibrium during water stress (DOY 220-230) (Fig. 5.6-5.7, 5.9, Table 5.2).
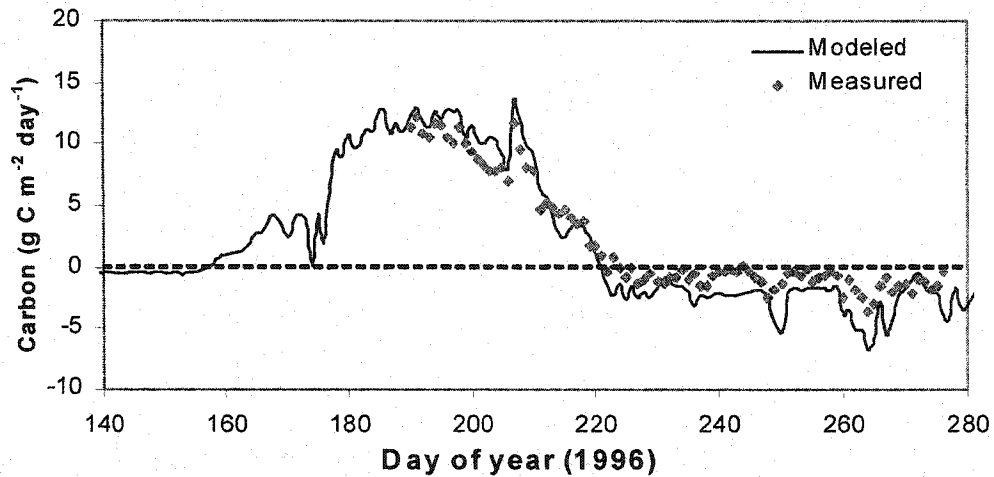
Fig. 5.8 Daily CO_2 fluxes from a barley field in 1996. Daily CO_2 fluxes are calculated by aggregated half-hourly (measured) and hourly (simulated) CO_2 fluxes into daily summation. Positive numbers denote CO_2 influxes into the ecosystem, negative numbers refer to CO_2 effluxes into atmosphere.
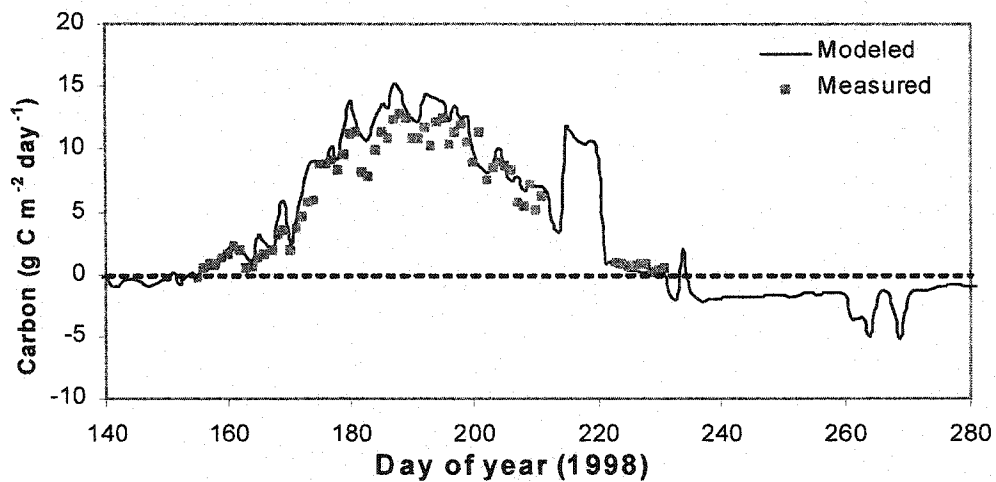
Fig. 5.9 Daily CO_2 fluxes from a barley field in 1998. Daily CO_2 fluxes are calculated by aggregated half-hourly (measured) and hourly (simulated) CO_2 fluxes into daily summation. Measured data from DOY 211 to 222 are not shown due to BREB breakdown. Positive numbers denote CO_2 influxes into the ecosystem, negative numbers refer to CO_2 effluxes into atmosphere.

There are some discrepancies between measured and modeled daily carbon fluxes. Generally, the measured data are slightly smaller than modeled data in both years, mainly because some missing measured data that were not included in the daily aggregation. However, the model captured the trend of carbon dynamics quite well. 1996 was a dry year, in which water stress started to develop earlier (after DOY 210) (Fig. 4.4). While the water status was better in 1998, and water stress developed only in later growing season (after DOY 220) when the crop had finished vegetative and reproductive development (Fig. 4.6). Therefore, the barley ecosystem became a net carbon source earlier in 1996 (DOY 220) than in 1998 (DOY 230) (Fig. 5.8-5.9).

5.4.2 Biomass accumulation

Seasonal variations in biomass accumulation in 1996 and 1998 are shown in Fig. 5.10 and 5.11, respectively. In 1996, biomass began to accumulate on DOY 145 and reached maximum around DOY 220, after which it declined (Fig. 5.10). Modeled results showed that maximum shoot (above ground) and root (below ground) biomass accumulation was 390 and 97 g C m^{-2}, respectively. Since the crop was seeded earlier in 1998 than in 1996, biomass began to accumulate on DOY 140 and reached its maximum around DOY 220 (Fig. 5.11). After DOY 220, biomass accumulation decreased less in 1998 than in 1996, and maximum modeled shoot and root biomass accumulation was about 502 and 100 g C m^{-2}, respectively.

Water stress influenced crop growth, and hence affected biomass accumulation. In 1996, biomass stopped accumulating after DOY 210 when water stress began to develop, as indicated by the slope of biomass accumulation line (Fig. 5.10). In 1998, biomass accumulation continued until DOY 220 when slight water stress developed (Fig. 5.11). Since crop photosynthesis was less influenced by water stress in 1998 (Fig. 5.2-5.7), the decline in net CO_2 fixation caused modeled crop biomass accumulation to be higher in 1998 than in 1996 (587 versus 476 g C m^{-2}).
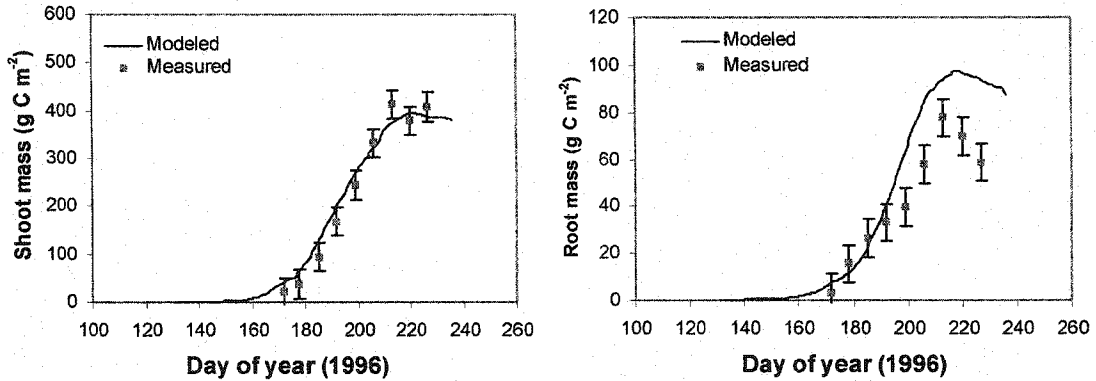
Fig. 5.10 Measured and modeled biomass accumulation during barley
growing season in 1996. Values are given in grams of equivalent dry
matter. Error bars are ±standard error.
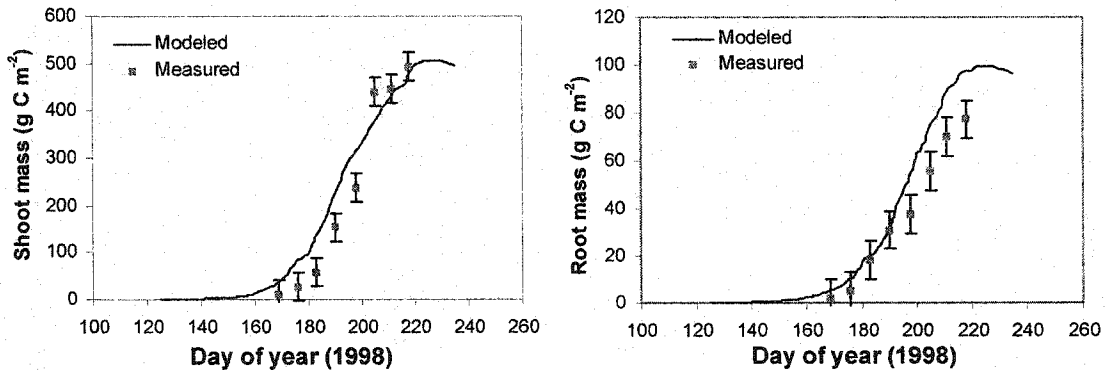
Fig. 5.11 Measured and modeled biomass accumulation during barley
growing season in 1998. Values are given in grams of equivalent dry
matter. Error bars are ±standard error.

Simulated living aboveground biomass and living root biomass showed that living aboveground biomass simulations closely followed measurements with an overestimation during the early and mid-growing season (Before DOY 200) and a slight underestimation during the later growing season (after DOY 200) (Fig. 5.10-5.11). Root biomass was overestimated for the whole growing season by the model, especially during the later growing season. This could have been caused by the technique used in

biomass measurement, which could recover most root material at the early stage of the growing season (shallow roots), but was expected to underestimate root biomass at later stages of crop growth. During the later growing season, it was very hard to uproot roots in deep soil layer, causing root biomass measurements to be less than total root biomass.

5.5 Annual carbon balance

Annual carbon balances were obtained by aggregating the hourly fluxes (modeled) and half-hourly fluxes (measured) over the whole year. For measured data, the same procedures were followed for gap filling and data quality checking as discussed under 5.4. The annual carbon balance consists of GPP (gross primary productivity), R_a (autotrophic respiration), NPP (net primary productivity), R_h (heterotrophic respiration, or soil respiration), NEP (net ecosystem productivity), NBP (net biome productivity). The equations for calculating these components were given in **Chapter 3**. In calculating the annual carbon balance of 1996, heterotrophic respiration from barley and fallow fields during the non-growing seasons was calculated from McGinn et al. (2000), who designed an automated chamber system to measure soil respiration. The measured data for heterotrophic respiration during the non-growing season of 1998 were not available and thus not included here. The results of annual carbon balance from a barley-fallow system in 1996 and 1998 are shown in Table 5.3.

Over the growing season, the modeled NPP (Equation 3.46) for barley was 505 and 610 g C m^{-2} in 1996 and 1998, respectively (Table 5.3). The NPP estimated from measured CO_2 fluxes for 1996 was 382 g C m^{-2}. Since there was no crop in the fallow field and therefore no carbon fixation, the NPP for the fallow field was zero. The modeled NPP for the whole barley-fallow system (an area percentage of 50% crop and 50% fallow) was 253 and 305 g C m^{-2} in 1996 and 1998, respectively. The NPP estimated from measurements for the whole system in 1996 was 191 g C m^{-2}.

The modeled R_h from the barley field for the whole year of 1996 and 1998 was -312 and -331 g C m^{-2}, respectively, while the R_h estimated from measurements from the barley in 1996 was -224 g C m^{-2}. For the same period, the modeled R_h from the fallow

field was -211 and -248 g C m^{-2} in 1996 and 1998, respectively, while the R$_h$ estimated from measurements from the fallow field in 1996 was -183 g C m^{-2}. The comparison of measured and modeled R$_h$ indicated that the model slightly overestimated R$_h$ for both the barley and the fallow field in 1996 (Table 5.3). Higher air temperature, higher precipitation and hence higher soil moisture in 1998 than in 1996 (Table 4.2), caused a higher soil respiration to be modeled in 1998 compared with 1996.

Table 5.3 The Annual carbon balance for a barley-fallow system in 1996 and 1998

| | | Annual Carbon Balance (g C m^{-2}) | | | | | |
| | | Estimated from measurements | | | Modeled | | |
	Year	Barley	Fallow	Barley-fallow	Barley	Fallow	Barley-fallow
NPP	1996	382	0	191	505	0	253
	1998				610	0	305
R$_h$	1996	-224	-183	-204	-312	-211	-262
	1998				-331	-248	-290
NEP	1996	158	-183	-13	194	-211	-9
	1998				279	-248	16
NBP	1996	24	-183	-80	86	-211	-63
	1998				98	-248	-75

Note: measured data for 1996 were calculated from McGinn et al. (2000). Positive numbers denote a sink of carbon to the ecosystem, while negative numbers indicate a loss of carbon from the ecosystem. To allocate carbon balance over the whole barley-fallow system, an area percentage of 50% crop and 50% fallow was used. NPP (net primary productivity) = GPP (gross primary productivity) – R$_a$ (autotrophic respiration); NEP (net ecosystem productivity) = NPP – R$_h$ (Heterotrophic respiration); NBP (net biome productivity) = NEP – Yield removal.

NEP indicates the net CO_2 exchange between the ecosystem and the atmosphere. The modeled NEP for barley in 1996 and 1998 was 194 and 279 g C m^{-2}, respectively, while the measured NEP from the barley field in 1996 was 158 g C m^{-2}. Both measured

and modeled results indicated that barley extracted CO_2 from the atmosphere by photosynthesis, and thus was a net carbon sink. This gain of carbon was accumulated as biomass, some of which was deposited into soil as litterfall, and some of which was harvested as grain yield. Since all green vegetation was eliminated by herbicide in the fallow field, carbon fixation was zero. The NEP under fallow field was equal to R_h. The modeled results indicated that the fallow field was a net source of 211 and 248 g C m^{-2} carbon to atmosphere in 1996 and 1998, respectively. Measured NEP in 1996 for the fallow field indicated a source of 183 g C m^{-2} carbon by soil respiration into atmosphere. For the whole barley-fallow system, the combined NEP showed that this system was a net carbon source of 13 (estimated)/9 g C m^{-2} (modeled) in drier year of 1996, and a net carbon sink of 16 g C m^{-2} (modeled) in wetter year of 1998 if the harvest yield is not considered.

The change of soil carbon is the difference between NEP and grain yield removal. The measured (modeled) grain yield was 134 g C m^{-2} (108 g C m^{-2}) in 1996, and 167 g C m^{-2} (175 g C m^{-2}) in 1998. The modeled results showed that soil under barley gained 86 g C m^{-2} and 98 g C m^{-2} in 1996 and 1998, respectively, and measured results indicated a gain of 24 g C m^{-2} under barley field in 1996. Since the modeled NPP, and hence NEP, was higher in the wetter year (1998) than that in the drier year (1996), the soil under barley gained more carbon in the wetter year than in the drier year (86 g C m^{-2} in 1996 versus 98 g C m^{-2} in 1998).

The effect of a barley-fallow rotation on the annual carbon balance can be evaluated by averaging the components of the annual carbon balance, using an area percentage (50% of barley and 50% of fallow) as an allocating coefficient. In the drier year of 1996, the barley-fallow system contributed 13 g C m^{-2} (measured)/9 g C m^{-2} (modeled) carbon to the atmosphere. After accounting for the grain yield removal from the field, there is a total carbon loss from the soil and the NBP was -80 g C m^{-2} (measured)/ -63 g C m^{-2} (modeled) in 1996. During the wetter year of 1998, the modeled results indicated that the barley-fallow system removed 16 g C m^{-2} from the atmosphere, but after harvest the overall loss in soil carbon was 75 g C m^{-2}.

The annual carbon balance of barley simulated by *ecosys* in 1996 and 1998 is shown in Table 5.4. Although the GPP and NPP were higher in 1998 than in 1996, the

ratio of aboveground to belowground biomass was higher in 1996 than in 1998 (24.0% in 1996 versus 19.5% in 1998), indicating more carbon was attributed to roots during water limited conditions.

Table 5.4 The components of gross primary productivity (GPP) of barley simulated by *ecosys* in 1996 and 1998 (Unit: g C m^{-2})

Year		1996	1998
Gross primary productivity		791	987
Autotrophic respiration	Aboveground	213	288
	Belowground	73	89
Net primary productivity	Aboveground	395	498
	Belowground	110	112
Senescence		10	7
Exudation		19	16
Biomass	Aboveground	385	491
	Belowground	91	96

5.6 Long-term soil carbon dynamics

Long-term soil carbon dynamics for a barley-fallow system modeled under current climate and climate change conditions is shown in Fig. 2.12. The results show that under crop-fallow rotation, there is a trend toward losing soil carbon over time. From 1991 to 2090, soil was modeled to lose 30% and 35% carbon in 0-135 cm layer, under current climate and climate change, respectively, which is equivalent to an average loss of 36 g C m^{-2} y^{-1} and 40 g C m^{-2} y^{-1}.
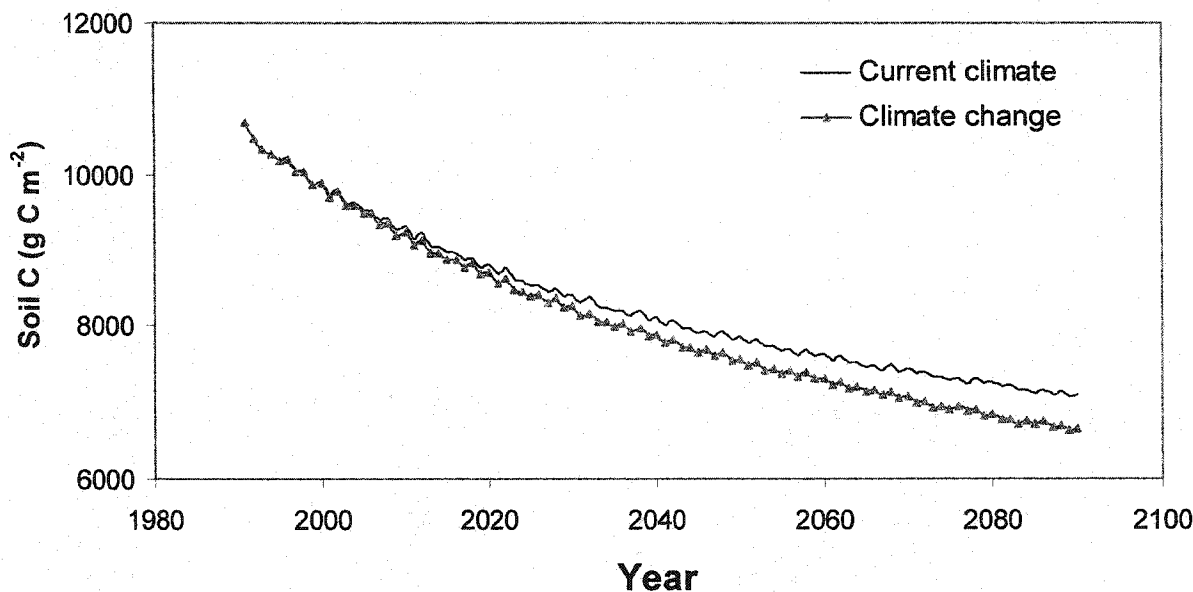
Fig. 5.12 Changes in soil carbon under current climate and climate change scenarios for a barley-fallow system. The climate change scenario was developed from the results of CRCM-II (Canadian Regional Climate Model) under the IS92a emissions scenario (Laprise et al., 1998).

The rate at which soil would lose carbon slows with the age of the ecosystem, as indicated by the slopes of the curves in Fig. 5.12. The ecosystem could roughly be classified into two stages, according to the rate of soil carbon loss. Before 2020, soil would lose carbon at a rate of 62 and 66 g C m^{-2} y^{-1}, under current climate and climate change, respectively. After 2020, the ecosystem would lose soil carbon at a slower rate of 22 and 27 g C m^{-2} y^{-1}, under current climate and climate change, respectively. Since crop-fallow rotation in the experimental fields was established after 1994, these results suggest that land use change (from continuous cropping to crop-fallow) would significantly accelerate the losses of soil carbon to the atmosphere at an earlier stage, but its effect on soil carbon loss would level off once the ecosystem reached a relatively stable stage. The rates of soil carbon loss modeled under current climate are comparable to those obtained from the calculation of annual carbon balance in 1996

128

and 1998, which show that 63 and 75 g C m^{-2} y^{-1} soil carbon was lost in 1996 and 1998, respectively (Table 5.3).

5.7 Discussion and conclusions

5.7.1 The effect of water stress on CO$_2$ exchange

Water stress commonly results in crop growth and photosynthesis reduction, which in turn should result in decreased growth respiration (Amthor, 1989). Water stress was observed after DOY 220 in the growing seasons of 1996 and 1998 (Fig. 4.4-4.6), during which both CO$_2$ fixation and soil respiration decreased, but the reduction in CO$_2$ fixation was much greater than in soil respiration (Fig. 5.2-5.7). This is consistent with other similar studies. Boyer (1970) observed the respiration and apparent photosynthesis in shoots of chamber-grown soybean, and found that even at very low water potential, respiration continued at about 50% of nonstress rates in soybean, while apparent photosynthesis was about 80% inhibited. Amthor (1989) stated that the effects of water stress on net photosynthesis were much greater than its effects on respiration. Brix (1962) noted that as the water potential of tomato leaves decreased, the respiration rate also decreased. Again, the photosynthetic rate was more significantly affected by the same decrease in leaf water potential. Such a response indicates an effect on respiration via an effect on assimilate levels and growth rate (Amthor, 1989). The impact of water stress (drought) on CO$_2$ exchange has also been demonstrated in studies elsewhere. In tropical savanna ecosystems a change from the wet to the dry season can switch the ecosystem from a carbon sink to a weak source (Miranda et al., 1997). Inter-annual variation in net ecosystem exchange of bunchgrass ecosystems, can also be highly modified by drought during summer periods. For three non-drought years the average summertime net ecosystem exchange indicated a net sink of 118 g C m^{-2}, however, during a drought year the lack of soil water combined with high surface temperatures converted the ecosystem into a net source of 155 g C m^{-2} (Meyers, 2001). These results show that water stress is a major reason that causes the diurnal variation of CO$_2$ exchanges in ecosystems in arid and semi-arid regions, which reduces the NPP.

5.7.2 The effects of crop rotation on soil carbon dynamics

Land use practices that involve soil disturbance and removal of vegetation have been widely observed to cause losses of soil carbon to the atmosphere (Matthews, 1983; Houghton, 1999, 2000). These losses account for about one-third of the atmospheric CO_2 that has accumulated since pre-industrial times, and they indicate widespread soil degradation. Davidson and Ackerman (1993) estimated that following the cultivation of the Great Plains of Northern America, soil organic matter was depleted by 15-30%. Similarly Monreal and Janzen (1993) reported that approximately 17% of the carbon was lost from Chernozemic soils. Therefore, land use and land-use change directly affect the exchange of greenhouse gases between terrestrial ecosystems and the atmosphere. The fact that land use change from continuous cropping to crop-fallow rotation causes loss of soil carbon has been demonstrated by many studies, which show conclusively that soil organic C will increase as the frequency of summer fallow in the crop rotation is decreased (Campbell et al., 1991; Janzen, 1987; Bremer et al., 1994). Horner et al. (1960), Ridley and Hedlin (1968) also showed that crop rotation with fallow produced more rapid loss of soil C. Bruce et al. (1999) stated that intensification of cropping systems by eliminating summer fallow not only increased the amount of carbon entering the soil, but also suppressed decomposition rates by cooling the soil through shading and by drying the soil. Our results obtained in Lethbridge showed that 63 and 75 g C m^{-2} y^{-1} soil carbon was lost from the soil in 1996 and 1998 (Table 5.3), which was consistent with the conclusion that the changing from continuous barley to a barley-fallow rotation could result in soil carbon loss. Bruce et al. (1999) reviewed carbon sequestration in soils and found that soils gain 20 g C m^{-2} y^{-1} when changing from crop-fallow rotation to continuous cropping.

The long-term soil carbon dynamics from a barley-fallow rotation in Lethbridge modeled under current climate conditions indicated that from 1991 to 2090, soil would lose 30% of the carbon in 0-135 cm layer, which is equivalent to an average loss of 36 g C m^{-2} y^{-1}. These results are comparable to soil carbon measurements in long-term experiments in Western Canada. Long-term experiments in Lethbridge showed that

under fallow-wheat rotation, soils lost approximately 20% of C in the surface 15 cm layer, and 22% in 15-30 cm layer from 1910 to 1990 (Janzen et al., 1997). The proportional decline in soil carbon in the 15-30 cm layer was similar, from 12.0 g kg^{-1} in 1910 to an average of 9.4 g kg^{-1} in 1990. According to this study and assuming a constant soil bulk density of 1.2 g cm^{-3}, soil under a fallow-wheat rotation in Lethbridge lost carbon at a rate of 10 g C m^{-2} y^{-1} in the 0-15 cm layer and 6 g C m^{-2} y^{-1} in the 15-30 cm layer from 1910 to 1990. McGill et al. (1988) estimated that typical organic carbon loss in the soils under the crop-fallow system of western Canada ranged from 15% to 30%. A study by Rasmussen and Parton (1994) indicated a loss of soil carbon at 20 g C m^{-2} y^{-1} in the upper 0.3 m layer and 18 g C m^{-2} y^{-1} at depths between 0.3 and 0.6 m under a 55-yr wheat-fallow rotation in Pendleton, Oregon. Using the Century Model, Smith et al. (1997) predicted soil carbon dynamics in agricultural soils under crop-fallow crop rotation in Canada. They estimated that about 26% of soil carbon was lost in the 0-30 cm soil layer from 1910 to 1990. Since our modeled results included the soil carbon loss from the surface layer to a depth of 1.35 m, they were relatively higher than those from field experiments which only considered the soil carbon loss from the surface horizons.

5.7.3 The effect of climate change on soil carbon dynamics

Atmospheric CO_2 concentration has increased during 1850–1998 from about 285 to 366 ppmv, and it will be double in the next century (IPCC, 2001). Since plants are always CO_2 limited for photosynthesis (Lemon, 1983), they response positively to increased CO_2 concentrations (Farquhar et al., 1980; IPCC, 2001). In C_3 plants, CO_2 and O_2 compete for the reaction sites on the photosynthetic carbon-fixing enzyme, Rubisco. Increasing the concentration of CO_2 in the atmosphere has two effects on the Rubisco reactions: increasing the rate of reaction with CO_2 (carboxylation) and decreasing the rate of oxygenation. Both effects increase the rate of photosynthesis, since oxygenation is followed by photorespiration which releases CO_2 (Farquhar et al., 1980). With increased photosynthesis, plants can develop faster, attaining the same final size in less time, or can increase their final mass. Both types of growth response to elevated CO_2 concentrations have been observed (Masle, 2000). C_3 crops show an

131

average increase in NPP of around 33% for a doubling of atmospheric CO_2 (Koch and Mooney, 1996). Therefore, under climate change conditions with an increased concentration of atmospheric CO_2, crop grain yields could be increased. As the grain yields are usually removed from the agricultural ecosystem, NBP will decrease, resulting in a decrease in the soil carbon pool, and NBP is the rate of soil carbon loss. The yields modeled under climate change showed an increase of about 8% and 11% in 1996 and 1998, respectively, compared with those modeled under current climate.

The long-term soil carbon dynamics for a barley-fallow system modeled under current climate and climate change conditions showed that soil will lose carbon faster under climate change than under current climate conditions (40 g C m^{-2} y^{-1} versus 36 g C m^{-2} y^{-1}) (Fig. 5.12), causing 35% and 30% of soil carbon loss in 0-135 cm layer from 1991 to 2090, under climate change and current climate, respectively. The higher soil carbon loss under climate change may be attributed to: 1) higher grain yield removal. About 10% of more yields would be harvested in 1996 and 1998 under climate change compared those under current climate; 2) increased temperature under climate change will result in a higher soil respiration. The global BNP also decreases as the CO_2 concentration increases, which was estimated globally to have averaged -0.2 ± 0.7 Pg C yr^{-1} during the 1980s and -1.4 ± 0.7 Pg C yr^{-1} during the 1990s, based on atmospheric measurements of CO_2 and O_2 (IPCC, 2001).

5.7.4 The contribution of crop-fallow rotation to CO_2 emission

Land use and land-use change directly affect the exchange of greenhouse gases between terrestrial ecosystems and the atmosphere. About 10 to 30% of the current total anthropogenic emissions of CO_2 are estimated to be caused by land-use conversion (IPCC, 2001). The annual flux of carbon from land-use change for the period from 1990 to 1995 has been estimated to be 1.6 Pg C yr^{-1} (Houghton, 2000; Houghton et al., 1999, 2000). In semi-arid areas where precipitation is limited, cropping system change from continuous cropping to crop-fallow rotation is thought to be an effective way to conserving soil moisture while ensuring stable crop yields. The estimation of area of

cropland under crop-fallow rotation in western Canada was 8.1 Mha in 1989 and 6.0 Mha in 1999 (Statistical Handbook, 1999).

The predicted results from long-term soil carbon dynamics showed that from 1991 to 2090, soil would lose carbon at an average loss of 36 g C m^{-2} y^{-1} and 40 g C m^{-2} y^{-1}, under current climate and climate change, respectively. Applying these rates of soil carbon loss from crop-fallow rotation in western Canada, it works out that the total soil carbon loss in western Canada in 1989 was 2.92×10^{12} g C and 3.24×10^{12} g C, under current climate and climate change, respectively. In 1999, the total soil carbon loss in western Canada was 2.16×10^{12} g C and 2.40×10^{12} g C, under current climate and climate change, respectively. Therefore, under current climate conditions, of the 1.6 Pg C yr^{-1} carbon emission from the global land-use change, the crop-fallow rotation in western Canada contributed 0.182 % and 0.135 % in 1989 and 1999, respectively. If climate change is considered, the contribution of the crop-fallow rotation in western Canada to global carbon emission from land-use change would be greater, which is 0.20% and 0.15% in 1989 and 1999, respectively. Anderson et al. (2001) estimated the soil carbon loss in summer fallow in western Canada's prairies using the Century Model, a mathematical ecosystem model. Their resulted indicated the average losses in summer fallow were 0.21 t of carbon per hectare per year (i.e. 21 g C m^{-2} y^{-1}), which is very close to the results obtained through the model *ecosys* in this study. Therefore, practical precautions must be taken in agricultural activities in order to mitigate the CO_2 emission from the crop-fallow system, especially under future climate conditions.

References

Amthor, J.S., 1989. Respiration and crop productivity. Springer-Verlag, New York.

Anderson, D., Grant, R.F., Rolfe, C., 2001. Climate of change: taking credit, Canada and the role of sinks in international climate negotiations. David Suzuki Foundation.

Anthoni, P.M., Law, B.E., Unsworth, M.H., 1999. Carbon and water vapor exchange of an open-canopied ponderosa pine ecosystem. Agric. Forest Meteorol. 95, 151-168.

Boyer, J.S., 1970. Leaf enlargement and metabolic rates in corn, soybean, and sunflower at various leaf water potentials. Plant Physiology 46, 233-235.

Bremer, E., Janzen, H.H., Johnson, A.M., 1994. Sensitivity of total, light fraction and mineralizable matter to management practices in a Lethbridge soil. Can. J. Soil Sci. 74, 131-138.

Brix, H., 1962. The effect of water stress on the rates of photosynthesis and respiration in tomato plants and loblolly pine seedlings. Physiologia Plantarum 15, 10-20.

Bruce, J.P., Frome, M., Haites, E., Jamzen, H., Lal, R., Paustian, K., 1999. Carbon sequestration in soils. Journal of Soil and Water conservation, 382-389.

Campbell, C.A., Biederbeck, V.O., Zentner, R.P., Lafond, G.P., 1991. Effects of crop rotations and cultural practices on soil organic matter, microbial biomass and respiration on a thin Black Chernozem. Can. J. Soil Sci. 71, 363-376.

Davidson, E.A., Ackerman, I.L., 1993. Changes in soil carbon inventories following cultivation of previously untilled soils. Biogeochemistry 20, 161-193.

Denmead, O.T., 1976. Temperate Cereals. In: Monteith, J.L. (Ed.), Vegetation and the atmosphere. Academic Press, London.

Farquhar, G.D., von Caemmerer, S., and Berry, J.A., 1980. A biological model of photosynthetic CO_2 assimilation in leaves of C_3 species. Planta 149, 78-90.

Horner, G.M., Oveson, M.M., Baker, G.O., Pawson, W.W., 1960. Effect of cropping practice on yield, soil organic matter, and erosion in the Pacific Northwest wheat region. Wash., Idaho, and Oregon Agric Exp. Stn. And ARS-USDA Coop. Bull. No. 1 Pullman, Wash.

Houghton, R.A. J.L. Hackler, and K.T. Lawrence, 1999. The U.S. carbon budget: contributions from land-use change. Science 285, 574–578.

Houghton, R.A., 1999. The annual net flux of carbon to the atmosphere from changes in land use 1850-1990. Tellus 52B, 298-313.

Houghton, R.A., 2000. A new estimate of global sources and sinks of carbon from land-use change. EOS 81, supplements 281.

Houghton, R.A., D.L. Skole, C.A. Nobre, J.L. Hackler, K.T. Lawrence, W.H. Chomentowski, 2000. Annual fluxes of carbon from deforestation and regrowth in the Brazilian Amazon. Nature 403, 301–304.

IPCC, 2001. IPCC Third Assessment Report - Climate Change 2001: The Scientific Basis. http://www.ipcc.ch.

Janzen, H.H., 1987. Soil organic matter characteristics after long-term cropping to various spring wheat rotation. Can. J. Soil. Sci. 67, 845-856.

Janzen, H.H., Johnston, A.M., Carefoot, J.M., and Lindwall, C.W., 1997. Soil organic dynamics in long-term experiments in southern Alberta. CRC Press.

Koch, G.W., Mooney, H.A., 1996. Response of terrestrial ecosystems to elevated CO_2: a synthesis and summary. In: Kock, G.W., Mooney, H.A. (eds.), Carbon Dioxide and Terrestrial Ecosystems. Academic Press, San Diego, 415-429.

Laprise, R., D. Caya, M. Giguere, G. Bergeron, H. Cote, J.-P. Blanchet, G.J. Boer, and N.A. McFarlane, 1998. Climate and Climate Change in Western Canada as simulated by the Canadian Regional Climate Model. Atmos. Oc. 36, 119-167.

Lemon, E.R., 1983. CO_2 and plants. The response of plants to rising levels of atmospheric carbon dioxide. AAAS Selected Symposium Series 84, Westview Press, Washington.

Masle, J., 2000. The effects of elevated CO_2 concentrations on cell division rates, growth patterns, and blade anatomy in young wheat plants are modulated by factors related to leaf position, vernalization, and genotype. Plant Physiology 122, 1399-1415.

Matthews, E., 1983. Global vegetation and land-use - new high-resolution data-bases for climate studies. Journal of Climate and Applied Meteorology 22, 474-487.

McGill, W.B., Dormaar, J.F., and Reinl-Dwyer, E., 1988. New perspectives on soil organic matter quality, and dynamics on the Canadian prairies, in Land Degradation and conservation Tillage. Proceedings of 34th Annual Canadian Society of Soil Science/Agricultural Institute of Canada Meeting, Calgary, Alberta.

McGinn, S.M., Akinremi, O.O., 2000. Carbon dioxide balance of a crop-fallow rotation in western Canada. Can. J. Soil Sci. 81, 121-127.

Meyers, T.P., 2001. A comparison of summertime water and CO_2 fluxes over rangeland for well-watered and drought conditions. Agric. Forest Meteorol. 106, 205-214.

Miranda, A.C., Miranda, H.S., Lloyd, J., Grace, J., Francey, R.J., McIntyre, J.A., Meir, P., Riggan, P., Lockwood, R., Brass, J., 1997. Fluxes of carbon, water and energy over Brazilian cerrado: an analysis using eddy covariance and stable isotopes. Plant Cell Environ. 20, 315-328.

Monreal, C.M., Janzen, H.H., 1993. Soil organic carbon dynamics after eighty years of cropping a Dark Brown Chernozem. Can. J. Soil Sci. 73, 133-136.

Rasmussen, P.E., Parton, W.J., 1994. Long-term effects of residue management in wheat-fallow. I. Inputs, yield and soil organic matter. Soil Sci. Soc. Am. J. 58, 523-530.

Ridley, A.O., Hedlin., R.A., 1968. Soil organic matter and crop yields as influenced by frequency of summer fallow. Can. J. Soil Sci. 48, 315-322.

Smith, W.N., Rochette, P., Monreal, C., Desjardins, R.L., Pattey, E., Jaques, A., 1997. The rate of carbon change in agricultural soils in Canada at the landscape level. Can. J. Soil Sci. 77, 219-229.

Statistical Handbook, 1999. Canadian Grains Industry, Winnipeg, MB.

Chapter 6   General discussion and conclusions

6.1 Summary

Bowen ratio/energy balance (BREB) and ecosystem modeling were used to examine the diurnal and season exchange of energy and CO_2 fluxes over a crop-fallow system in the growing seasons of 1996 and 1998 in Lethbridge, southern Alberta. Simultaneous measurements of net radiation (Rn), sensible heat (H), latent heat (LE) and CO_2 fluxes were made by two Bowen ratio systems, which were used to test modeled results from the ecosystem model *ecosys* after initialized with the boundary conditions, site and topographic information, soil and crop attributes, soil management information, crop management information that followed those from the field experimental sites. Diurnal and season exchange of energy and CO_2 fluxes, annual carbon balance of the crop-fallow rotation was examined based on the measurements and simulation results. The model *ecosys* was also used to predict long-term soil carbon dynamics under the current climate and the climate change scenarios, based on which the effects of land use change and climate change on soil carbon dynamics were examined and discussed. This work is important in determining the contribution of agriculture to greenhouse gas emission, and to the global change studies.

6.2 General discussion and conclusions

1.   Bowen ratio (BREB) and modeling methods provide effective ways for studying the diurnal and seasonal energy and carbon dioxide exchanges, and for studying annual carbon balance in the barley-fallow system. Using the *ecosys* model, the net radiation flux (Rn) was slightly overestimated at lower values, but was fairly well simulated at higher values. The overall overestimation of average Rn by *ecosys* is 25-30 W m^{-2}, which is in the same range as the typical accuracy of net radiation measurements (Halldin and Lindroth, 1992; Smith et al., 1997). Due to the inequality of

137

heat and water vapor eddy diffusivities during sensible heat advection (Blad and Rosenberg, 1974; Verma et al., 1978), and the systematic overestimation of available energy (Rn-G) by BREB (Fritschen and Simpson, 1989; Cooper et al., 1998), BREB usually underestimates latent heat fluxes (LE), while it overestimates sensible heat fluxes (H), causing an apparent overestimation of LE and an apparent underestimation of H fluxes by the model *ecosys*. The average LE was overestimated by the model by about 20%, which is in the same range of the potential errors carried by BREB (Baldocchi et al., 1988). However, statistical analysis showed that the linear regression between measured and modeled energy and CO_2 fluxes was highly significant with a correlation coefficient (r^2) at an extremely significant level. Standard error of energy exchange and carbon fluxes were smaller than 50 W m^{-2} and 3.5-4.5 μmol m^{-2} s^{-1}, respectively, which were very close to those reported in a similar study (50 W m^{-2} and 3 to 4 μmol m^{-2} s^{-1}, respectively) in which *ecosys* had been proved to confidently stimulate fluxes over crop fields (Grant et al., 1993).

2. Water status is a major factor controlling energy exchange over the barley-fallow systems in the semi-arid region, which determines the partitioning of solar radiation between latent (LE) and sensible heat (H) fluxes. During wet periods, radiative energy received by the canopy during daytime was dissipated more as latent heat than as sensible heat, causing higher latent heat while lower sensible heat fluxes to be measured and modeled. While during dry periods, latent heat was decreasing, but sensible heat was increasing. Soil water status determines partitioning of available energy (Rn-G) between LE and H mainly through its regulation on stomatal apertures, which also play an important role in determining the CO_2 transfer in the ecosystem.

3. Water status is also a major factor controlling CO_2 exchanges over crop-fallow systems in semi-arid regions, which determines the season carbon fixation and annual carbon balance. Both CO_2 influxes (carbon fixation) and CO_2 effluxes (soil respiration) were reduced by water stress, but the reduction in CO_2 fixation was much greater than in soil respiration (Brix, 1962; Amthor, 1989), causing NPP to decline, and causing a ecosystem to change from a carbon sink to a carbon source in the end. Before grain

yield removal, the barley-fallow system can be a small C source in drier year (1996), but a small sink in wetter year (1998). However, soil lost carbon in both years after accounting for the grain yield removal from the ecosystem, causing a negative NBP.

4. Land use change from continuous cropping to a crop-fallow rotation could result in soil carbon loss (Matthews, 1983; Houghton, 1999, 2000). The rate at which soil would lose carbon slows with the age of the ecosystem. Generally, cultivation of grasslands caused a rapid decline in organic carbon and nitrogen during the first 10 to 30 years of cultivation (Rasmussen et al., 1980). Anderson et al. (2001) also stated that land use change would within a decade or two cause a rapid loss of much of the gains in carbon storage, because gains during the first decade are mostly in litterfall residues in the upper 5-10 cm of the soil that are still decomposing rapidly and so are vulnerable to accelerated decomposition if disturbed. Since the soils in Lethbridge were originally developed under grasslands where high levels of soil organic matter had been accumulated, cultivation of these grasslands to croplands therefore would cause a higher rate of soil carbon loss at earlier stages. The effect of conversion of natural ecosystems for shifting of cultivation on soil carbon loss would level off once the ecosystem reached a relatively stable stage. Therefore, when land use changes from natural grasslands to continuous cropping, and then to crop-fallow rotation, the rate of soil carbon loss slows with the time. Before 2020 soil would lose carbon at a rate of 62 and 66 g C m^{-2} y^{-1}, under current climate and climate change, respectively. After 2020, the ecosystem would lose soil carbon at a slower rate of 22 and 27 g C m^{-2} y^{-1}, under current climate and climate change, respectively. The overall loss of soil carbon resulted from land use change from continuous barley to barley-fallow rotation in Lethbridge, would be 30% carbon in 0-135 cm layer from 1991 to 2090, which is equivalent to an average loss of 36 g C m^{-2} y^{-1} under current climate. These results are comparable to soil carbon measurements under crop-fallow rotations in long-term experiments in Western Canada, which reported that soil organic carbon loss ranged from 15% to 30% in 0-60 cm layer (McGill et al., 1988; Janzen et al., 1997). Therefore, barley-fallow rotation is a net carbon source to atmosphere. Practical precautions must be taken in

agricultural activities in order to mitigate the CO_2 emission from the crop-fallow system.

5. Climate change with increased atmospheric CO_2 concentration would accelerate the loss of soil carbon from the barley-fallow rotation. From 1991 to 2090, soil would lose 30% and 35% carbon in 0-135 cm layer, which is equivalent to an average loss of 36 g C m^{-2} y^{-1} and 40 g C m^{-2} y^{-1}, under current climate and climate change, respectively. Higher rates of soil carbon loss under climate change may be attributed to 1) Higher grain yield removal from the ecosystem. Since the plants are always CO_2 limited for photosynthesis (Lemon, 1983), they respond positively to increased CO_2 concentration (Farquhar et al., 1980; IPCC, 2001). With increased photosynthesis, higher yields can be obtained and be removed, causing a decrease in NBP (net biome productivity) (Masle, 2000); 2) Higher soil respiration resulted from increased temperature would cause a reduction in soil carbon storage (Shaver et al., 1992; Townsend et al., 1992; Oechel et al., 1993; Schimel et al., 1994). Higher temperatures would also cause a higher decomposition rate of soil organic matter and hence a higher rate of soil respiration and soil carbon loss, NBP is thus reduced.

6. Land use change from natural grasslands to continuous cropping, and then to crop-fallow rotations contributes to the CO_2 emission from agricultural ecosystem. About 10 to 30% of the current total anthropogenic emissions of CO_2 are estimated to be caused by land-use conversion (IPCC, 2001). The annual flux of carbon from land-use change for the period from 1990 to 1995 has been estimated to be 1.6 Pg C yr^{-1} (Houghton, 2000; Houghton et al., 1999, 2000). According to these results and the estimated area of crop-fallow rotation in western Canada (Statistical Handbook, 1999), under current climate conditions, the land-use change from continuous cropping to crop-fallow rotation in western Canada contributed 0.182 % and 0.135 % of the global carbon emission resulted from the land-use change in 1989 and 1999, respectively. While under climate change conditions, the contribution would be increased, which would be 0.20% and 0.15% in 1989 and 1999, respectively. Therefore, practical

precautions must be taken in agricultural activities in response to the climate change, in order to mitigate the CO_2 emission from the crop-fallow system.

6.3 Future considerations

1. Further research is required to improve the ability to detect, attribute and understand climate change, to reduce uncertainties and to project future climate changes, in order to study the possible effect of climate on annual carbon balance and soil carbon dynamics under the crop-fallow rotation. In particular, there is a need for long-term systematic and sustained observations to make accurate estimates of annual carbon budgets for the crop-fallow system.

2. Sustain and expand the observational foundation for energy and carbon dioxide exchange studies by providing accurate, long-term, consistent data including implementation of a strategy for integrated global observations, and enhancing the development of reconstructions of past climate periods.

3. Improve the observations of the spatial distribution of CO_2 exchange and annual carbon balance by coupling the process-based model *ecosys* with GCMs and remote sensing. Using Geographical Information System (GIS) to visually display the outputs in three-dimension and at landscape, regional or even global levels.

4. Improve understanding of the mechanisms and factors leading to changes in energy and CO_2 exchange, annual carbon balance, long-term soil carbon dynamics in the crop-fallow system. Study the feedback of climate change on these processes, coupling with descriptions of human activities (land use change, tillage, fertilization, irrigation, etc.).

5. Investigate the effective ways in agricultural practices that can increase carbon sequestration in soil.

6. Sensitivity analysis: perform sensitivity test of the model in order to quantify the general variability in the modelled responses to model inputs and parameters, and to the changing climates.

References

Amthor, J.S., 1989. Respiration and crop productivity. Springer-Verlag, New York.

Anderson, D., Grant, R.F., Rolfe, C., 2001. Climate of change: taking credit, Canada and the role of sinks in international climate negotiations. David Suzuki Foundation.

Baldocchi, D.D., Hicks, B.B., Meyers, T.P., 1988. Measuring biosphere-atmosphere exchanges of biologically related gases with micrometeorological methods. Ecology 69, 1331-1340.

Blad, B.L., Rosenberg, N.J., 1974. Lysimetric calibration of the Bowen ratio/energy balance method for evapotranspiration estimation in the central Great Plains. J. Appl. Meteorol. 13, 227-236.

Brix, H., 1962. The effect of water stress on the rates of photosynthesis and respiration in tomato plants and loblolly pine seedlings. Physiologia Plantarum 15, 10-20.

Cooper, D.I., Alves, L.M., Matthias, A.D., and Gay, L.W., 1998. Comparison of Bowen ration and eddy correlation methods for sensible heat flux estimates. 117-140.

Farquhar, G.D., von Caemmerer, S., and Berry, J.A., 1980. A biological model of photosynthetic CO_2 assimilation in leaves of C_3 species. Planta 149, 78-90.

Fritschen, L.J., Simpson, J.R., 1989. Surface energy balance and radiation systems: general description and improvements. J. Appl. Meteorol. 28, 680-689.

Grant, R. F., Rochette, P., Desjardins, R. L., 1993. Energy exchange and water use efficiency of field crops: validation of a simulation model. Agron. J. 85, 916-928.

Halldin, S., Lindroth, A., 1992. Errors in net radiometry: comparison and evaluation of six radiometer designs. J. Atmos. Ocean. Technol. 9, 762-783.

Houghton, R.A. J.L. Hackler, and K.T. Lawrence, 1999. The U.S. carbon budget: contributions from land-use change. Science 285, 574–578.

Houghton, R.A., 1999. The annual net flux of carbon to the atmosphere from changes in land use 1850-1990. Tellus 52B, 298-313.

Houghton, R.A., 2000. A new estimate of global sources and sinks of carbon from land-use change. EOS 81, supplements 281.

Houghton, R.A., D.L. Skole, C.A. Nobre, J.L. Hackler, K.T. Lawrence, W.H. Chomentowski, 2000. Annual fluxes of carbon from deforestation and regrowth in the Brazilian Amazon. Nature 403, 301–304.

IPCC, 2001. IPCC Third Assessment Report - Climate Change 2001: The Scientific Basis. http://www.ipcc.ch.

Janzen, H.H., Johnston, A.M., Carefoot, J.M., and Lindwall, C.W., 1997. Soil organic dynamics in long-term experiments in southern Alberta. CRC Press.

Lemon, E.R., 1983. CO_2 and plants. The response of plants to rising levels of atmospheric carbon dioxide. AAAS Selected Symposium Series 84, Westview Press, Washington.

Masle, J., 2000. The effects of elevated CO_2 concentrations on cell division rates, growth patterns, and blade anatomy in young wheat plants are modulated by factors related to leaf position, vernalization, and genotype. Plant Physiology 122, 1399-1415.

Matthews, E., 1983. Global vegetation and land-use - new high-resolution data-bases for climate studies. Journal of Climate and Applied Meteorology 22, 474-487.

McGill, W.B., Dormaar, J.F., and Reinl-Dwyer, E., 1988. New perspectives on soil organic matter quality, and dynamics on the Canadian prairies, in Land Degradation and conservation Tillage. Proceedings of 34th Annual Canadian Society of Soil Science/Agricultural Institute of Canada Meeting, Calgary, Alberta.

Oechel, W.C., Hastings, S.J., Vourlitis, G., Jenkins, M., Riechers, G., Grulke, N., 1993. Recent change of Artic tundra ecosystems from a net carbon sink to a source. Nature 361, 520-523.

Rasmussen, P.E., Allmaras, R.R., Rohde, C.R., Roager Jr., N.C., 1980. Crop residue influences on soil carbon and nitrogen in a wheat-fallow system. Soil Sci. Soc. Am. J. 44, 596-600.

Schimel, D.S., Braswell Jr., B.H., Holland, E.A., 1994. Climatic edaphic, and biotic controls over carbon and turnover of carbon in soils. Global Biogeochemical Cycles 8, 279-293.

Shaver, G.R., Billings, W.D., Chapin III, F.S., Giblin, A.E., Nadelhoffer, K.J., Oechel, W.C., Rastetter, E.B., 1992. Global change and the carbon balance of Artic ecosystems. BioScience 42, 433-441.

Smith, E.A., Hodges, G.B., Bacrania, M., Cooper, H.J., Owens, M.A., Chappel, R., Kincannon, W., 1997. BOREAS net radiometer engineering study. NASA-Goddard Space Flight Center, Greenbelt, USA.

Statistical Handbook, 1999. Canadian Grains Industry, Winnipeg, MB.

Townsend, A.R., Vitousek, P.M., Holland, E.A., 1992. Tropical soils could dominate the short-term carbon cycle feedbacks to increased global temperatures. Climate Change 22, 293-303.

Verma, S.B., Rosenberg, N.J., Blad, B.L., 1978. Turbulent exchange coefficients for sensible heat and water vapor under advective conditions. J. Appl. Meteorol. 17, 330-338.

Appendix-Equation and glossary used in the model

Energy Balance

$$R_{N_i} + LE_i + LV_i + H_i + G_i = 0 \tag{3.1}$$

$$R_{N_g} + LE_g + H_g + G_g = 0 \tag{3.2}$$

$$R_{N_i} = R_{S_i} + F_{P_i}(R_{La} + R_{Lg} - 2R_{Li}) \tag{3.3}$$

$$R_{N_g} = F_g[R_{Sg} + (1 - F_{P_i})R_{La} + F_{P_i}R_{Li}] - R_{Lg} \tag{3.4}$$

$$LE_i = F_{Si}L(e_a - e_i)/(r_{Ai} + r_{Ci}) \tag{3.5}$$

$$LV_i = F_{Si}L(e_a - e_i')/r_{Ai} \tag{3.6}$$

$$LE_g = F_g[L(e_a - e_g)/r_{Ag}] \tag{3.7}$$

$$H_i = F_{si}c_a(T_a - T_i)/r_{Ai} \tag{3.8}$$

$$H_g = F_g c_a(T_a - T_g)/r_{Ag} \tag{3.9}$$

$$r_{Ai} = \frac{\ln((z_R - d_i + z_{Ci})/z_{Ci})\ln((z_R - d_i + z_{Vi})/z_{Vi})}{K^2 u_a(1.0 - 10.0Ri)} \tag{3.10}$$

$$r_{Ci} = r_{C_i} + (r_{C\max} - r_{C_i})e^{(-\beta\Psi_{Ti})} \tag{3.11}$$

$$r_{C_i} = 0.64 F_{P_i}(C_{Bi} - C_{\Gamma_i})/V_{B_i'} \tag{3.12}$$

$$G_i = c_i(T_{i(t-1)} - T_{i(t)})/\Delta t \tag{3.13}$$

$$G_r = c_r \frac{T_{r(t-1)} - T_{r(t)}}{\Delta t} + 2\kappa_r \frac{T_{s(t-1)} - T_{r(t)}}{z_r + z_s} \tag{3.14}$$

$$G_s = c_s \frac{T_{s(t-1)} - T_{s(t)}}{\Delta t} + 2\kappa_s \frac{T_{l(t-1)} - T_{s(t)}}{z_s + z_l} \tag{3.15}$$

$$G_{l,l+1} = 2\kappa_{l,l+1}(T_l - T_{l+1})/(z_l + z_{l+1}) + c_w T_l W_{l,l+1} \tag{3.16}$$

Water Relations

$$\Psi_{Ti} = \Psi_{Ci} - \Psi_{\pi i} \tag{3.17}$$

$$\Psi_{\pi i} = \Psi_{\pi_i}F_{DM}/F_{DM'} - [X]_i F_{DM}RT_i/M \tag{3.18}$$

$$U_i = \sum_{l=1}^{L}\sum_{r=1}^{2}U_{i,l,z} \tag{3.19}$$

$$U_{i,l,z} = (\Psi_{C_i} - \Psi_{Sl})/(\Omega_{S_{i,l,z}} + \Omega_{R_{i,l,z}} + \sum_{x=1}^{2}\Omega_{A_{i,l,z,x}}) \tag{3.20}$$

$$\Omega_{S_{i,l,z}} = \ln[(d_{i,l,z}/r_{i,l,z})/(2\pi L_{i,l,z}\kappa_{R_{i,l,z}})]\theta_l'/\theta_{i,l,z} \tag{3.21}$$

$$\Omega_{R_{i,l,z}} = \Omega_{R_{i,z}}/L_{i,l,z} \tag{3.22}$$

$$\Omega_{A_{i,l,z,1}} = \Omega_{A_{i,r}} z_l / \{n_{i,l,z,1}(r_{i,l,z,1} / r'_{i,2,z})^4\} \tag{3.23}$$

$$\Omega_{A_{i,l,z,2}} = \Omega_{A_{i,r}} 0.5(L_{i,l,z,2} / n_{i,l,z,2}) / \{n_{i,l,z,2}(r_{i,l,z,2} / r'_{i,2,z})^4\} \tag{3.24}$$

$$\Psi_{R_{i,l,z}} = \frac{\{\Psi_{Sl}(\Omega_{R_{i,l,z}} + \Omega_{A_{i,l,z,1}} + \Omega_{A_{i,l,z,2}}) + \Psi_{Ci}\Omega_{Si,l,z}\}}{(\Omega_{Si,l,z} + \Omega_{Ri,l,z} + \Omega_{Ai,l,z,1} + \Omega_{Ai,l,z,2})} \tag{3.25}$$

Gross primary productivity (GPP)

$$V_{C_{i,j,k,l,m,n,o}} = \frac{V_{C\max_{i,j,k}}(C_{C_{i,j,k,l,m,n,o}} - \Gamma_{i,j,k})}{C_{C_{i,j,k,l,m,n,o}} + K_{Ci}} \tag{3.26}$$

$$K_{Ci} = K_{C'_i}(1 + O_C / K_{O'_i}) \tag{3.27}$$

$$V_{C\max_{i,j,k}} = V'_i f_{C_i} R_{C_i} 3.0(N_{i,j,k} / M_{i,j,k})(M_{i,j,k} / A_{i,j,k}) \tag{3.28}$$

$$\Gamma_{i,j,k} = \frac{V_{O\max_{i,j,k}} K_{C'_i} O_c}{2V_{C\max_{i,j,k}} K_{O'_i}} \tag{3.29}$$

$$V_{J_{i,j,k,l,m,n,o}} = J_{i,j,k,l,m,n,o} Y_{i,j,k,l,m,n,o} \tag{3.30}$$

$$J_{i,j,k,l,m,n,o} = \frac{QR_{P_{i,l,m,n,o}} + J_{\max_{i,j,k}} - [(QR_{P_{i,l,m,n,o}} + J_{\max_{i,j,k}})^2 - 4\alpha QR_{P_{i,l,m,n,o}} J_{\max_{i,j,k}}]^{0.5}}{2\alpha} \tag{3.31}$$

$$J_{\max_{i,j,k}} = J'_i f_{C_i} E_{C_i} 3.0(N_{i,j,k} / M_{i,j,k})(M_{i,j,k} / A_{i,j,k}) \tag{3.32}$$

$$f_{C_i} = T_i\{e^{[A - H_a/(RT_i)]}\} / \{1 + e^{[(H_{dl} - ST_i)/(RT_i)]} + e^{[(ST_i - H_{dh})/(RT_i)]}\} \tag{3.33}$$

$$Y_{i,j,k,l,m,n,o} = \frac{C_{C_{i,j,k,l,m,n,o}} - \Gamma_{i,j,k}}{\varepsilon C_{C_{i,j,k,l,m,n,o}} + 10.5\Gamma_{i,j,k}} \tag{3.34}$$

$$V_{B_{i,j,k,l,m,n,o}} = \min\{V_{C_{i,j,k,l,m,n,o}}, V_{J_{i,j,k,l,m,n,o}}\} \tag{3.35}$$

$$V_{G_{i,j,k,l,m,n,o}} = \frac{C_{B_i} - C_{I_{i,j,k,l,m,n,o}}}{r_{L_{i,j,k,l,m,n,o}}} \tag{3.36}$$

$$C_{B_i} = C_A - \frac{1.33 r_{A_i}(V_N + V_S) \times 10^6}{12 \times 3600 \times 44.6 \times 273.15 / T_i} \tag{3.37}$$

$$r_{L_{i,j,k,l,m,n,o}} = r'_{L_{i,k,l,m,n,o}} + (r_{L\max} - r'_{L_{i,j,k,l,m,n,o}}) \times e^{-\beta\psi_{T_i}} \tag{3.38}$$

$$r'_{L_{i,j,k,l,m,n,o}} = (C_{B_i} - C_{I'_i}) / V_{B'_{i,j,k,l,m,n,o}} \tag{3.39}$$

$$C_{I_{i,j,k,l,m,n,o}}\Big|V_{X_{i,j,k,l,m,n,o}} = V_{B_{i,j,k,l,m,n,o}} = V_{G_{i,j,k,l,m,n,o}} = GPP \tag{3.40}$$

Autotrophic respiration

$$Q_{T_{i,j}} = Q'_T X_{i,j} f_{Q_i} \tag{3.41}$$

$$Q_{M_{i,j}} = Q'_M \, N_{i,j} f_{M_i} \tag{3.42}$$

$$Q_{G_{i,j}} = \max\{0, (Q_{T_{i,j}} - Q_{M_{i,j}}) \max[0, (\Psi_{T_i} - \Psi_{T'_i})]\} \tag{3.43}$$

$$Q_{S_{i,j}} = \max\{0, Q_{M_{i,j}} - Q_{T_{i,j}}\} \tag{3.44}$$

$$\frac{\partial M_{i,j}}{\partial t} = \frac{Q_{G_{i,j}} F_{X_{i,j}}}{1.0 - F_{X_{i,j}}} - Q_{S_{i,j}} - Q_{D_{i,j}} \tag{3.45}$$

$$V_{N_{i,j}} = V_{X_{i,j}} - \min\{Q_{T_{i,j}}, Q_{M_{i,j}}\} - Q_{G_{i,j}} - Q_{S_{i,j}} = NPP \tag{3.46}$$

Heterotrophic respiration

Decomposition

$$D_{S_{i,j,c}} = D'_{S_{i,j,c}} M_{i,a,c} f_{tg} \tag{3.47}$$

$$D_{Z_{i,j,c}} = D'_{Z_{i,j,c}} M_{i,a,c} f_{tg} \tag{3.48}$$

$$D'_{S_{i,j,c}} = \{P_{S_{i,j,c}} [S_{i,c}]\} / \{[S_{i,c}] + K_{mS_{i,c}} (1.0 + [M_{i,a,c}] / K_{iS_{i,c}})\} \tag{3.49}$$

$$D'_{Z_{i,j,c}} = \{P_{Z_{i,j,c}} [Z_{i,c}]\} / \{[Z_{i,c}] + K_{mZ_{i,c}} (1.0 + [M_{i,a,c}] / K_{iZ_{i,c}})\} \tag{3.50}$$

$$f_{tg} = T_i \{e^{[A - H_a/(RT_i)]}\} / \{1 + e^{[(H_{dl} - ST_i)/(RT_i)]} + e^{[(ST_i - H_{dh})/(RT_i)]}\} \tag{3.51}$$

$$D_{Si,j,n} = D_{Si,j,c} (S_{i,j,n} / S_{i,j,c}) \tag{3.52}$$

$$D_{Zi,j,n} = D_{Zi,j,c} (Z_{i,j,n} / Z_{i,j,c}) \tag{3.53}$$

$$H_{Si=residue,j=lignin,c} = D_{Si=residue,j=lignin,c} F_H \tag{3.54}$$

Microbial growth

$$R_{gi,c} = \{R'_{gi,c} [Q_{i,c}]\} / [K_{mPc} + [Q_{i,c}]\} f_{tg} \tag{3.55}$$

$$R_{m_{i,j,c}} = R_m M_{i,j,n} f_{tm} \tag{3.56}$$

$$f_{tm} = e^{0.09(T_i - 303.16))} \tag{3.57}$$

$$R_{i,c} = R_{gi,c} + R_{mi,j,c} = Rh \tag{3.58}$$

$$\partial M_{i,j,c} / \partial t = F_j U_{i,c} - F_j R_{i,c} - D_{Mi,j,c} \qquad [R_{i,c} > R_{mi,j,c}] \tag{3.59a}$$

$$\partial M_{i,j,c} / \partial t = F_j U_{i,c} - R_{mi,j,c} - D_{Mi,j,c} \qquad [R_{i,c} < R_{mi,j,c}] \tag{3.59b}$$

$$U_{i,c} = U'_{i,c} [C_N / (C_N + K_{CN})] \tag{3.60a}$$

$$U'_{i,c} = R_{gi,c} (1 + \Delta G / E_m) \tag{3.60b}$$

$$I_{i,j,n} = (M_{i,j,c} C_{Nj} - M_{i,j,n}) \qquad (I_{i,j,n} < 0) \tag{3.61a}$$

$$I_{i,j,n} = (M_{i,j,c} C_{Nj} - M_{i,j,n})[N] / ([N] + K_N) \qquad (I_{i,j,n} > 0) \tag{3.61b}$$

$$D_{Mi,j,c} = D_{Mi,j} M_{i,j,c} f_{tg} \tag{3.62}$$

$$D_{Mi,j,n} = D_{Mi,j} M_{i,j,n} f_{tg} \tag{3.63}$$

$$H_{M_{i,j,c}} = D_{M_{i,j,c}} F_H \tag{3.64}$$

Glossary of the terms used in equations

Subscripts used to define spatial resolution of variables

a   Atmosphere
g   Soil or residue surface (r=residue, s=soil)
i   Plant species or type of soil organic matter
j   Tiller or branch of plant species
k   Node of tiller or branch
l   Canopy or soil layer
m   Azimuth class of leaf in canopy layer
n   Inclination class of leaf azimuth class
o   Irradiance class of leaf inclination class (sunlit or shaded)
r   Residue at ground surface
s   Soil at ground surface
x   Root axis order (1=primary, 2=secondary)
z   Root type (root or mycorrhize)

Definition of variables that are used in equations

Ψ_{π_i} Canopy osmotic potential (MPa) [Eq. 3.17]

Ψ_{π_i}' $\Psi_{\pi i}$ at $\Psi_{Ci}= 0$ (MPa) [Eq. 3.18]

Ψ_{Ci} Canopy water potential (MPa) [Eq. 3.17, 3.20]

Ψ_{Sl} Soil water potential (MPa) [Eq. 3.20, 3.25]

Ψ_{Ti} Canopy turgor potential (MPa) [Eq. 3.11, 3.17, 3.38, 3.43]

Ψ_{T_i}' Canopy turgor potential (MPa) below which $\partial M_{i,j}/\partial t \leq 0$ [Eq. 3.38]

$\Psi_{Ri,l,z}$ Root water potential (MPa) [Eq. 3.25]

$\Omega_{Ai,r}$ Axial resistance to water transport through secondary root or mycorrhizae (MPa h m^{-4}) [Eq. 3.22, 3.23]

$\Omega_{Ai,l,z,1}$ Axial resistances to water transport through primary root axes (MPa h m^{-1}) [Eq. 3.23, 3.25].

$\Omega_{Ai,l,z,2}$ Axial resistances to water transport through secondary root axes (MPa h m^{-1}) [Eq. 3.24, 3.25].

$\Omega_{R_{i,z}}$ radial resistivity to water transport from surface to axis root or mycorrhizae (MPa h m^{-2}) [Eq. 3.22]

$\Omega_{Ai,l,z,x}$ Axial resistance to water transport through root or mycorrhizal system (MPa h m^{-1}) [Eq. 3.20]

$\Omega_{Ri,l,z}$ Radial resistance to water transport from root surface to root axis (MPa h m^{-1}) [Eq. 3.20, 3.22, 3.25]

$\Omega_{Si,l,z}$ Radial resistance to water transport from soil to root surface (MPa h m^{-1}) [Eq. 3.20, 3.21]

κ_r Thermal conductivity of residue-soil (W m^{-1} K^{-1}) [Eq. 3.14]

κ_s	Thermal conductivity of surface soil (W m^{-1} K^{-1}) [Eq. 3.15]
$\kappa_{l,l+1}$	Thermal conductivity between adjacent soil layers (W m^{-1} K^{-1}) [Eq. 3.16]
$\kappa_{Ri,l,z}$	Hydraulic conductivity between soil and root surface (m^2 MPa^{-1} h^{-1}) [Eq. 3.21]
α	Shape parameter for respiration of $J_{i,j,k,l,m,n,o}$ to $R_{Pi,l,m,n,o}$ [Eq. 3.31]
β	Stomatal resistance parameter [Eq. 3.11, 3.38]
ε	The electron requirement for CO_2 fixation [Eq. 3.34]
$\Gamma_{i,j,k}$	CO_2 compensation point (μm) at ambient O_C [Eq. 3.26, 3.29]
$\theta_{i,l,z}$	Soil water content at root surface (m^3 m^{-3}) [Eq. 3.21]
θ'_l	Soil porosity (m^3 m^{-3}) [Eq. 3.21]
A	Parameter such that f_{Ci} and f_{tg}=1.0 at T_i and T_l=303.15K [Eq. 3.33, 3.51]
$A_{i,j,k}$	Leaf surface area (m^2 m^{-2}) [Eq. 3.28]
C_A	CO_2 concentration in atmosphere (μmol mol^{-1}) [Eq. 3.37]
c_a	Heat capacity of atmosphere (J m^{-3} K^{-1}) [Eq. 3.8-3.9]
C_{Bi}	CO_2 concentration in canopy air (μmol mol^{-1}) [Eq. 3.12, 3.36, 3.37]
$C_{I''i}$	CO_2 concentration in canopy leaves (μmol mol^{-1}) at ψ_{Ci}=0 MPa [Eq. 3.12, 3.39]
$C_{Ci,j,k,l,m,n,o}$	Chloroplast CO_2 concentration (μM) in soluble equilibrium with $C_{Ii,j,k,l,m,n,o}$ [Eq. 3.26, 3.34]
c_i	Heat capacity of canopy (J m^{-3} K^{-1}) [Eq. 3.13]
$C_{Ii,j,k,l,m,n,o}$	CO_2 concentration in canopy leaves (μmol mol^{-1}) [Eq. 3.36, 3.40]
c_r	Heat capacity of surface residue (J m^{-3} K^{-1}) [Eq. 3.14]
c_s	Heat capacity of soil surface layer (J m^{-3} K^{-1}) [Eq. 3.15]
c_w	Heat capacity of water (J g^{-1} K^{-1}) [Eq. 3.16]
C_N	Ratio of $M_{i,j,n}$ to $M_{i,j,c}$ (g N g C^{-1}) [Eq. 3.60]
C_{Nj}	Maximum ratio of $M_{i,j,n}$ to $M_{i,j,c}$ maintained by $M_{i,j,c}$ (g N g C^{-1}) [Eq. 3.61]
d_i	zero plane displacement height (m) [Eq. 3.10]
$d_{i,l,z}$	Half distance between adjacent root (m) [Eq. 3.21]
$D_{Mi,j,c}$	Decomposition rate of $M_{i,j,c}$ (g C m^{-2} h^{-1}) [Eq. 3.59, 3.62, 3.64]
$D_{Mi,j,n}$	Decomposition rate of $M_{i,j,n}$ (g N m^{-2} h^{-1}) [Eq. 3.63]
$D_{Si,j,c}$	Decomposition rate of $S_{i,j,c}$ by $M_{i,a,c}$ (g C m^{-2} h^{-1}) [Eq. 3.47]
$D'_{Si,j,c}$	Specific decomposition rate of $S_{i,j,c}$ by $M_{i,a,c}$ at 30°C and saturating [$S_{i,c}$] (g C g C^{-1} h^{-1}) [Eq. 3.47, 3.49]
$D_{Si,j,n}$	Decomposition rate of $S_{i,j,n}$ by $M_{i,a,c}$ (g N m^{-2} h^{-1}) [Eq. 3.52]
$D_{Zi,j,c}$	Decomposition rate of $Z_{i,j,c}$ by $M_{i,a,c}$ (g C m^{-2} h^{-1}) [Eq. 3.48]
$D'_{Zi,j,c}$	Specific decomposition rate of $Z_{i,j,c}$ by $M_{i,a,c}$ at 30°C and saturating [$Z_{i,c}$] (g C g C^{-1} h^{-1}) [Eq. 3.48, 3.50]
$D_{Zi,j,n}$	Decomposition rate of $Z_{i,j,n}$ by $M_{i,a,c}$ (g N m^{-2} h^{-1}) [Eq. 3.53]
$D_{Mi,j}$	Specific decomposition rate of $M_{i,j,c}$ at 30°C (g C g C^{-1} h^{-1}) [Eq. 3.62, 3.63]
e_a	Atmosphere vapor density (g m^{-3}) at T_a and ambient humidity (Eq. 3.5-3.7)
E_{Ci}	Specific leaf chlorophyll content (g g^{-1} leaf protein) [Eq. 3.32]
e_g	Vapor density at ground surface (g m^{-3}) at T_g and Ψ_{Sg} [Eq. 3.7]
e_i	Canopy vapor density (g m^{-3}) at T_i and Ψ_{Ci} [Eq. 3.5-3.7]
e'_i	Saturation vapor density (g m^{-3}) at T_i [Eq. 3.6]

E_m	Energy requirement for growth of $M_{i,a,c}$ [Eq. 3.60]
f_{Ci}	Temperature sensitivity of V'_i and J'_i [Eq. 3.28, 3.32, 3.33]
F_{DM}	Ratio of leaf+sheath dry mass to symplasmic water (g g^{-1}) [Eq. 3.18]
$F_{DM'}$	F_{DM} when Ψ_{Ci}=0 (g g^{-1}) [Eq. 3.18]
F_g	Fraction of ground surface covered by residue r or soil s (m^2 m^{-2}) [Eq. 3.4]
F_H	Fraction of products from lignin hydrolysis and microbial decomposition that are humified (function of clay content) [Eq. 3.54,3.64]
f_{Mi}	Temperature sensitivity of Q'_M [Eq. 3.42]
F_{Pi}	Photosynthetic photon flux density absorbed by canopy (μmol m^{-2} s^{-1}) [Eq. 3.3]
f_{Qi}	Temperature sensitivity of Q'_T [Eq. 3.41]
F_{Si}	Fraction of incident shortwave radiation absorbed by canopy (m^2 m^{-2}) [Eq. 3.5]
f_{tg}	Temperature function for growth respiration [Eq. 3.47, 3.48, 3.51]
f_{tm}	Temperature function for maintenance respiration [Eq. 3.56-3.57]
$F_{Xi,j}$	Biosynthesis efficiency (g g^{-1}) [Eq. 3.45]
F_j	J=l: fraction of microbial growth allocated to labile component $M_{i,l,c}$ [Eq.3.59] J=r: fraction of microbial growth allocated to resistant component $M_{i,r,c}$ [Eq.3.59]
G_g	Change in thermal energy stored in ground surface (W m^{-2})[Eq. 3.2]
G_i	Change in thermal energy stored in crop phytomass (W m^{-2})[Eq. 3.1, 3.13]
$G_{l,l+1}$	Heat flux between adjacent soil layers (W m^{-2}) [Eq. 3.16]
G_r	Change in thermal energy stored in surface residue (W m^{-2})[Eq. 3.14]
G_s	Change in thermal energy stored in soil surface layer (W m^{-2})[Eq. 3.15]
ΔG	Energy yield from aerobic oxidation of $Q_{i,c}$ [Eq.3.60]
H_a	Energy of activation (J mol^{-1}) [Eq. 3.33, 3.51]
H_{dh}	Energy of high-temperature deactivation (J mol^{-1}) [Eq. 3.33, 3.51]
H_{dl}	Energy of low-temperature deactivation (J mol^{-1}) [Eq. 3.33, 3.51]
H_g	Sensible heat flux between ground surface and atmosphere (W m^{-2}) [Eq. 3.2]
H_i	Sensible heat flux between canopy and atmosphere (W m^{-2}) [Eq. 3.1]
$H_{Mi,j,c}$	Humification rate of microbial decomposition products (g C m^{-2} h^{-1}) [Eq. 3.64]
$H_{Si,j,c}$	Humification rate of lignin hydrolysis products (g C m^{-2} h^{-1}) [Eq. 3.54]
J'_i	Specific electron transport by chlorophyll (μmol e$^-$ g^{-1} s^{-1}) at T_i=30°C and saturating R_{Pi} [Eq. 3.32]
$J_{i,j,k,l,m,n,o}$	Electron transport rate (μmol e$^-$ m^{-2} s^{-1}) [Eq. 3.30-3.31]
$J_{max\ i,j,k}$	Electron transport rate (μmol e$^-$ m^{-2} s^{-1}) at saturating R_{Pi} [Eq. 3.31-3.32]
K	von Karman's constant [Eq. 3.10]
K_{Ci}	Michaelis-Menten constant (μM) for carboxylation under ambient O_2 [Eq. 3.26, 3.27]
$K_{C'i}$	Michaelis-Menten constant (μM) for carboxylation in the absence of O_2 [Eq. 3.27]
$K_{iSi,c}$	Inhibition constant for $M_{i,a,c}$ on $S_{i,c}$ (g C Mg^{-1}) [Eq. 3.49]
$K_{iZi,c}$	Inhibition constant for $M_{i,a,c}$ on $Z_{i,c}$ (g C Mg^{-1}) [Eq. 3.50]
K_{mPc}	Michaelis-Menten constant for $R_{gi,c}$ on $[Q_{i,c}]$ [Eq. 3.55]
$K_{mSi,c}$	Michaelis-Menten constant for $D_{Si,j,c}$ (g C Mg^{-1}) [Eq. 3.49]

$K_{mZi,c}$	Michaelis-Menten constant for $D_{Zi,j,c}$ (g C Mg^{-1}) [Eq. 3.50]
K_N	Michaelis-Menten constant for microbial uptake of solution N (g N m^{-3}) [Eq. 3.61]
K_{CN}	Ratio of $M_{i,a,n}$ to $M_{i,a,c}$ at which $U_{i,c} = 1/2\ U'_{i,c}$ [Eq. 3.60]
$K_{O'i}$	Michaelis-Menten constant (μM) for carboxylation in the absence of CO_2 [Eq. 3.27, 3.29]
L	Latent heat of evaporation (J g^{-1}) [Eq. 3.1-3.2, 3.5-3.7]
LE_g	Latent heat flux between ground surface and atmosphere (W m^{-2}) [Eq. 3.2, 3.7]
LE_i	Latent heat flux between canopy and atmosphere (W m^{-2})[Eq. 3.1, 3.5]
$L_{i,l,z}$	Length of roots (m m^{-2}) [Eq. 3.21, 3.22]
$L_{i,l,z,2}$	Length of secondary roots (m m^{-2}) [Eq. 3.24]
LV_i	Latent heat flux between canopy surface and atmosphere (W m^{-2})[Eq. 3.1, 3.6]
M	Average molecular mass of X_i (g mol^{-1}) [Eq. 3.18]
$M_{i,a,c}$	Active microbial C (g C m^{-2}) [Eq. 3.47-3.50]
$M_{i,j}$	Mass of tiller (branch) (g C m^{-2}) [Eq. 3.45]
$M_{i,j,c}$	C content of microbial biomass $M_{i,j}$ (g C m^{-2}) [Eq. 3.59, 3.61-3.62]
$M_{i,j,k}$	Mass of leaf (g C m^{-2}) [Eq. 3.28]
$M_{i,j,n}$	N content of microbial biomass $M_{i,j}$ (g N m^{-2}) [Eq. 3.56, 3.61, 3.63]
$N_{i,j}$	Nitrogen content of tiller (branch) (g N m^{-2}) [Eq. 3.42]
$N_{i,j,k}$	Nitrogen content of leaf (g N m^{-2}) [Eq. 3.28]
$n_{i,l,z,1}$	Number of primary axes (m^{-2}) [Eq. 3.23]
$n_{i,l,z,2}$	Number of secondary axes (m^{-2}) [Eq. 3.24]
$[N]$	[NH_4^+] or [NO_3^-] in soil solution (g N m^{-3}) [Eq. 3.61]
O_C	Soluble O_2 concentration (μm) in chloroplasts [Eq. 3.27]
$P_{Si,j,c}$	Specific decomposition rate of $S_{i,j,c}$ by $M_{i,a,c}$ at 30°C (g C g C^{-1} h^{-1}) [Eq. 3.49]
$P_{Zi,j,c}$	Specific decomposition rate of $Z_{i,j,c}$ by $M_{i,a,c}$ at 30°C (g C g C^{-1} h^{-1}) [Eq. 3.50]
Q	Quantum yield (μmol e$^-$ μmol quanta^{-1}) [Eq. 3.31]
$Q_{i,c}$	Hydrolysis products of $(D_{si,j,c} + D_{Zi,j,c})$(g C m^{-2})
$Q_{Di,j}$	Litterfall caused by senescence respiration of tiller (branch) (g C m^{-2} h^{-1}) [Eq. 3.45]
$Q_{Gi,j}$	Growth respiration (g C m^{-2} h^{-1}) [Eq. 3.43, 3.45, 3.46]
Q'_M	Specific maintenance respiration (g C m^{-2} h^{-1}) at $T_i = 30$°C [Eq. 3.42]
$Q_{Mi,j}$	Maintenance respiration of tiller (branch) (g C m^{-2} h^{-1}) [Eq. 3.42-3.44, 4.46]
$Q_{Si,j}$	Senescence respiration of tiller (branch) (g C m^{-2} h^{-1}) [Eq. 3.44-3.46]
Q'_T	Specific respiration of $X_{i,j}$ (g C m^{-2} h^{-1}) [Eq. 3.41]
$Q_{Ti,j}$	Total respiration of $X_{i,j}$ (g C m^{-2} h^{-1}) [Eq. 3.41, 3.43-3.44, 3.46]
$[Q_{i,c}]$	Solution concentration of hydrolysis products (g C Mg^{-1}) [Eq. 3.55]
$r_{Li,j,k,l,m,n,o}$	Leaf stomatal resistance to CO_2 flux (s m^{-1}) [Eq. 3.36, 3.38]
$r'_{Li,j,k,l,m,n,o}$	Leaf stomatal resistance to CO_2 flux (s m^{-1}) at $\Psi_{Ci} = 0$ MPa [Eq. 3.38-3.39]
$r'_{i,2,z}$	Secondary root radius (m) at $\Psi_{Ti,l,z} = 1.0 MPa$ [Eq. 3.23, 3.24]
r_{Ag}	Aerodynamic resistance to vapor flux from ground surface (μmol m^{-2} s^{-1}) [Eq. 3.7, 3.9]
r_{Ai}	Aerodynamic resistance to vapor flux from canopy (s m^{-1}) [Eq. 3.5-3.6, 3.8,

	3.10, 3.37]
$r_{C'i}$	Minimum r_{Ci} (s m^{-1}) at ψ_{Ci}=0 MPa [Eq. 3.11, 3.12]
r_{Ci}	Canopy stomatal resistance to vapor flux (s m^{-1}) [Eq. 3.5, 3.11]
r_{Cmax}	canopy cuticular resistance to vapor flux (s m^{-1}) [Eq. 3.11]
$r_{i,l,z}$	Root radius (m) [Eq. 3.21]
$r_{i,l,z,1}$	Primary root radius (m) [Eq. 3.23]
$r_{i,l,z,2}$	Secondary root radius (m) [Eq. 3.24]
r_{Lmax}	Leaf cuticular resistance to CO_2 flux (s m^{-1}) [Eq. 3.38]
R	Gas constant (J mol^{-1} K^{-1}) [Eq. 3.18, 3.33, 3.51]
R_{Ci}	Specific leaf rubisco content (g g^{-1}) [Eq. 3.28]
$R_{gi.c}$	Growth respiration under ambient O_2 (g C m^{-2} h^{-1}) [Eq. 3.55]
$R'_{gi.c}$	Growth respiration under non-limiting O_2 (g C m^{-2} h^{-1}) [Eq. 3.55]
R_i	Richardson number [Eq. 3.10]
$R_{i,c}$	Total C from growth and maintenance respiration (g C m^{-2} h^{-1}) [Eq. 3.58]
R_{La}	Longwave radiation emitted from atmosphere(W m^{-2}) [Eq. 3.3, 3.4]
R_{Lg}	Longwave radiation emitted from ground surface (W m^{-2}) [Eq. 3.3, 3.4]
R_{Li}	Longwave radiation emitted from canopy (W m^{-2}) [Eq. 3.3, 3.4]
R_m	Specific maintenance respiration at 30°C (g C m^{-2} h^{-1}) [Eq. 3.56]
$R_{mi,j,c}$	Maintenance respiration by $M_{i,j,c}$ (g C m^{-2} h^{-1}) [Eq. 3.56]
R_{Ng}	Net radiation absorbed by canopy (W m^{-2}) [Eq. 3.2]
R_{Ni}	Net radiation absorbed by canopy (W m^{-2}) [Eq. 3.1]
$R_{Pi,l,m,n,o}$	Photosynthetic photon flux density absorbed by leaf surface (μmol quanta m^{-2} s^{-1}) [Eq. 3.31]
R_{Sg}	Shortwave radiation absorbed by ground surface (W m^{-2}) [Eq. 3.4]
R_{si}	Shortwave radiation absorbed by canopy (W m^{-2}) [Eq. 3.3, 3.5, 3.6]
S	Change in entropy (J mol^{-1} K^{-1}) [Eq. 3.33, 3.51]
$S_{i,j,c}$	Mass of solid or sorbed organic C in soil (g C m^{-2}) [Eq. 3.52]
$S_{i,j,n}$	Mass of solid or sorbed organic N in soil (g N m^{-2}) [Eq. 3.52]
$S'_{Si,j,c}$	Specific decomposition rate of $S_{i,j,c}$ by $M_{i,a,c}$ at 30°C and saturating [$S_{i,c}$] (g C g C^{-1} h^{-1}) [Eq. 3.49]
$S'_{Zi,j,c}$	Specific decomposition rate of $Z_{i,j,c}$ by $M_{i,a,c}$ at 30°C and saturating [$Z_{i,c}$] (g C g C^{-1} h^{-1}) [Eq. 3.50]
[$S_{i,c}$]	Concentration of $\sum_{j=1}^{J} S_{i,j,c}$ in soil (g C Mg^{-1}) [Eq. 3.49]
t	Current time step [Eq.3.13-3.15]
$t-1$	Previous time step [Eq.3.13-3.15]
T_a	Air temperature (K) [Eq. 3.8-3.9]
T_g	Ground surface temperature (K) [Eq. 3.8-3.9]
T_i	Canopy temperature (K) [Eq. 3.8, 3.13]
T_l	Temperature of soil layer below surface (K) [Eq. 3.15, 3.16]
T_r	Surface residue temperature (K) [Eq. 3.14]
T_s	Soil surface temperature (K) [Eq. 3.14-3.15]
u_a	wind speed at z_R (m s^{-1}) [Eq. 3.10]
U_i	Water uptake by canopy root system (m^3 m^{-2} h^{-1}) [Eq. 3.19]

$U_{i,c}$	Uptake of $Q_{i,c}$ by $M_{i,a,c}$ under limiting nutrient availability (g C m^{-2} h^{-1}) [Eq. 3.59, 3.60]
$U'_{i,c}$	Uptake of $Q_{i,c}$ by $M_{i,a,c}$ under non-limiting nutrient availability (g C m^{-2} h^{-1}) [Eq. 3.59, 3.60]
$U_{i,l,z}$	Water uptake by canopy roots or mycorrhiae in layer l (m^3 m^{-2} h^{-1}) [Eq. 3.19]
$V_{Ci,j,k,l,m,n,o}$	CO_2-limited leaf carboxylation rate (μmol m^{-2} s^{-1}) at $C_{Ci,j,k,l,m,n,o}$ [Eq. 3.26]
$V_{Ji,j,k,l,m,n,o}$	Irradiance-limited leaf carboxylation rate (μmol m^{-2} s^{-1}) at $R_{Pl,m,n,o}$ [Eq. 3.30]
$V_{Gi,j,k,l,m,n,o}$	Leaf CO_2 diffusion rate (μmol m^{-2} s^{-1}) [Eq. 3.36, 3.40]
$V_{B'i}$	potential canopy carboxylation rate (μmol m^{-2} s^{-1}) at ψ_{Ci}=0 MPa [Eq. 3.12]
$V_{B'_{i,j,k,l,m,n,o}}$	potential leaf carboxylation rate (μmol m^{-2} s^{-1}) at ψ_{Ci}=0 MPa [Eq. 3.39]
$V_{Bi,j,k,l,m,n,o}$	Leaf carboxylation rate (μmol m^{-2} s^{-1}) [Eq. 3.35]
$V_{Cmax\ i,j,k}$	Leaf carboxylation rate (μmol m^{-2} s^{-1}) at saturating CO_2 in the absence of O_2 [Eq. 3.26, 3.28]
V'_i	Specific carboxylation activity of rubisco (μmol g^{-1} s^{-1}) at T_i=30°C and saturating CO_2 in the absence of O_2 [Eq. 3.28]
$V_{Gi,j,k,l,m,n,o}$	Leaf CO_2 diffusion rate (μmol m^{-2} s^{-1}) (Equations 3.36, 3.40)
V_N	Net CO_2 fixation (g C m^{-2} h^{-1}) [Eq. 3.37]
$V_{Ni,j}$	Tiller (branch) net CO_2 fixation (g C m^{-2} h^{-1}) [Eq. 3.46]
$V_{Omax\ i,j,k}$	Leaf oxygenation rate (μmol m^{-2} s^{-1}) at saturating O_2 in the absence of CO_2 [Eq. 3.29]
V_S	Soil CO_2 flux (g C m^{-2} h^{-1}) [Eq. 3.37]
$V_{Xi,j}$	Tiller (branch) gross CO_2 fixation (g C m^{-2} h^{-1}) [Eq. 3.46]
$V_{Xi,j,k,l,m,n,o}$	Leaf gross CO_2 fixation rate (μmol m^{-2} s^{-1}) at ambient Ψ_{Ci} [Eq. 3.40]
$W_{l,l+1}$	Water flux between adjacent soil layers (g m^{-2} s^{-1}) [Eq. 3.16]
$X_{i,j}$	Primary photosynthate storage pool (g C m^{-2}) [Eq. 3.41]
$[X]_i$	Concentration of X in leaf + sheath (g g^{-1}) [Eq. 3.18]
$Y_{i,j,k,l,m,n,o}$	Carboxylation yield (μmol CO_2 μmol e^{--1}) [Eq. 3.30, 3.34]
z_{Ci}	Momentum roughness parameter (m) [Eq. 3.10]
$Z_{i,j,c}$	Mass of microbial residue C in soil (g C m^{-2}) [Eq. 3.53]
$Z_{i,j,n}$	Mass of microbial residue N in soil (g N m^{-2}) [Eq. 3.53]
z_l	Depth of soil layer below surface (m) [Eq. 3.15, 3.23]
z_R	Height of wind speed measurement (m) [Eq. 3.10]
z_r	Depth of surface residue (m) [Eq. 3.14]
z_s	Depth of soil surface layer (m) [Eq. 3.14-3.15]
z_{Vi}	Vapor roughness parameter (m) [Eq. 3.10]
$[Z_{i,c}]$	Concentration of $\sum_{j=1}^{J} Z_{i,j,c}$ in soil (g C Mg^{-1}) [Eq. 3.50]